

NEAR EAST UNIVERSITY

Faculty of Engineering

Department of Electrical & Electronic Engineering

**Upsampling Based on Combination of Lagrange and
Orthogonal Polynomials**

Master Thesis

Student: Jalal Swailam (991480)

Supervisor: Prof.Dr. Fakhraddin Mamedov

Nicosia - 2004



26 39 51 27 80

NEU

JURY REPORT

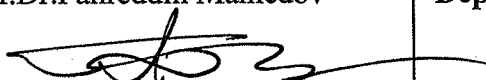
**DEPARTMENT OF
ELECTRICAL & ELECTRONIC ENGINEERING**

Academic Year: 2003-2004

STUDENT INFORMATION

Full Name	Jalal Swailam		
Undergraduate degree	BSc.	Date Received	Spring 1999-2002
University	Near East University	CGPA	2.00

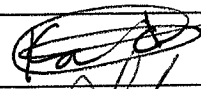


THESIS

THESIS			
Title	Upsampling Based on Combination of Lagrange and Orthogonal Polynomials		
Description The process of the upsampling and downsampling for discrete signal. Signal reconstruction by inserting new values of samples to original signal by upsampling application			
Supervisor	Prof.Dr.Fahreddin Mamedov 	Department	Electrical & Electronic Engineering

DECISION OF EXAMINING COMMITTEE

The jury has decided to accept / ~~reject~~ the student's thesis.
The decision was taken unanimously / ~~by majority~~.

COMMITTEE MEMBERS

Number Attending	3	Date	14/07/2004
Name			Signature
Assist. Prof. Dr. Kadri Buruncuk, Chairman of the jury			
Prof. Dr. Perviz Alizada, Member			
Assoc.Prof. Dr. Sameer Ikhdair, Member			

APPROVALS

Date
July 2004

Chairman of Department
Assoc. Prof. Dr. Adnan Khashman

DEPARTMENT OF ELECTRICAL & ELECTRONIC ENGINEERING
DEPARTMENTAL DECISION

Date: 14/07/2004

Subject: Completion of M.Sc. Thesis

Participants: Prof.Dr. Fahraddin Mamedov, Assist. Prof. Dr. Kadri Buruncuk, Prof. Dr. Perviz Alizada, Assoc.Prof. Dr. Sameer Ikhdair, Alaa Eleyan, Mehmet Göğebakan, Mr. Jamal Abu Hasna, Mohammed Al Hams, Ramiz Salama, Mohammed Mdukh, Nashat AL Mansour, Hazem Abu Shaban.

DECISION

We certify that the student whose number and name are given below, has fulfilled all the requirements for a MSc. degree in Electrical & Electronic Engineering.

CGPA

991480

Jalal Swailam

3.14

Assist. Prof. Dr. Kadri Buruncuk, Committee Chairman , Electrical &
Electronic Engineering Department, NEU

Prof. Dr. Perviz Alizada,

Committee Member , Electrical and Electronic
Engineering Department, NEU

Assoc.Prof. Dr. Sameer Ikhdair,

Committee Member, Electrical and Electronic
Department, NEU

Prof.Dr. Fakhraddin Mamedov,


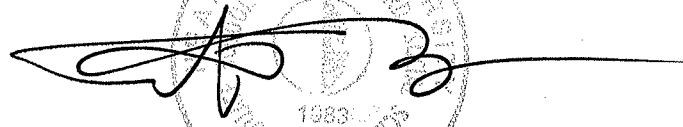
Supervisor, Electrical and Electronic Engineering
Department, NEU

Chairman of Department
Assoc. Prof. Dr. Adnan Khashman

Jalal Swailam : Upsampling Based on Combination of Lagrange and Orthogonal Polynomials

Approval of the Graduate School of Applied and Social Sciences

Prof. Dr. Fakhraddin Mamedov
Director



We certify this thesis is satisfactory for the award of the Degree of Master of Science in Electrical and Electronic Engineering

Examining Committee in charge:

Assist. Prof. Dr. Kadri Buruncuk, Committee Chairman , Electrical & Electronic Engineering Department, NEU



Prof. Dr. Perviz Alizada,



Committee Member , Electrical and Electronic Engineering Department, NEU

Assoc.Prof. Dr. Sameer Ikhdair,



Committee Member, Electrical and Electronic Department, NEU

Prof.Dr. Fakhraddin Mamedov,



Supervisor, Electrical and Electronic Engineering Department, NEU

ACKNOWLEDGMENTS

I could not have prepared this thesis without the generous help of my supervisor, colleagues, friends, and family.

I would like to express my gratitude to my supervisor Prof. Dr. Fakhraddin Mamedov for providing invigorating environment in which I could write this thesis.

My deepest thanks due to Assoc. Prof. Dr. Adnan Khashman for his help and answering any question I asked him.

My deepest thanks due to Assoc. Prof. Dr. Sameer Ikhdair for his enlightening comments regarding the correction of my thesis.

Finally, I could never have prepared this thesis without the encouragement and support of my parents, brothers, sisters, my fiancé Rinad.

ABSTRACT

The condition under which the signal is exactly recoverable from the samples is embodied in the sampling theorem. For exact reconstruction, this theorem requires that the signal to be sampled be band limited and that the sampling frequency be greater than the twice the highest frequency in signal to be sampled. Under these conditions exact reconstruction of the original signal is carried out by means of ideal filtering.

However in practice we face the problem to recover the original signal from its limited number of samples located at large intervals than sampling intervals defined by Shannon theorem. In this case, it is impossible to exact recover the original signal from its samples.

To increase precision of reconstruction we propose inserting extra interpolated samples between the original samples and then orthogonal filtering the combination of original and extra samples.

CONTENTS

AKNOWLEDEMENTS	i
ABSTRACT	ii
CONTENTS	iii
INTRODUCTION	vi
1. DISCRETE-TIME SIGNALS AND SYSTEMS	1
1.1 Overview	1
1.2 Sampling Theorem	1
1.3 Practical Issues	4
1.3.1 Interpolation/Filtering	4
1.3.2 Aliasing	4
1.3.3 The Treachery of Aliasing	5
1.4 An Important Class of Linear Time-Invariant Discrete-Time (LTID) Systems	5
1.5 Linear Convolution in Discrete-Time	7
1.6 Some Applications of the Sampling Theorem	7
1.7 Dual of Time-Sampling	8
1.7.1 The Spectral Sampling Theorem	8
1.7.2 Spectral Interpolation	9
1.8 Numerical Computation of the Fourier Transform	10
1.8.1 The Discrete Fourier Transform (DFT)	10
1.8.2 Number of Samples	11
1.8.3 Point of Discontinuity	11
1.8.4 Zero padding	12
1.9 Summary	12
2. BASIC PRINCIPLES OF SAMPLING AND SAMPLING RATE CONVERSION	13
2.1 Overview	13
2.2 Uniform Sampling and the Sampling Theorem	14

2.2.1	Uniform Sampling Viewed as a Modulation Process	14
2.2.2	Spectral Interpretations of Sampling	17
2.2.3	The Sampling Theorem	20
2.2.4	Reconstruction of an Analog Signal from Its Samples	22
2.2.5	Summary of the Implications of the Sampling Theorem	24
2.3	Sampling Rate Conversion - An Analog Interpretation	25
2.4	Decimation and Interpolation of Bandpass Signals	32
2.4.1	The Sampling Theorem Applied to Bandpass Signals	32
2.4.2	Integer-Band Decimation and Interpolation	33
2.5	Summary	40
3	DIGITAL FILTER BANK IN MULTIRATE SIGNAL PROCESSING	41
3.1	Overview	41
3.2	Definitions	41
3.3	Uniform DFT Filter Banks	42
3.3.1	Nyquist (L th Band) Filters	44
3.3.2	Half-Band Filters	46
3.4	Two-Channel Quadrature-Mirror Filter Bank	47
3.4.1	The Filter Bank Structure	48
3.4.2	An Alias-Free Realization	49
3.5	L -Channel QMF Bank	52
3.5.1	Analysis of the L -Channel Filter Bank	52
3.5.2	Matrix Representation	53
3.5.3	Polyphase Representation	55
3.6	Filter Banks with Equal Pass-Band Widths	57
3.7	Filter Banks with Unequal Pass-Band Widths	60
3.8	Summary	64
4	INTERPOLATION USING ORTHOGONAL FUNCTION	65
4.1	Overview	65
4.2	Orthogonal Filters	65
4.3	Completeness of an Orthogonal Set, the Fourier Series	67
4.4	Trigonometric Polynominal Approximation	69

4.5 Expansions in Orthogonal Functions	70
4.6 Orthogonal Filters	73
4.6.1 Hermite Series	73
4.6.2 Hermite Rodriguez Function	75
4.7 Signal Duration and Bandwidth	76
4.8 Scaling	77
4.9 Optimizing the Weights of the Orthogonal Series	78
4.10 Summary	79
5. PRACTICAL IMPLEMENTATION USING MATLAB	80
5.1 Overview	80
5.2 MATLAB Implementation	80
5.3 Design of Algorithms and Devices for Upsampling	88
5.4 Summary	98
CONCLUSION	99
REFERENCES	100
APPENDIX 1	102
APPENDIX 2	103

INTRODUCTION

The theory of conventional single rate digital signal processing of the continuous time signal is based on the Shannon Sampling Theorem. In accordance to this theorem, any continuous time signal can be represented from its samples taken at least twice the maximal frequency of the content signal.

On process of control it is necessary to reconstruct CTS from limited numbers of discrete samples .the problem is carried in control of parameter that difficult to access (eg. Special system, petrol and chemistry industries).

In this cases application only Lagrange orthogonal polynomial for reconstruction yields unacceptable errors between nodes of interpolation to increase precision and enhancing process of interpolation in this we use combination of above measured two types method of interpolation.

In chapter 1, the theoretical discrete time signals and systems are presented. The problems of prefiltering to avoid aliasing, analysis of quantizing error, decimation and interpolation and up sampling methods are described.

Chapter 2 introduces basic Sampling and Sampling Rate Conversion. The impulse and frequency responses, properties of Linear-phase filters with symmetrical and antisymmetrical impulse responses are analyzed.

The Matrix and polyphase representation condition of perfect reconstruction by(Quadrature Mirror Filter) QMF filters, bank filter with equal and unequal pass band are analyzed. Conclusion states therefore results obtained by author in investigation multirate signal processing system.

Chapter 3 gives basic of the digital bank filter and its application for multirate signal processing. Uniform(Discrete Fourier Transform) DFT filters having different central frequencies, full and half (Number of Band) Lth band filter are presented. Design and error analysis of the 2-channel QMF bank filters are given.

Chapter 4 introduces many different sets of orthogonal function may be chosen to represent a given signal, and finally the expansion of the signals in special orthogonal functions.

Finally in chapter 5 introduces extra samples between measured original samples using lagrange interpolation and orthogonal function practical and simulation of systems are described by using MATLAB program.

1. DISCRETE-TIME SIGNALS AND SYSTEMS

1.1 Overview

The world around us is analog, that is, continuous in time and amplitude. However, because of progresses in digital technology, it is common to take samples of signals and perform all kind of processing (including storage and transmission) in digital domain, i.e., discrete in time and amplitude.

In this chapter, we introduce discrete-time signals as sampled versions of continuous-time signals. We also introduce difference equations as discrete-time equivalent of differential equations. The concept of convolution in discrete-time will also be introduced.

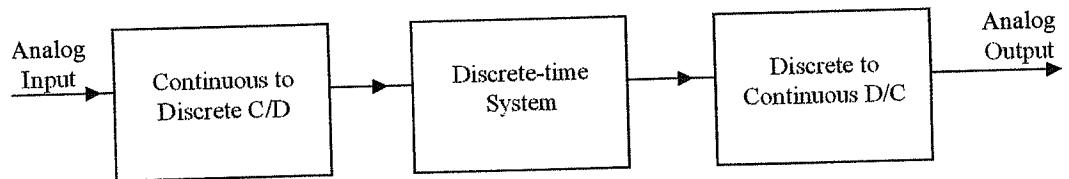


Figure 1.1 Operation of Obtaining Analog Output Signal from Analog Input after Converting to Discrete Signal.

1.2 Sampling Theorem

Shannon (sampling) theorem states that if a continuous time signal $f(t)$ is band-limited to B Hz, i.e., $|F(\omega)| = 0$ for $|\omega| > 2\pi B$, then the samples of $f(t)$, taken at a frequencies $F_s \geq 2B$, are sufficient for reconstruction of $f(t)$. That is, there will be no loss of information in using the sampled signal in place of its continuous time version. The frequency $F_m = 2B$ is called Nyquist frequency of $f(t)$.

To prove the sampling theorem, we define the sampled version of $f(t)$ as

$$\bar{f}(t) = f(t)\delta_T(t) = \sum_n f(nT)\delta(t - nT) \quad (1.1)$$

where $T = 1/F_s$ and

$$\delta_T(t) = \sum_n \delta(t - nT) \quad (1.2)$$

since $\delta_T(t)$ is a periodic signal, it has a Fourier series. Moreover, recalling that $\delta_T(t)$ is symmetric with respect to origin, its Fourier series is of the form

$$\delta_T(t) = a_0 + a_1 \cos w_s t + a_2 \cos 2w_s t + \dots$$

where

$$w_s = \frac{2\pi}{T} = 2\pi F_s \quad (1.3)$$

$$a_0 = \frac{1}{T} \int_{-T/2}^{T/2} \delta_T(t) dt = \frac{1}{T}$$

and

$$a_n = \frac{2}{T} \int_{-T/2}^{T/2} \delta_T(t) \cos w_s t dt = \frac{2}{T}; \quad n = 1, 2, \dots \quad (1.4)$$

Thus,

$$\delta_T(t) = \frac{1}{T} [1 + 2 \cos w_s t + 2 \cos 2w_s t + \dots] \quad (1.5)$$

Hence,

$$\bar{f}(t) = \frac{1}{T} [f(t) + 2f(t) \cos w_s t + 2f(t) \cos 2w_s t + \dots] \quad (1.6)$$

The above results are depicted in figure 1.2.

Notes:

1. Sampling results in repetition of the spectrum at the intervals
2. When $F_s \geq 2B$ for $\omega_s > 2\pi B$ the original spectrum and the Fourier transform pairs $F(w)$ can be extracted from $\bar{F}(w)$ through a lowpass filtering.

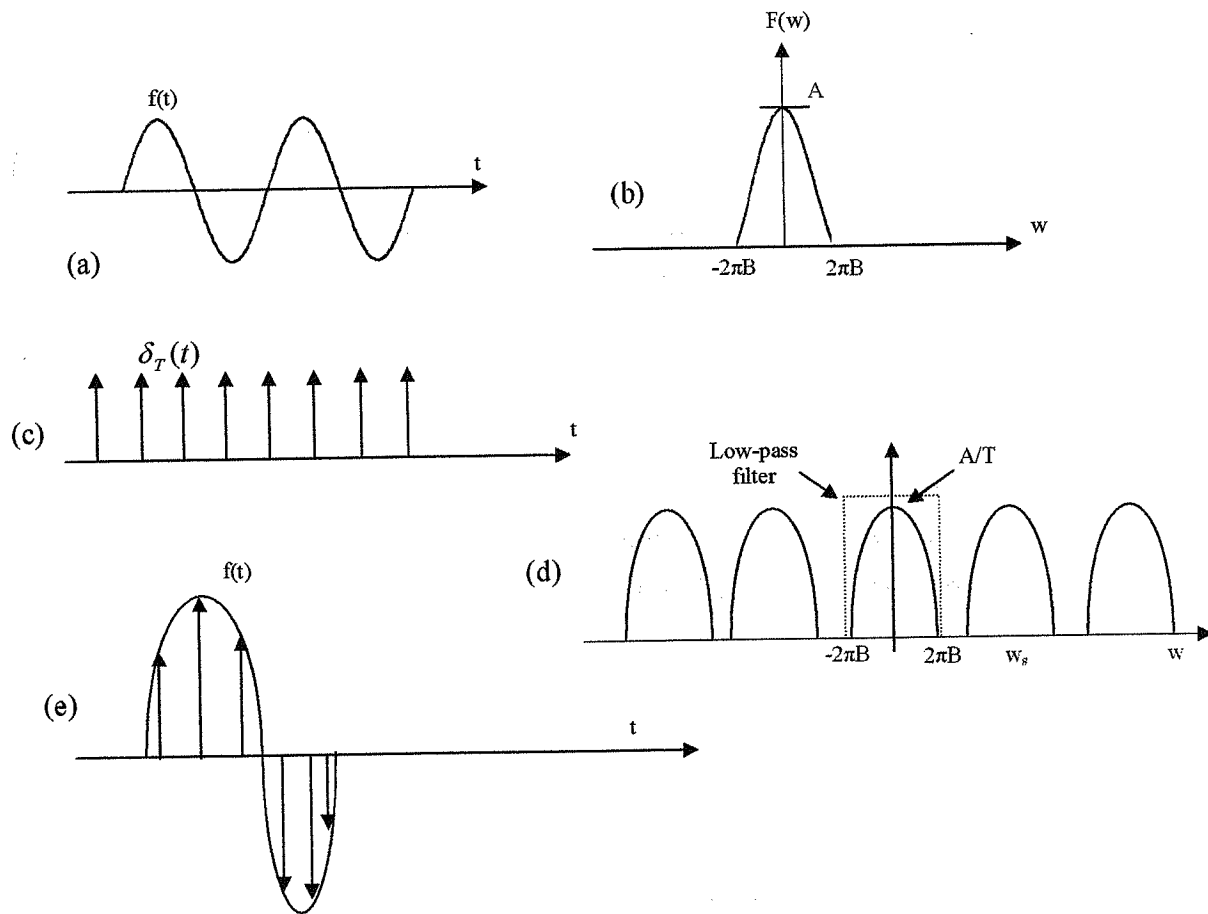


Figure 1.2 Sampling Results in Repetition of the Spectrum at the Intervals

- (a) Function of time signal
- (b) Function of frequency signal
- (c) Impulse train signal
- (d) Sampling frequency intervals
- (e) After sampling for time signal

1.3 Practical Issues

1.3.1 Interpolation/Filtering

In practice, the realization of the ideal lowpass filter mentioned above is not possible, as it is non-causal. It is thus replaced by a filter which is realizable. Such a filter requires a non-zero transition band. This means that signals have to be sampled at a rate above Nyquist, to introduce a guard band such that transition bands could be accommodated.

We shall also note that a practical filter can never cancel the replicas of signal spectrum, completely. Thus, interpolation error is inevitable in practice. However, this error will be reduced by using a higher order filter or by choosing a larger sampling frequency such that a sufficient guard band will be present.

1.3.2 Aliasing

Strictly speaking, the assumption that a signal is band-limited is not satisfied in most of the practical applications. Most of the signals have a spectrum which stretches over a relatively wide band. However, there is usually negligible energy above a certain band.

When a signal is sampled at a rate which is less than Nyquist rate, higher frequency components will fold over and mix with the lower frequency components, as shown in figure 1.3. The phenomenon of folding the higher frequencies to the lower frequencies is called aliasing.

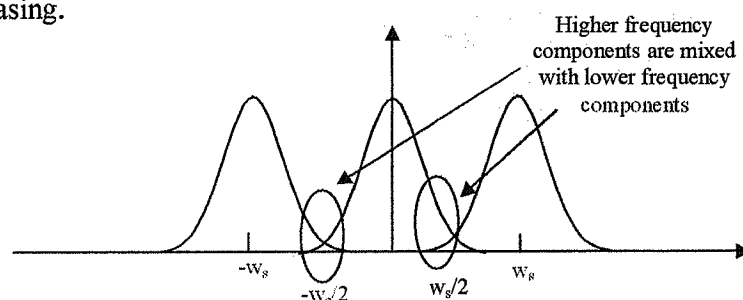


Figure 1.3 Definition of Aliasing

1.3.3 The Treachery of Aliasing

When a signal is sampled below Nyquist rate, there are two consequences to the aliasing: (i) the components above $\omega_s/2$ are cancelled in the process of signal reconstruction; (ii) the aliased (folded) components distort the signal components below $\omega_s/2$. Therefore the damage done to the signal is two-fold.

To resolve the two-fold problem just mentioned, analog antialiasing filters are used to cancel any signal components beyond $\omega_s/2$. In this way, the loss of information in the sampled signal is only due to cancellation of components above $\omega_s/2$. The signal components below $\omega_s/2$ remain untouched.

1.4 An Important Class of Linear Time-Invariant Discrete-Time (LTID) Systems

For LTID systems the equivalent systems are those whose input and output are related by constant coefficients difference equations of the form

$$\begin{aligned} y[k] + a_{n-1}y[k-1] + a_{n-2}y[k-2] + \dots + a_0y[k-n] \\ = b_m f[k] + b_{m-1}f[k-1] + \dots + b_0f[k-m] \end{aligned} \quad (1.7)$$

A simple example of LTID systems is the one whose input and output are related according to the difference equation

$$y[k] - \alpha y[k-1] = f[k] \quad (1.8)$$

Figure 1.4 depicts a realization of this system

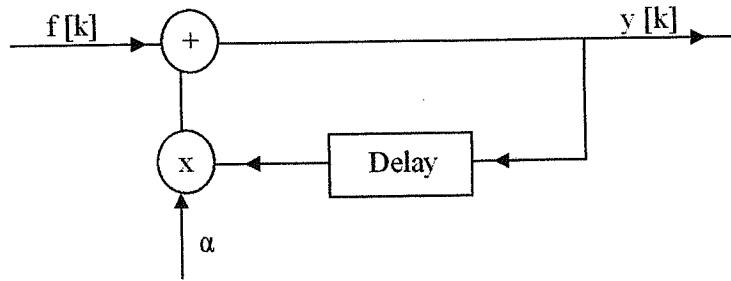


Figure 1.4 LTID System

The impulse response of this system is obtained by letting $f[k] = \delta[k]$ and finding the samples of output. The result is (assuming $y[k] = 0$ for $k < 0$)

$$\begin{aligned} y[0] &= \alpha \times 0 + \delta[0] = 1 \\ y[1] &= \alpha \times y[0] + \delta[1] = \alpha \\ y[2] &= \alpha \times y[1] + \delta[2] = \alpha^2 \\ &\vdots \end{aligned}$$

Thus, the system impulse response is $h[k] = \alpha^k u[k]$. This is similar to the sampled version of the impulse response of a LTIC system

$$h(t) = e^{-t/\tau} u(t) \quad (1.9)$$

Replacing k by kt in equation (1.8) and making use of (1.9) and then putting $t = T$ gives

$$\tau = -\frac{1}{\ln \alpha} \quad (1.10)$$

By simple generalization of this observation, we may say that any LTIC system governed by a differential equation, has a LTID equivalent governed by a difference equation.

1.5 Linear Convolution in Discrete-Time

We note that a signal $f[k]$ may be written as

$$f[k] = \sum_n f[n]\delta[k-n] \quad (1.11)$$

i.e., a summation of impulses.

Applying this as input to an LTID system and considering the linearity and time shifting properties, we obtain

$$f[k] = \sum_n f[n]h[k-n] \quad (1.12)$$

which is linear convolution in discrete-time.

1.6 Some Applications of the Sampling Theorem

The immediate and most important application of sampling theorem is to convert the samples of the sampled signal to a set of digital numbers. Once these digital numbers are obtained they can be used to store the signal in a computer or transmit the information bits through a communication channel. The digital numbers can also be used for processing the signal in a very convenient way, e.g., filtering the signal using a digital filter.

In particular, there are many advantages in working with digital signals instead of their analog counterparts:

- Ease of transmission
- Accurate regeneration/reconstruction
- Ease of implementation
- Coding can be applied to achieve very low probability of error
- Multiplexing is straightforward
- Lower cost

1.7 Dual of Time-Sampling

1.7.1 The Spectral Sampling Theorem

Let us begin with the time-limited signal $f(t)$ and its Fourier transform $F(w)$ as shown in figure 1.5.

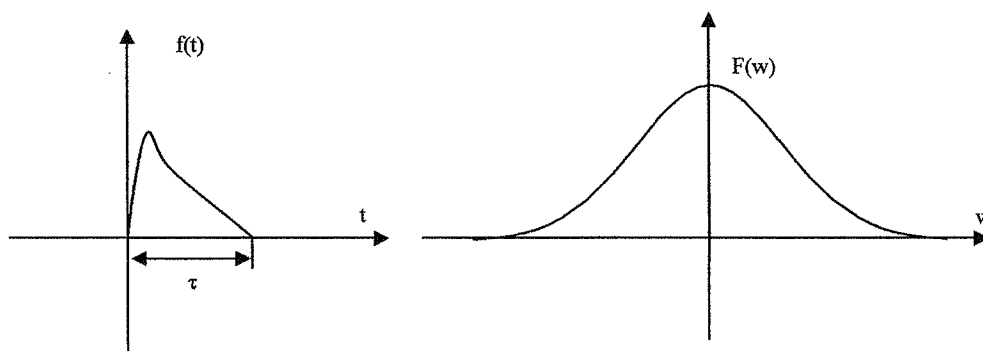


Figure 1.5 (a) Time-Limited Signal $f(t)$; (b) Fourier Transform $F(w)$

$$F(w) = \int_{-\infty}^{\infty} f(t)e^{-j\omega t} dt = \int_0^{\tau} f(t)e^{-j\omega t} dt \quad (1.13)$$

Next define the periodic signal $f_{T_0}(t)$ and its complex Fourier series coefficients D_n as shown in figure 1.6.

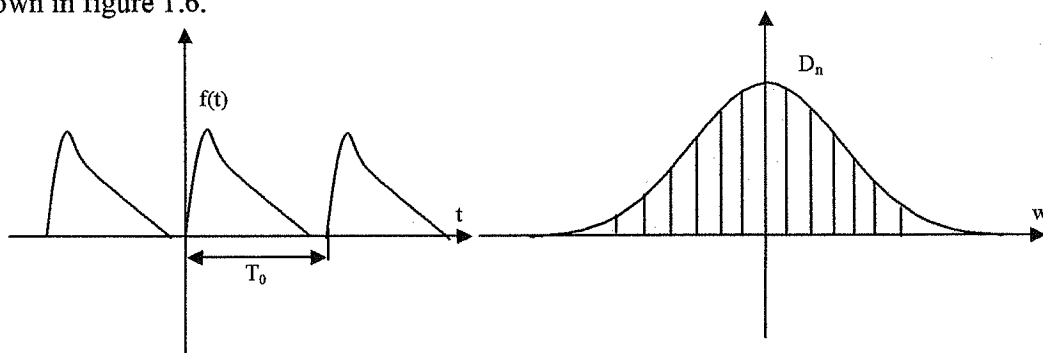


Figure 1.6 (a) Periodic Signal $f_{T_0}(t)$; (b) Complex Fourier Coefficient D_n .

From the Fourier series (assuming $T_0 > \tau$)

$$f_{T_0}(t) = \sum_{n=-\infty}^{\infty} D_n e^{jn\omega_0 t} \quad (1.14)$$

where

$$\omega_0 = \frac{2\pi}{T_0}$$

and

$$D_n = \frac{1}{T_0} \int_0^{T_0} f(t) e^{-jn\omega_0 t} dt = \frac{1}{T} \int_0^T f(t) e^{-jn\omega_0 t} dt \quad (1.15)$$

which implies that

$$D_n = \frac{1}{T_0} F(n\omega_0) \quad (1.16)$$

i.e., D_n is $\frac{1}{T_0}$ times the sample $F(n\omega_0)$ of $F(\omega)$.

1.7.2 Spectral Interpolation

Following the same line of derivations to the time interpolation, we get

$$F(\omega) = \sum_n F(n\omega_0) \text{sinc} \left(\frac{\omega\tau}{2} - n\pi \right) \quad (1.17)$$

where

$$\omega_0 = \frac{2\pi}{\tau}$$

1.8 Numerical Computation of the Fourier Transform

1.8.1 The Discrete Fourier Transform (DFT)

Given a time-limited signal $f(t)$ and its sampled version $\bar{f}(t)$, we have the Fourier transform pairs shown below in figure 1.7

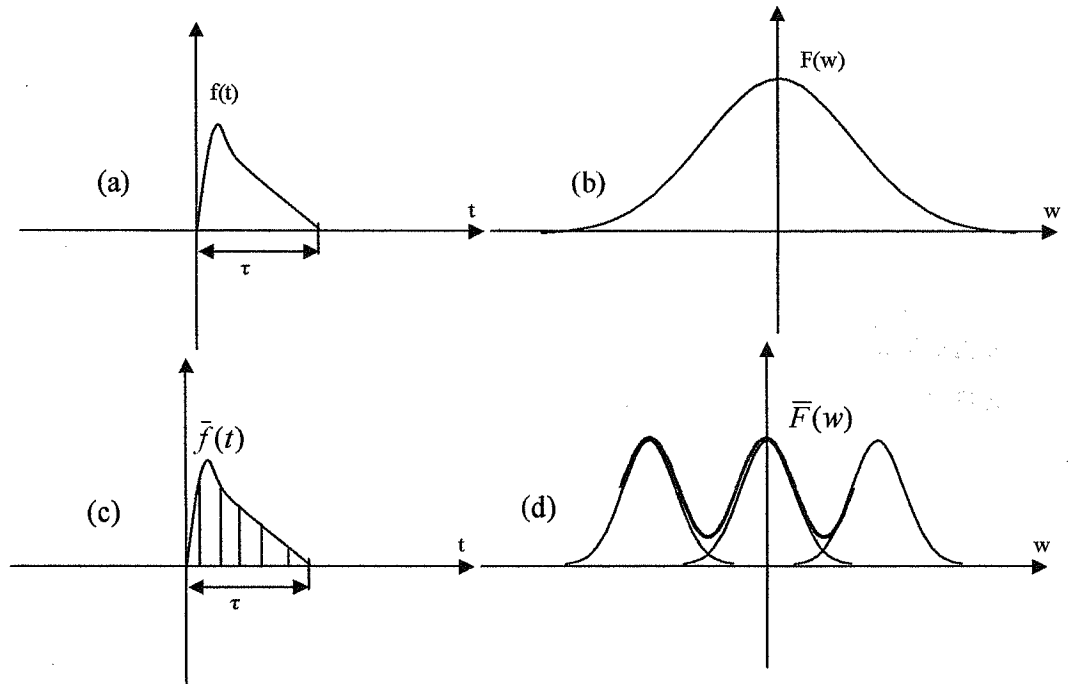


Figure 1.7 Time-Limited Signal $f(t)$ and its Sampled Version $\bar{f}(t)$

Now, if we repeat $\bar{f}(t)$ after every T seconds the associated Fourier transform will be a sampled version of $\bar{F}(w)$.

Figure 1.7 assumes a value of T that is not small enough to avoid aliasing. By reducing T one can avoid aliasing or, at least, reduce aliasing to a negligible level. Thus, by reducing T , as shown in figure 1.8, in which aliasing is negligible.

Note: When a signal is time limited, its spectrum is band unlimited. This means that aliasing cannot be cancelled completely, unless T reduces to zero!

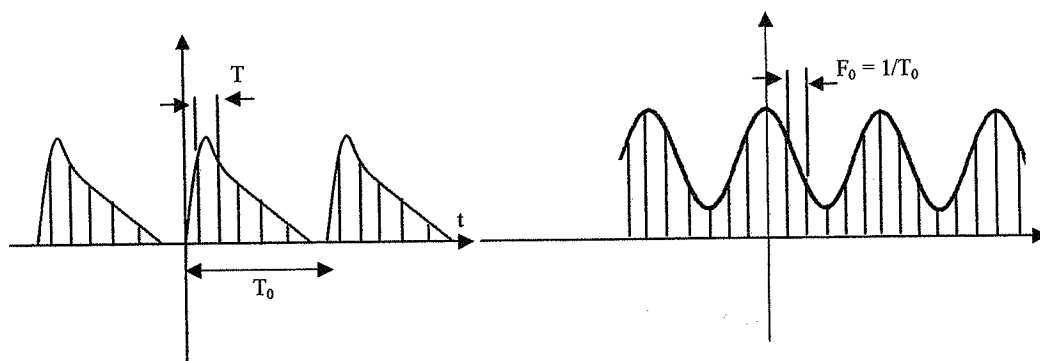


Figure 1.8 Aliasing is Negligible.

1.8.2 Number of Samples

Let N_0 denote number of samples in each period of the time domain signal, and N'_0 denote the number of samples in each period of the frequency domain signal. Then,

$$N_0 = \frac{T_0}{T} \text{ and } N'_0 = \frac{F_s}{F_0} \quad (1.18)$$

where $F_s = \frac{1}{T}$ and $F_0 = \frac{1}{T_0}$, it gives

$$N_0 = \frac{T_0}{T} = \frac{F_s}{F_0} = N'_0 \quad (1.19)$$

1.8.3 Point of Discontinuity

When $f(t)$ has a discontinuity at a sampling point, the sample value should be taken as the average of the values on the two sides of the discontinuity, because this leads to the best regeneration of the time domain signal from the frequency domain samples.

1.8.4 Zero Padding

For a time-limited signal with duration of τ we usually consider a choice of $T_0 > \tau$. Since $F_0 = \frac{1}{T_0}$, this increases the frequency resolution, i.e., more samples of $F(w)$ are calculated. When the sampling period, T , is kept constant and T_0 is increased, this is equivalent to increasing N_0 , or thinking of samples N_0 is increased by padding zeros behind the samples $f_k = Tf(kT)$.

1.9 Summary

The theoretical discrete time signals and systems were presented. The problems of prefiltering to avoid aliasing, analysis of quantizing error, decimation and interpolation and up sampling methods were described.

2. BASIC PRINCIPLES OF SAMPLING AND SAMPLING RATE CONVERSION

2.1 Overview

The purpose of this chapter is to provide the basic theoretical framework for uniform sampling and for the signal processing operations involved in sampling rate conversion. As such we begin with a discussion of the sampling theorem and consider its interpretations in both the time and frequency domains. We then consider sampling rate conversion systems (for decimation and interpolation) in terms of both analog and digital operations on the signals for integer changes in the sampling rate. By combining concepts of integer decimation and interpolation, we generalize the results to the case of rational fraction changes of sampling rates for which a general input-output relationship can be obtained. These operations are also interpreted in terms of concepts of periodically time-varying digital systems.

Next we consider more complicated sampling techniques and modulation techniques for dealing with bandpass signals instead of lowpass. We show that sampling rate conversion techniques can be extended to bandpass signals as well as lowpass signals and can be used for purposes of modulation as well as sampling rate conversion.

2.2 Uniform Sampling and the Sampling Theorem

2.2.1 Uniform Sampling Viewed as a Modulation Process

Let $X_c(t)$ be a continuous function of the continuous variable t . We are interested in sampling $X_c(t)$ at the uniform rate that is, one every interval of duration T .

$$t = nT, \quad -\infty < n < \infty \quad (2.1)$$

Figure 2.1 shows an example of a signal $X_c(t)$ and the associated sampled signal $x(n)$ for two different values of T .

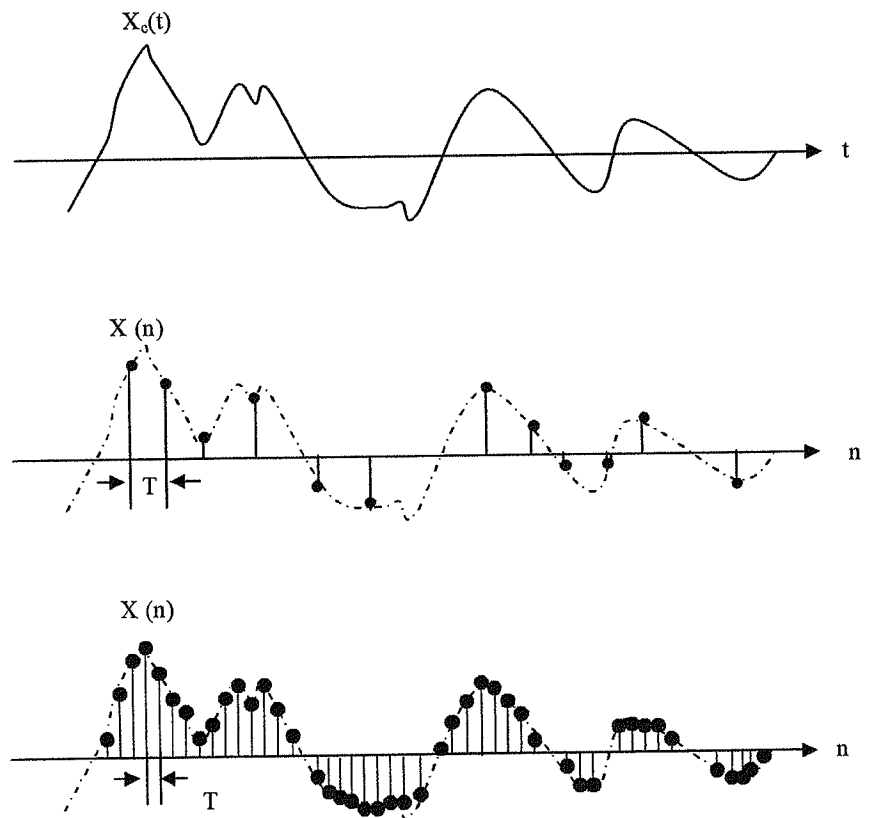


Figure 2.1 Continuous Signal and Two Sampled Versions of it.

One convenient way of interpreting this sampling process is as a modulation or multiplication process, as shown in figure 2.2(a). The continuous signal $X_c(t)$ is multiplied (modulated) by the periodic impulse train (sampling function) $s(t)$ to give the

pulse amplitude modulation (PAM) signal $X_c(t)s(t)$. This PAM signal is then discretized in time to give $x(n)$, that is,

$$x(n) = \lim_{\varepsilon \rightarrow 0} \int_{t=nT-\varepsilon}^{nT+\varepsilon} x_c(t)s(t)dt \quad (2.2)$$

where

$$s(t) = \sum_{l=-\infty}^{\infty} u_0(t-lT) \quad (2.3)$$

where $u_0(t)$ denotes an ideal unit impulse function. In the context of this interpretation, $x(n)$ denotes the area under the impulse at time nT . Since this area is equal to the area under the unit impulse (area = 1), at time nT , weighted by $X_c(nT)$, it is easy to see that

$$x(n) = x_c(nT) \quad (2.4)$$

Figure 2.2(b), (c), and (d) show $X_c(t)$, $s(t)$, and $x(n)$ for a sampling period of T seconds.

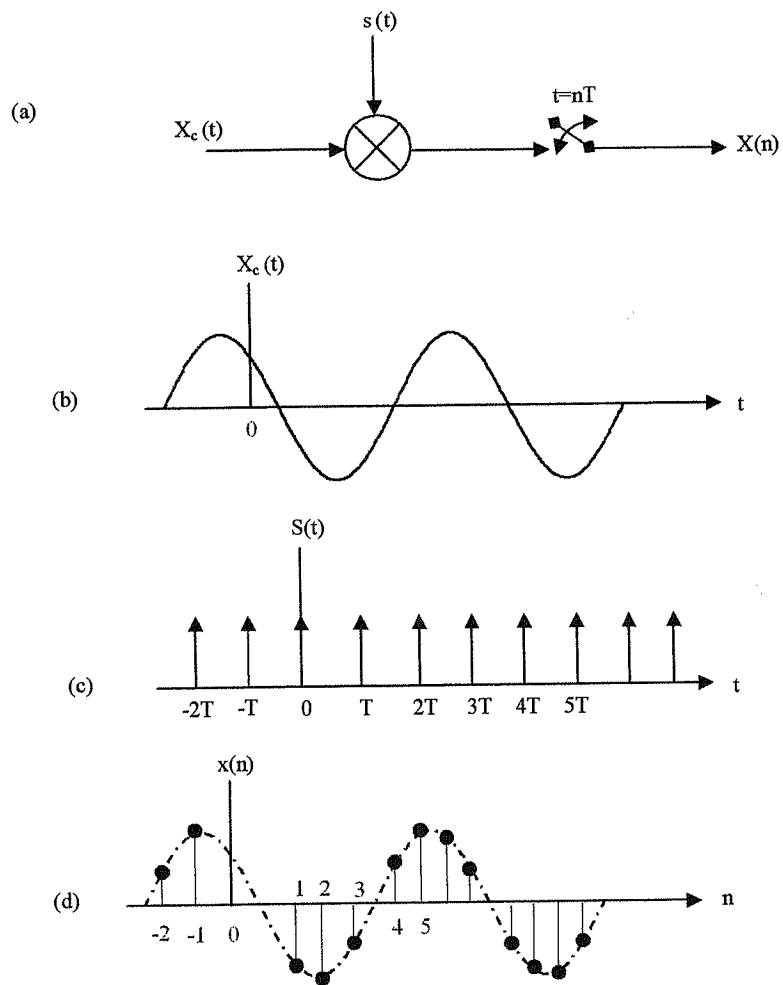


Figure 2.2 Periodic Sampling of $X_c(t)$ via Modulation to obtain $x(n)$.

2.2.2 Spectral Interpretations of Sampling

We assume that $x_c(t)$ has the Fourier transform $X_c(j\Omega)$ defined as

$$X_c(j\Omega) = \int_{-\infty}^{\infty} x_c(t) e^{-j\Omega t} dt \quad (2.5)$$

where Ω denotes the analog frequency (in rad/sec). Similarly, the Fourier transform of the sampling function $s(t)$ can be defined as

$$S(j\Omega) = \int_{-\infty}^{\infty} s(t) e^{-j\Omega t} dt \quad (2.6)$$

and it can be shown that by applying equation (2.3) to equation (2.6), $S(j\Omega)$ has the form

$$S(j\Omega) = \frac{2\pi}{T} \sum_{l=-\infty}^{\infty} u_0 \left[\Omega - \frac{2(\pi)l}{T} \right] \quad (2.7)$$

by defining

$$F = \frac{1}{T} \quad (2.8)$$

$$\Omega = 2\pi f \quad (2.9a)$$

and

$$\Omega_F = 2\pi F \quad (2.9b)$$

$S(j\Omega)$ also has the form

$$S(j\Omega) = \Omega_F \sum_{l=-\infty}^{\infty} u_0(\Omega - l\Omega_F) \quad (2.10)$$

That is, a uniformly spaced impulse train in time, $s(t)$, transforms to a uniformly spaced impulse train in frequency, $S(j\Omega)$.

Since multiplication in the time domain is equivalent to convolution in the frequency domain, we have the relation

$$X_c(j\Omega) * S(j\Omega) = \int_{-\infty}^{\infty} [x_c(t)s(t)] e^{-j\Omega t} dt \quad (2.11)$$

where $*$ denotes a linear convolution of $X_C(j\Omega)$ and $S(j\Omega)$ in frequency. Figure 2.3 shows typical plots of $X_C(j\Omega)$, $S(j\Omega)$, and the convolution $X_C(j\Omega) * S(j\Omega)$, where it is assumed that $X_C(j\Omega)$ is band-limited and its highest-frequency component $2\pi F_C$ is less than one-half of the sampling frequency, $\Omega_F = 2\pi F$. From this figure it is seen that the process of pulse amplitude modulation periodically repeats the spectrum $X_C(j\Omega)$ and $S(j\Omega)$.

Because of the direct correspondence between the sequence $x(n)$ and the pulse amplitude modulated signal $x_C(t)s(t)$, as seen in equations (2.2) and (2.4) it is clear that the information content and the spectral interpretations of the two signals are synonymous. This correspondence can be shown more formally by considering the (discrete) Fourier transform of the sequence $x(n)$, which is defined as

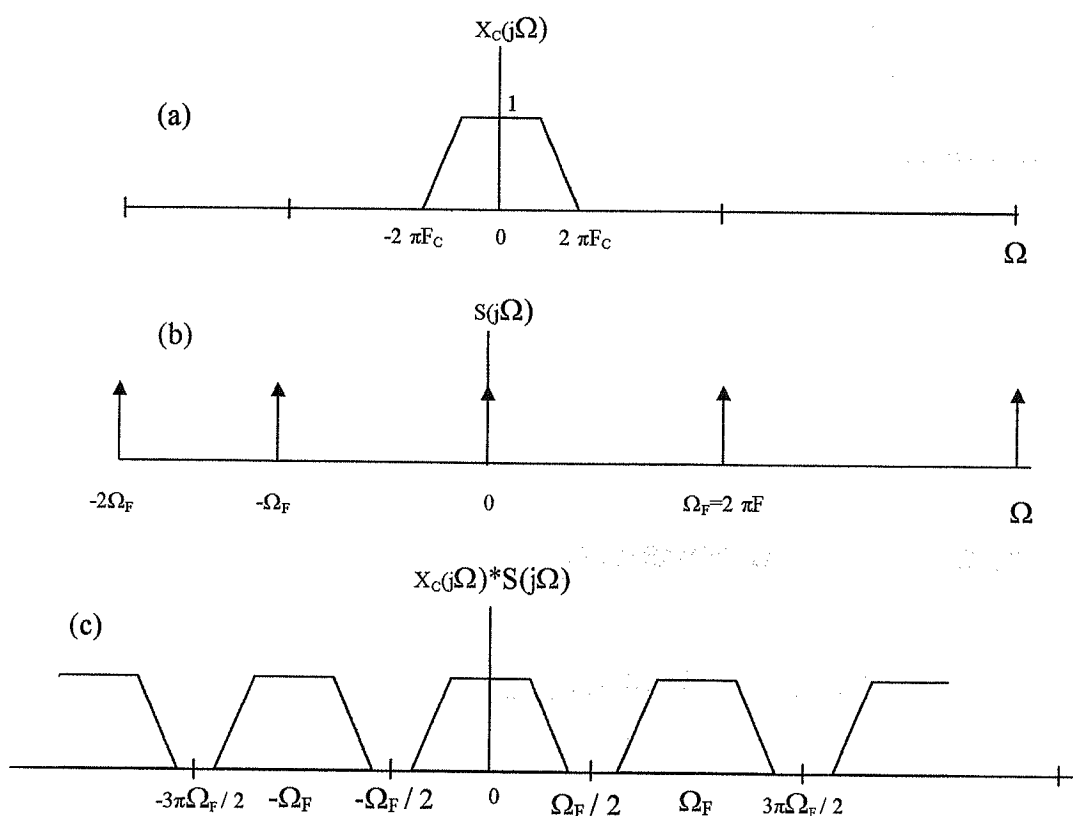


Figure 2.3 Spectra of Signals Obtained from Periodic Sampling via Modulation.

$$X(e^{j\omega}) = \sum_{n=-\infty}^{\infty} x(n)e^{-j\omega n} \quad (2.12)$$

where ω denotes the frequency (in radians relative to the sampling rate F), defined as

$$w = \Omega T = \frac{\Omega}{F} \quad (2.13)$$

Since $x_c(t)$ and $x(n)$ are related by equation (2.4), a relation can be derived between $X_c(j\Omega)$ and $X(e^{jw})$ with the aid of equations (2.5) and (2.12) as follows. The inverse Fourier transform of $X_c(j\Omega)$ gives $x_c(t)$ as

$$x_c(t) = \frac{1}{2\pi} \int_{-\infty}^{\infty} X_c(j\Omega) e^{j\Omega t} d\Omega \quad (2.14)$$

Evaluating equation (2.14) for $t = nT$, we get

$$x(n) = x_c(nT) = \frac{1}{2\pi} \int_{-\infty}^{\infty} X_c(j\Omega) e^{j\Omega nT} d\Omega \quad (2.15)$$

The sequence $x(n)$ may also be obtained as the (discrete) inverse Fourier transform of $X(e^{jw})$,

$$x(n) = \frac{1}{2\pi} \int_{-\pi}^{\pi} X(e^{jw}) e^{jwn} dw \quad (2.16)$$

Combining equations (2.15) and (2.16), we get

$$\frac{1}{2\pi} \int_{-\pi}^{\pi} X(e^{jw}) e^{jwn} dw = \frac{1}{2\pi} \int_{-\infty}^{\infty} X_c(j\Omega) e^{j\Omega nT} d\Omega \quad (2.17)$$

By expressing the right-hand side of equation (2.17) as a sum of integrals (each width $2\pi / T$), we get

$$\begin{aligned}
 \frac{1}{2\pi} \int_{-\infty}^{\infty} X_c(j\Omega) e^{j\Omega nT} d\Omega &= \frac{1}{2\pi} \sum_{l=-\infty}^{\infty} \int_{(2l-1)\pi/T}^{(2l+1)\pi/T} X_c(j\Omega) e^{j\Omega nT} d\Omega \\
 &= \frac{1}{2} \sum_{l=-\infty}^{\infty} \int_{-\pi/T}^{\pi/T} \left[X_c \left[j\Omega + j \frac{2\pi l}{T} \right] \right] e^{j\Omega nT} e^{j2\pi l n} d\Omega \\
 &= \frac{1}{2\pi} \int_{-\pi/T}^{\pi/T} \left[\sum_{l=-\infty}^{\infty} X_c \left[j\Omega + j \frac{2\pi l}{T} \right] \right] e^{j\Omega nT} d\Omega
 \end{aligned} \tag{2.18}$$

since $e^{j2\pi l n} = 1$ for all integer values of l and n . Combining equations (2.17) and (2.18), setting $\Omega = w/T$ and $\Omega_F = 2\pi/T$, gives

$$\frac{1}{2\pi} \int_{-\pi}^{\pi} [X(e^{jw})] e^{jwm} dw = \frac{1}{2\pi} \int_{-\pi}^{\pi} \left[\frac{1}{T} \sum_{l=-\infty}^{\infty} X_c(j\Omega + j l \Omega_F) \right] e^{jwm} dw \tag{2.19}$$

Finally, by equating terms within the brackets, we get

$$X(e^{jw}) = \frac{1}{T} \sum_{l=-\infty}^{\infty} X_c(j(\Omega + l\Omega_F)) = \frac{1}{T} \sum_{l=-\infty}^{\infty} X_c \left[\frac{j}{T} (w + 2\pi l) \right] \tag{2.20}$$

Equation (2.20) provides the fundamental link between continuous and digital systems. The correspondence between these relations and the spectral interpretation of the PAM signal $X_c(j\Omega) * S(j\Omega)$ in figure 2.3 is also apparent; that is, the spectrum of the digital signal corresponds to harmonically translated and amplitude scaled repetitions of the analog spectrum.

2.2.3 The Sampling Theorem

Given the analog signal $X_c(t)$ it is always possible to obtain the digital signal $x(n)$. However, the reverse process is not always true; that is, $X_c(t)$ uniquely specifies $x(n)$; but $x(n)$ does not necessarily uniquely specify $X_c(t)$. In practice it is generally desired to have a unique correspondence between $x(n)$ and $X_c(t)$ and the conditions under which this uniqueness holds is given by the well-known *sampling theorem*:

If a continuous signal $X_c(t)$ has a band-limited Fourier transform $X_c(j\Omega)$, that is, $|X_c(j\Omega)| = 0$ for $|\Omega| > 2\pi F_c$, then $X_c(t)$ can be uniquely reconstructed without error from equally spaced samples $X_c(nT)$, $-\infty < n < \infty$, if $F > 2F_c$, where $F = 1/T$ is the sampling

frequency.

The sampling theorem can be conveniently understood in terms of the spectral interpretations of the sampling process and equation (2.20). Figure 2.4 shows an example of the spectrum of a band-limited signal [part (a)] and the resulting spectrum of the digital signal for a sampling period which is shorter than required by the sampling theorem [part (b)], a sampling period equal to that required by the sampling theorem [part (c)], and a sampling period longer than required by the sampling theorem [part (c)]. From figure 2.4 we readily see that for parts (b) and (c) (when the conditions of the sampling theorem are met) the higher-order spectral components (the terms in equation (2.20) for $|l| > 1$) do not overlap the baseband and distort the digital spectrum. Thus one basic interpretation of the sampling theorem is that the spectrum of the sampled signal must be the same as (to within a constant multiplier) the spectrum of the continuous signal for the baseband of frequencies $(-2\pi F_c < \omega < 2\pi F_c)$.

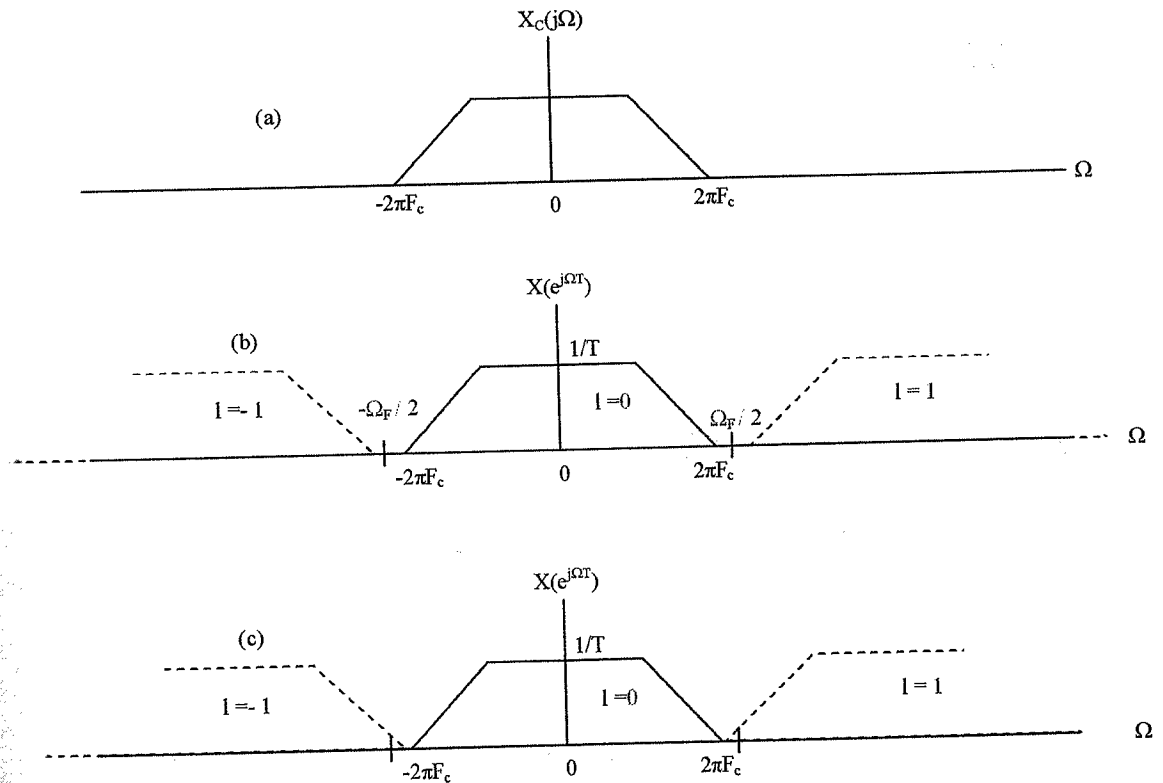


Figure 2.4 Spectral Interpretations of the Sampling Theorem.

2.2.4 Reconstruction of an Analog Signal from Its Samples

The major consequence of the sampling theorem is that the original sequence $X_c(t)$ can be uniquely and without error reconstructed from its samples $X(n)$ if the samples are obtained at a sufficiently high rate. To see how this reconstruction is accomplished. We consider the spectrum of the continuous-time modulated signal $X_c(t)s(t)$ as shown in figure 2.3(c). This spectrum is identical to that of the sampled signal $x(n)$. To recover $X_c(j\Omega)$ from the convolution $X_c(j\Omega) * S(j\Omega)$, we merely have to filter the signal $X_c(t)$ by an ideal lowpass filter whose cutoff frequency is between $2\pi F_c$ and $\Omega_F - 2\pi F_c$. This processing is illustrated in figure 2.5. To implement this process, an ideal digital-to-analog converter is required to get $X_c(t)s(t)$ from $x(n)$. Assuming that we do not worry about the realizability of such an ideal converter, the reconstruction formula from figure 2.5 is

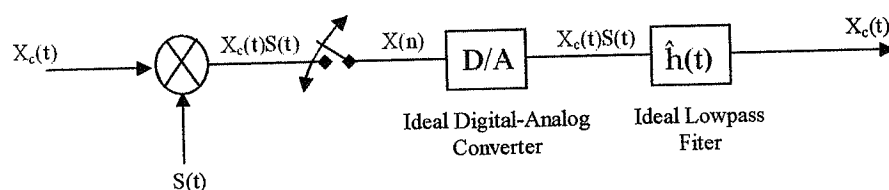


Figure 2.5 Sampling and Reconstruction of a Continuous Signal.

$$X_c(t) = \int_{\tau=-\infty}^{\infty} x_c(\tau)s(\tau)\hat{h}(t-\tau)d\tau \quad (2.21)$$

and applying equations (2.2) to (2.4) gives

$$X_c(t) = \sum_{n=-\infty}^{\infty} x(n)\hat{h}(t-nT) \quad (2.22)$$

For an ideal lowpass filter with cutoff frequency F_{LP} , the ideal impulse response $\hat{h}_I(t)$ is of the form

$$\hat{h}_I(t) = \frac{\text{Sin}(2\pi F_{LP}t)}{2\pi F_{LP}t} \quad (2.23)$$

Generally, F_{LP} is chosen as

$$F_{LP} = \frac{F}{2} = \frac{1}{2T} \quad (2.24)$$

leading to the well-known reconstruction formula

$$x_c(t) = \sum_{n=-\infty}^{\infty} x(n) \left[\frac{\sin[\pi(t-nT)/T]}{\pi(t-nT)/T} \right] \quad (2.25)$$

Figure 2.6 illustrates the application of equation (2.25) to a typical signal. It is seen that the ideal lawpass filter acts like an interpolator for the band-limited signal $x_c(t)$, allowing the determination of *any* value of $X_c(t)$ from the *infinite* set of its samples taken at a sufficiently high rate.

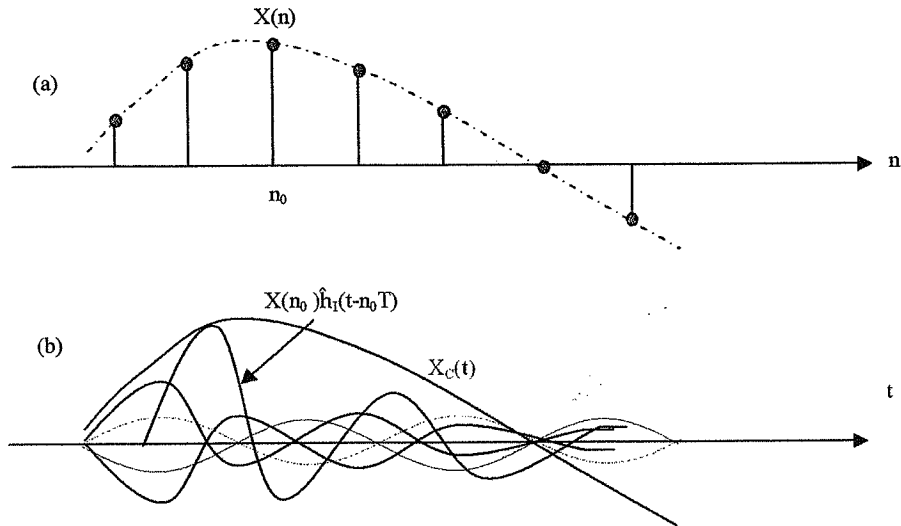


Figure 2.6 Illustration of a Band-limited Reconstruction from Shifted and Scaled Lowpass Filter Responses.

In practice the "ideal" filter is unrealizable because it requires values of $x(n)$ for $-\infty < n < \infty$ in order to evaluate a single value of $X_c(t)$. Therefore, some realizable approximation to $\hat{h}_1(t)$ must be used. Figure 2.7 illustrates an example of an impulse response for a realizable reconstruction or interpolating lowpass filter, $\hat{h}(t)$, that extends over a finite number of samples of $x(n)$. In this figure we show plots of $X_c(t)$ (bottom figure) and $x(n)$, and the range of $h(t-nT)$ evaluated in the region of the n_0 th sample [Le., at $t = n_0T$ (top figure)]. To the extent that the frequency response of the actual lawpass filter approximates the ideal lawpass filter, the reconstruction error of $X_c(t)$ can be kept small.

2.2.5 Summary of the Implications of the Sampling Theorem

The main result of the sampling theorem is that there is a minimum rate (related directly to the bandwidth of the signal at which a signal can be sampled and for which theoretically exact reconstruction of the signal is possible from its samples. If the signal is sampled below this minimum rate, then distortions, in the form of spectral fold over or *aliasing* [e.g., see figure 2.4(c)], occur from which no recovery is generally possible.

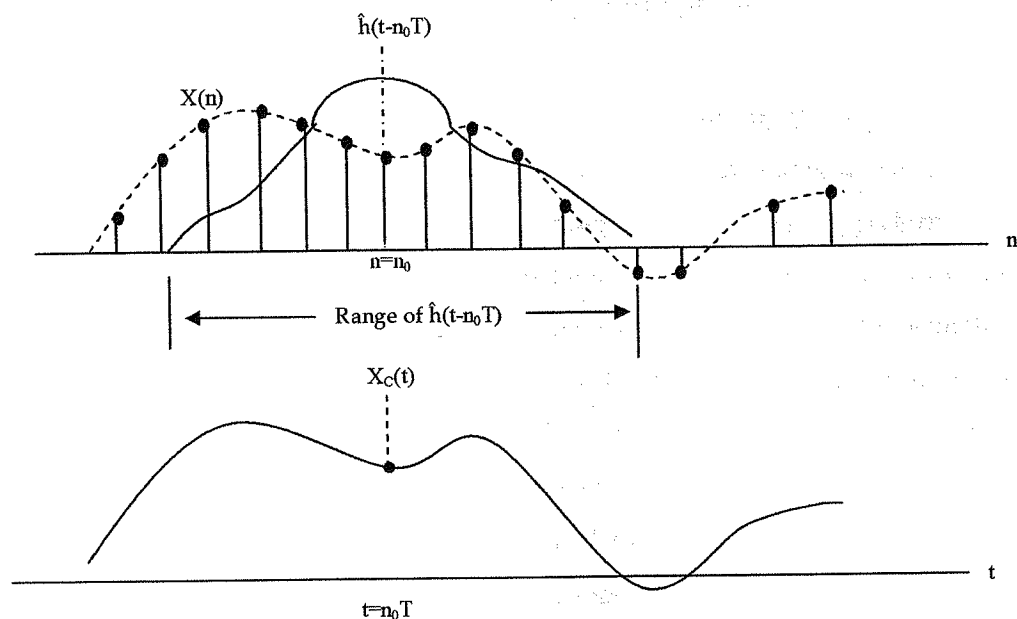


Figure 2.7 Illustration of Reconstruction of a Band-limited Signal from its Samples using a nonideal Finite Duration Impulse Response Lowpass Filter.

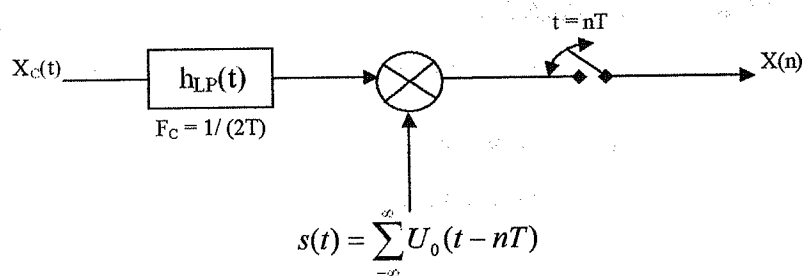


Figure 2.8 Representation of a Practical Sampling System with Prefiltering to Avoid Aliasing.

Thus to ensure that the conditions of the sampling theorem are met for a given application, the signal to be sampled is generally first filtered by a lowpass filter whose

cutoff frequency is less than (or equal to) half the sampling frequency. Such a filter is often called an *anti-aliasing prefilter* because its purpose is to guarantee that no aliasing occurs due to sampling. Thus the standard representation of a system for sampling a signal (analog-to-digital conversion) is as shown in figure 2.8. We will see in the following sections that a lowpass filter of the type shown in figure 2.8 is required for almost all sampling rate conversion systems.

2.3 Sampling Rate Conversion - An Analog Interpretation

The process of sampling rate conversion is one of converting the sequence $x(n)$ obtained from sampling $X_c(t)$ with a period T , to another sequence $y(m)$ obtained from sampling $X_c(t)$ with a period T' . The most straightforward way to perform this conversion is to reconstruct $X_c(t)$ (or the lowpass filtered version of it) from the samples of $x(n)$ and then resample $X_c(t)$ (assuming that it is sufficiently band-limited for the new sampling rate) with period T' to give $y(m)$. The processing involved in this procedure is illustrated in figure 2.9. Figure 2.10 shows typical waveforms which illustrate the signal processing involved in implementing the system of figure 2.9. Because $\hat{h}(t)$, the impulse response of the analog lowpass filter, is assumed to be of finite duration, the value of $x_c(t)$ at $t = m_o T'$ is determined *only* from the finite set of samples of $x(n)$ shown in part (a) of this figure. Thus for any m , the value of $y(m)$ can be obtained as

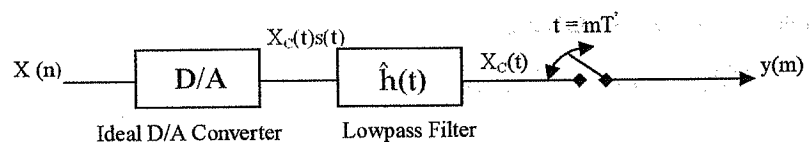


Figure 2.9 Conversion of a Sequence $x(n)$ to another Sequence $y(m)$ by Analog Reconstruction and Resampling.

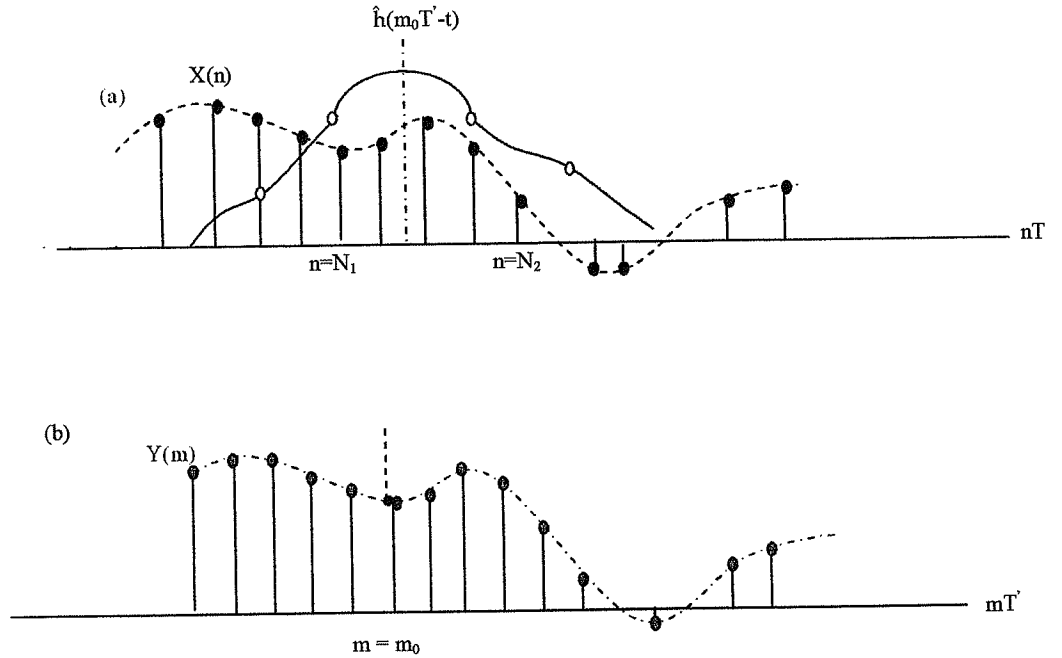


Figure 2.10 Typical Waveforms for Sampling Rate Conversion by Analog Reconstruction and Resampling.

$$y(m) = x_c(t) \big|_{t=mT'} = \sum_{n=N_1}^{N_2} x(n) \hat{h}(mT' - nT) \quad (2.26)$$

where N_1 and N_2 denote minimum and maximum of the range of values of n involved in the computation of $y(m)$. From equation (2.26) and figure (2.10) we see that only specific values of n and specific values of $\hat{h}(t)$ are used to generate $y(m)$, that is,

$$y(m) = x(N_1) \hat{h}(mT' - N_1 T) + \dots + x(N_2) \hat{h}(mT' - N_2 T) \quad (2.27)$$

The values of $\hat{h}(t)$ that are used to give $y(m)$ are spaced T apart in time. In effect the signal $x(n)$ samples (and weights) the impulse response $\hat{h}(t)$ to give $y(m)$. It is interesting to note that when $T' = T$, the form of equation (2.26) reduces to that of the familiar discrete convolution

$$y(m) = \sum_n x(n) \hat{h}((m-n)T) \quad (2.28)$$

The limits on the summation of equation (2.26) are determined from the range of values for which $\hat{h}(t)$ is nonzero. If we assume that $\hat{h}(t)$ is zero for $t < t_1$ and $t > t_2$, that is,

$$\hat{h}(t) = 0, \quad t > t_2, t < t_1 \quad (2.29)$$

this leads to the result

$$\hat{h}(mT' - nT) = 0, \quad mT' - nT > t_2, mT' - nT < t_1 \quad (2.30)$$

or (see figure 2.10)

$$n < \frac{mT' - t_2}{T} \quad (2.31a)$$

$$n > \frac{mT' - t_1}{T} \quad (2.31b)$$

Thus by integrizing equations (2.31) we get

$$N_1 = \left\lceil \frac{mT' - t_2}{T} \right\rceil \quad (2.32a)$$

$$N_2 = \left\lfloor \frac{mT' - t_1}{T} \right\rfloor \quad (2.32b)$$

It can be seen from equations (2.32) that the set of samples $x(n)$ involved in the determination of $y(m)$ is a complicated function of the sampling periods T and T' , the endpoints of the filter t_1 and t_2 , and the sample m being determined.

Figure 2.11 illustrates this effect for the case $T' = T/2$, and for two impulse response durations, $t_2 = -t_1 = 2.3T$ and $t_2 = -t_1 = 2.8T$. As shown in parts (a) and (b), the determination of $y(m)$ for m even for both $t_2 = -t_1 - 2.3T$ [part (a)] and $t_2 = -t_1 - 2.8T$ [part (b)] involves the identical set of samples of $x(n)$. However, the determination of $y(m)$ for m odd involves different sets of samples of $x(n)$ for $t_2 = -t_1 - 2.3T$ [part (c)] than for $t_2 = -t_1 - 2.8T$ [part (d)].

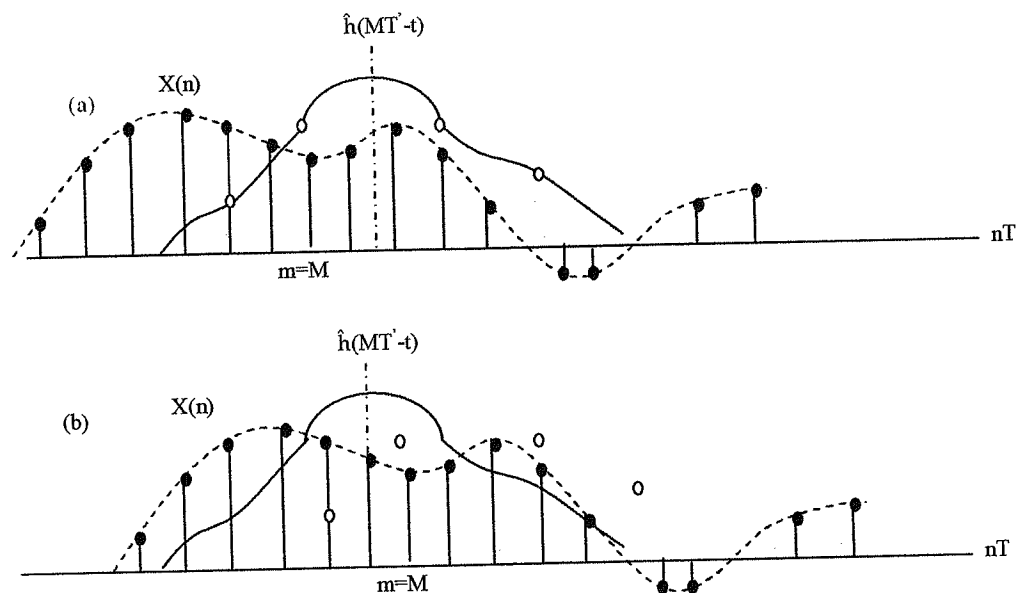


Figure 2.11 Examples Showing the Samples of $x(n)$ Involved in the Computation of $y(m)$ for two Different Impulse Response Durations and for even and odd Samples of $y(m)$ for a 2-to-1 Increase in the Sampling Rate.

A second important issue in the implementation described above involves the set of samples of $h(t)$ used in the determination of $y(m)$. For each value of m , a distinct set of samples of $h(t)$ are used to give $y(m)$. Figure 2.12 illustrates this point for the case $T' = T/2$ (i.e., a 2-to-1 increase in the sampling rate). Figure 2.12(a) shows $x(n)$, $\hat{h}(m_e T' - t)$, and $y(m)$ for the computation of $y(m_e)$, where m_e is an even integer, and figure 2.12(b) shows the same waveforms for $m_o = m_e + 1$ (i.e., an odd value of m). It can be seen that two distinctly different sets of values of $h(t)$ are involved in the computation of $y(m)$ for even and odd m . For the case $T' = 2T$ (i.e., a 2-to-1 decrease in the sampling rate), the same set of samples of $\hat{h}(t)$ are used to determine *all* output samples $y(m)$.

By introducing the change of variables

$$k = \left\lfloor \frac{mT'}{T} \right\rfloor - n \quad (2.33)$$

the form of equation (2.26) can be modified to another form that more explicitly reveals

the nature of the indexing problem associated with the evaluation of $y(m)$ in the sampling rate conversion process described above. This form will be used extensively in later sections. Applying equation (2.33) to equation (2.26) gives the expression

$$y(m) = \sum_{k=K_1}^{K_2} x \left[\left\lfloor \frac{mT'}{T} \right\rfloor - k \right] \hat{h} \left[mT' - \left\lfloor \frac{mT'}{T} \right\rfloor T + kT \right] \quad (2.34)$$

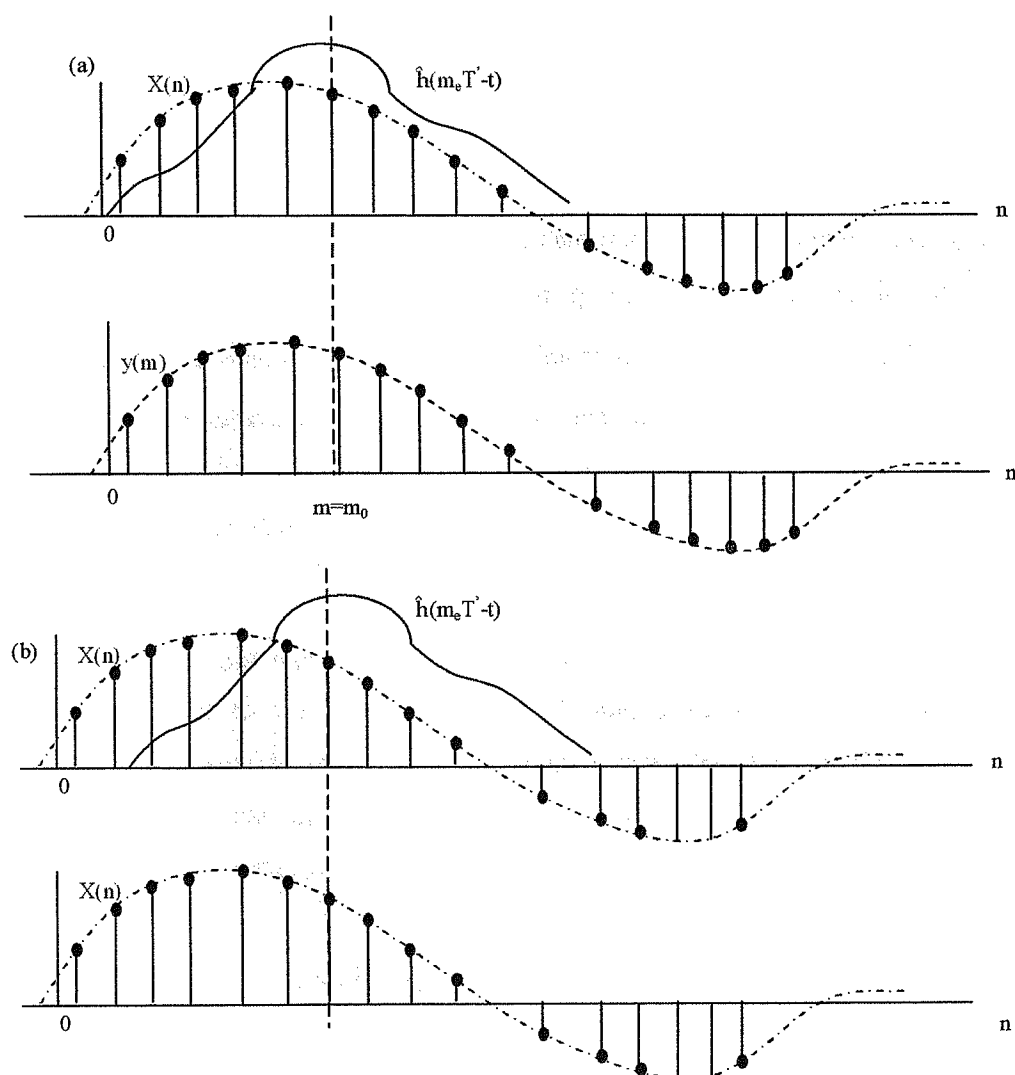


Figure 2.12 Examples Showing the Samples of $\hat{h}(t)$ Involved in the Computation of: (a) Even Values of $y(m)$, and; (b) Odd Values of $y(m)$ for a 2-to-1 Increase in the Sampling Rate.

And rearranging terms gives the desired form

$$y(m) = \sum_{k=K_1}^{K_2} \hat{h}((k + \delta_m)T) x \left[\left\lfloor \frac{mT'}{T} \right\rfloor - k \right] \quad (2.35)$$

where δ_m is defined as

$$\delta_m = \frac{mT'}{T} - \left\lfloor \frac{mT'}{T} \right\rfloor \quad (2.36)$$

It is clear that δ_m corresponds to the difference of a number mT'/T and its next lowest integer,

$$0 \leq \delta_m < 1 \quad (2.37)$$

Thus from equation (2.35) it can be seen that the determination of a sample value $y(m)$ involves samples of $\hat{h}(t)$ spaced T apart and offset by the fractional sample time $\delta_m T$, where δ_m varies as a function of m . It is also interesting to note that when $T' = T$, equation (2.35) again reduces to a familiar convolutional form

$$y(m) = \sum_k \hat{h}(KT) x(m - k) \quad (2.38)$$

Figure 2.13 depicts the samples of $\hat{h}(t)$ and $x(n)$ involved in determining $y(m)$ based on equation (2.35). As in the earlier interpretation of equation (2.26), it is seen that the finite range of $\hat{h}(t)$ restricts the number of samples $x(n)$ that are actually used in determining $y(m)$. By again applying the conditions of equation (2.29) it can be shown that the limits on the summation, K_1 and K_2 , can be determined from the condition

$$\hat{h}((k + \delta_m)T) = 0, (k + \delta_m)T > t_2, (k + \delta_m)T < t_1 \quad (2.39)$$

or

$$k > \frac{t_2}{T} - \delta_m \quad (2.40a)$$

$$k < \frac{t_1}{T} - \delta_m \quad (2.40b)$$

and integerizing equations (2.40) gives

$$K = \left\lceil \frac{t_1}{T} - \delta_m \right\rceil = \left\lceil \frac{t_1}{T} - \frac{mT'}{T} \right\rceil + \left\lfloor \frac{mT'}{T} \right\rfloor \quad (2.41a)$$

$$K = \left\lceil \frac{t_2}{T} - \delta_m \right\rceil = \left\lceil \frac{t_2}{T} - \frac{mT'}{T} \right\rceil + \left\lfloor \frac{mT'}{T} \right\rfloor \quad (2.41b)$$

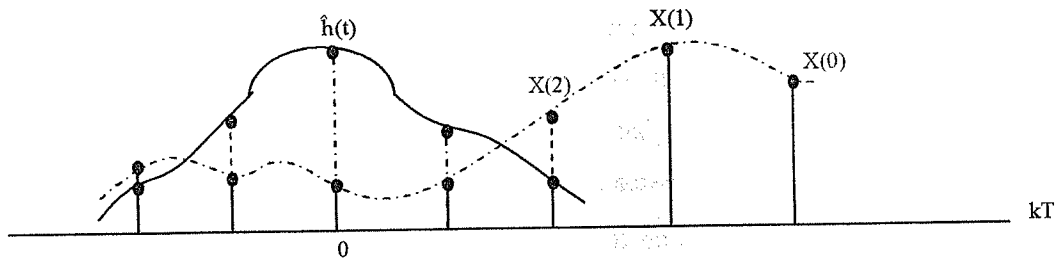


Figure 2.13 Alternative Form for Sampling Rate Conversion Process Showing Samples of $\hat{h}(t)$ and $x(n)$ Involved in Determining $y(m)$.

2.4 Decimation and Interpolation of Bandpass Signals

2.4.1 The Sampling Theorem Applied to Bandpass Signals

In the preceding sections it was assumed that the signals that we are dealing with are lowpass signals and therefore the filters required for decimation and interpolation are lowpass filters which preserve the baseband signals of interest. In many practical systems, however, it is often necessary to deal with bandpass signals, as well as lowpass signals. In this section we show how the concepts of decimation and interpolation can be applied to systems in which bandpass signals are present.

Figure 2.14(a) shows an example of the discrete Fourier transform of a digital bandpass signal $S(e^{j2\pi fT})$ which contains spectral components only in the frequency range $f_1 < |f| < f_1 + f_\Delta$. If we apply directly the concepts of lowpass sampling F_w , necessary to represent this signal must be twice that of the highest-frequency component in $S(e^{j2\pi fT})$, that is, $F_w \geq 2(f_1 + f_\Delta)$. Alternatively, let S^+ denote the component of $S(e^{j2\pi fT})$ associated with $f > 0$ and S^- denote the component of $S(e^{j2\pi fT})$ associated with $f < 0$, as seen in fig. 2.14. Then, by lowpass translating (modulating) S^+ to the band 0 to f_Δ and S^- to the band $-f_\Delta$ to 0, as illustrated by figure 2.14(b), it is seen that a new signal $S_\gamma(e^{j2\pi fT})$ can be generated which is "equivalent" to $S(e^{j2\pi fT})$ in the sense that $S(e^{j2\pi fT})$ can uniquely be reconstructed from $S_\gamma(e^{j2\pi fT})$ by the inverse process of bandpass translation. [Actually, it is seen that $S(e^{j2\pi fT})$ is the "single-sideband" modulated version of $S_\gamma(e^{j2\pi fT})$]. By applying concepts of lowpass sampling to $S_\gamma(e^{j2\pi fT})$, however, it can be seen that the sampling frequency necessary to represent this signal is now $F_\Delta \geq 2f_\Delta$, which can be much lower than the value of F_w specified above (if $f_1 \gg f_\Delta$). Thus it is seen that by an appropriate combination of modulation followed by lowpass sampling, any real bandpass signal with (positive frequency) bandwidth f_Δ can be uniquely sampled at a rate $F_\Delta \geq 2f_\Delta$ (i.e., such that the original bandpass signal can be uniquely reconstructed from the sampled representation)

In practice, there are many ways in which the combination of modulation and sampling described above can be carried out. In this section we consider three specific methods in detail: integer-band sampling, quadrature modulation, and single-sideband modulation (based on a quadrature implementation).

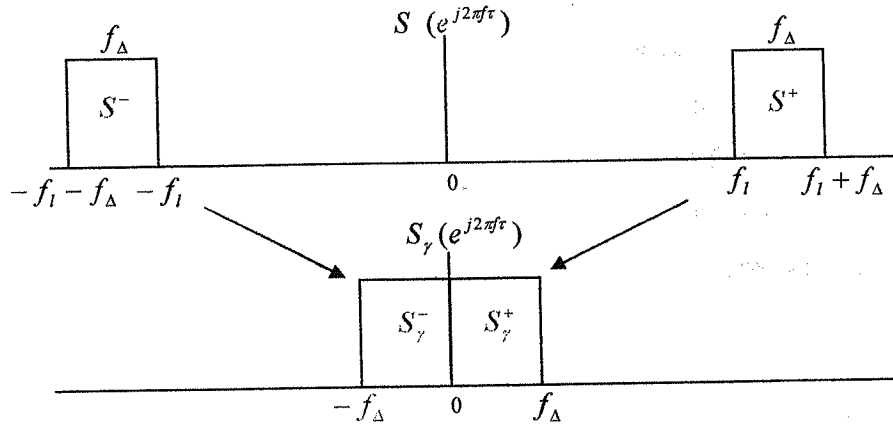


Figure 2.14 Bandpass Signal and its Lowpass Translated Representation.

2.4.2 Integer-Band Decimation and Interpolation

Perhaps the simplest and most direct approach to decimating or interpolating digital bandpass signals is to take advantage of the inherent frequency translating (i.e., aliasing or imaging) properties of decimation and interpolation. Sampling and sampling rate conversion can be viewed as a modulation process in which the spectrum of the digital signal contains periodic repetitions of the baseband signal (images) spaced at harmonics of the sampling frequency. This property can be used to advantage when dealing with bandpass signals by associating the bandpass signal with one of these images instead of with the baseband.

Figure 2.15(a) illustrates an example of this process for the case of decimation by the integer factor M . The input signal $x(n)$ is first filtered by the bandpass filter $h_{BP}(n)$ to isolate the frequency band of interest. The resulting bandpass signal, $x_{BP}(n)$, is then directly reduced in sampling rate by an M -sample compressor giving the final output, $y(m)$. It is seen that this system is identical to that of the integer lowpass decimator, with the exception that the filter is a bandpass filter instead of a lowpass filter. Thus the

output signal $Y(e^{jw'})$ can be expressed as

$$Y(e^{jw'}) = \frac{1}{M} \sum_{l=0}^{M-1} H_{BP}(e^{j(w'-2\pi l)/M}) X(e^{j(w'-2\pi l)/M}) \quad (2.42)$$

From equation (2.42) it is seen that $Y(e^{jw'})$ is composed of M aliased components of $X(e^{jw'})H_{BP}(e^{jw'})$ modulated by factors of $2\pi l/M$. The function of the filter $H_{BP}(e^{jw'})$ is to remove (attenuate) all aliasing components except those associated with the desired band of interest. Since the modulation is restricted to values of $2\pi l/M$, it can be seen that only specific frequency bands are allowed by this method. As a consequence the choice of the filter $H_{BP}(e^{jw'})$ is restricted to approximate one of the M ideal characteristics

$$\tilde{H}_{BP}(e^{jw}) = \begin{cases} 1, & k \frac{\pi}{M} < |w| < (k+1) \frac{\pi}{M} \\ 0, & \text{otherwise} \end{cases} \quad (2.43)$$

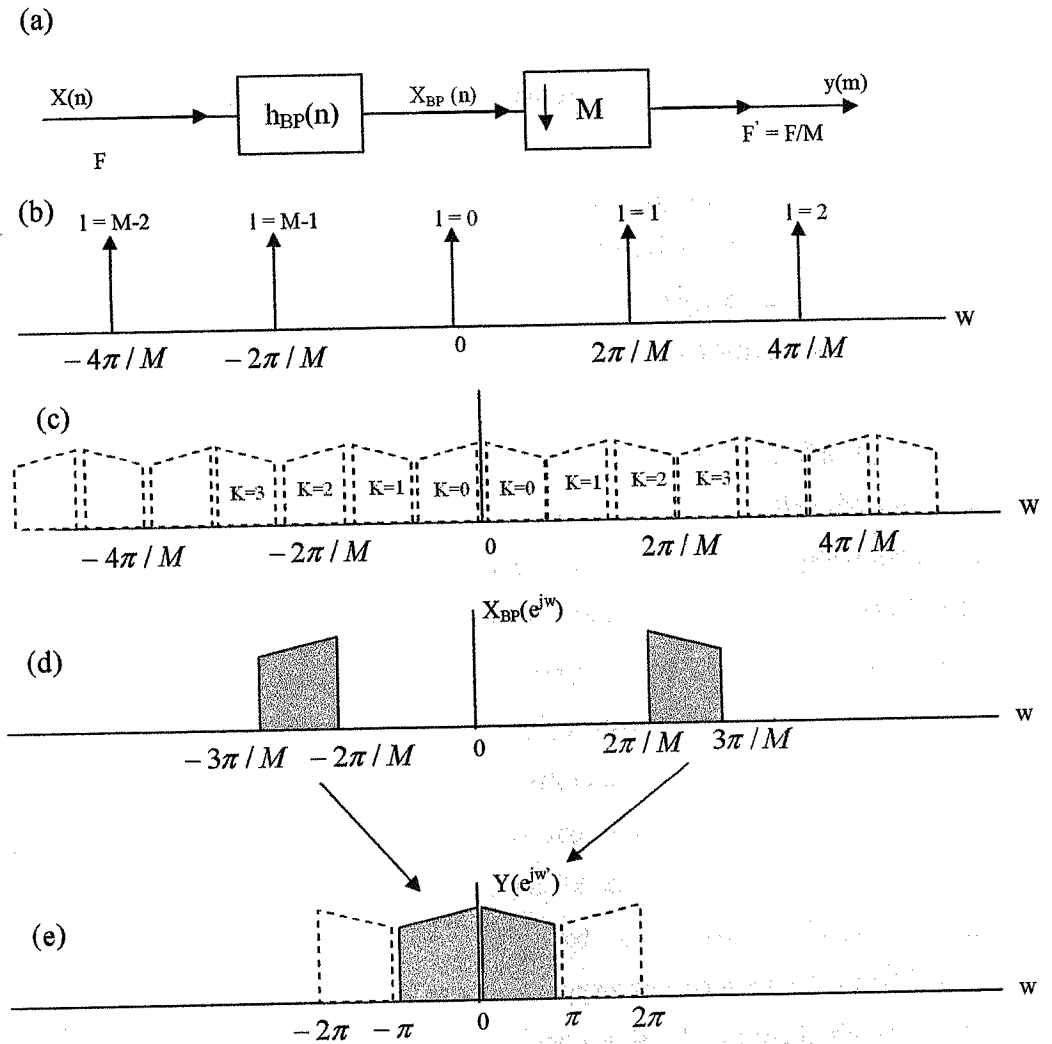


Figure 2.15 Integer-band Decimation and a Spectral Interpretation for the $k = 2$.
 where $k = 0, 1, 2, \dots, M-1$; that is, $H_{BP}(e^{jw})$ is restricted to bands $w = k\pi/M$ to
 $w = (k+1)\pi/M$, where π/M is the bandwidth.

Figure 2.15(b) to (e) illustrates this approach. Figure 2.15(b) shows the M possible modulating frequencies which are a consequence of the M -to-1 sampling rate reduction; that is, the digital sampling function (a periodic train of unit samples spaced M samples apart) has spectral components spaced $2\pi/M$ apart. Figure 2.15(c) shows the "sidebands" that is associated with these spectral components, which correspond to the

M choices of bands as defined by equation (2.43). They correspond to the bands that are aliased into the baseband of the output signal $Y(e^{j\omega'})$ according to equation (2.42). [As seen by equations (2.42) and (2.43) and figures 2.15(b) and 2.15(c), the relationship between k and l is nontrivial.]

Figure 2.15(d) illustrates an example in which the $k = 2$ band is used, such that $X_{BP}(e^{j\omega})$ is band-limited to the range $2\pi/M < |\omega| < 3\pi/M$. Since the process of sampling rate compression by M to 1 corresponds to a convolution of the spectra of $X_{BP}(e^{j\omega'})$ [Figure 2.15(d)] and the sampling function [Figure 2.15(b)], this band is lowpass translated to the baseband of $Y(e^{j\omega'})$ as seen in Figure 2.15(e). Thus the processes of modulation and sampling rate reduction are achieved simultaneously by the M -to-1 compressor.

Figure 2.16 illustrates a similar example for the $k = 3$ band such that $X_{BP}(e^{j\omega})$ is band-limited to the band $3\pi/M < |\omega| < 4\pi/M$. In this case it is seen that the spectrum is inverted in the process of lowpass translation. If the noninverted representation of $y(m)$ is desired, it can easily be achieved by modulating $y(m)$ by $(-1)^m$ [i.e., $\hat{y}(m) = (-1)^m y(m)$], which corresponds to inverting the signs of odd samples of $y(m)$. In general, bands associated with even values of k are directly lowpass translated to the baseband of $Y(e^{j\omega'})$, whereas bands associated with odd values of k are translated and inverted [see figure 2.15(c)]. This is a consequence of the fact that even numbered bands (k even) correspond to "upper sidebands" of the modulation frequencies $2\pi/M$, whereas odd-numbered bands (k odd) correspond to "lower sidebands" of the modulation frequencies (e.g., the $k = 2$ band is an upper sideband for $l = 2$ and $l = M - 1$ and the $k = 3$ band is a lower sideband for $l = 2$ and $l = M - 2$, as seen in figure 2.15).

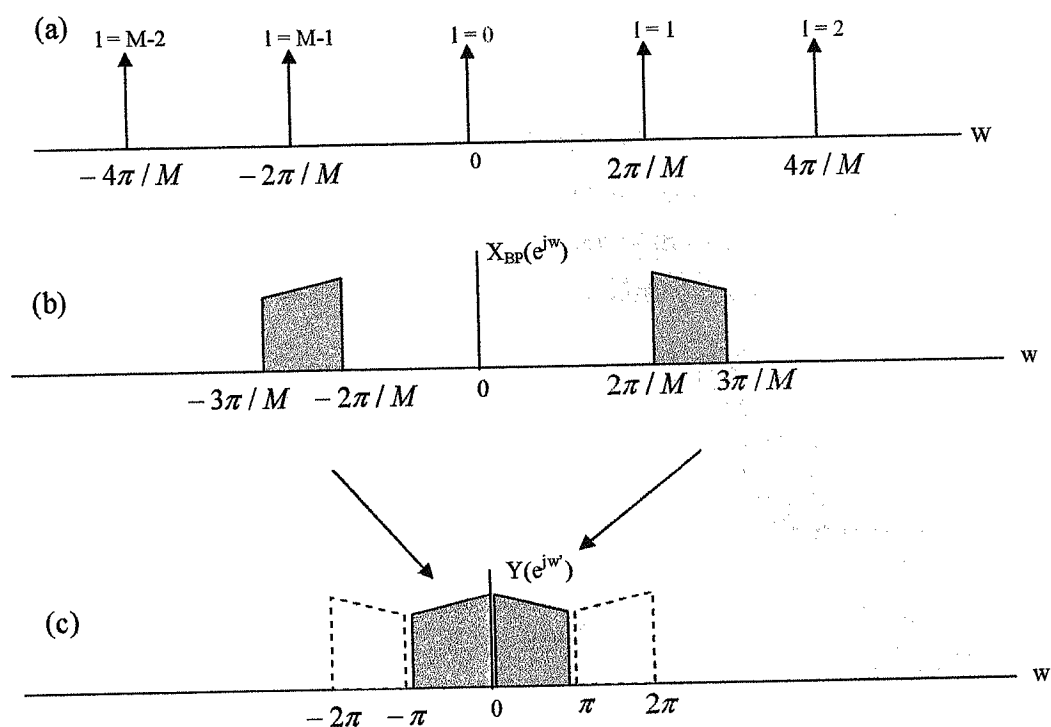


Figure 2.16 Spectral Interpretation of Integer-band Decimation for the Band $k = 3$.

Figure 2.17 illustrates an example in which the integer-band constraints of equation (2.43) are not satisfied. It is seen that nonrecoverable aliasing occurs in the baseband of $Y(e^{jw'})$, and therefore the signal $X_{BP}(e^{jw'})$, when integer-band constraints are violated, cannot be reconstructed from its decimated version.

The process of integer-band interpolation is the inverse to that of integer-band decimation; that is, it performs the reconstruction (interpolation), of a bandpass Figure 2.17 illustrates an example in which the integer-band constraints of equation (2.43) are not satisfied. It is seen that nonrecoverable aliasing occurs in the baseband of $Y(e^{jw'})$, and therefore the signal $X_{BP}(e^{jw'})$, when integer-band constraints are violated, cannot be reconstructed from its decimated version.

Figure 2.18(a) illustrates this process. The input signal, $x(n)$, is sampling rate expanded by L [by inserting $L-1$ zero-valued samples between each pair of samples of $x(n)$] to produce the signal $w(m)$. From the discussion of integer interpolation, it is seen

that the spectrum of $w(m)$ can be expressed as

$$W(e^{jw'}) = X(e^{jw'L}) \quad (2.44)$$

and it corresponds to periodically repeated images of the baseband of $X(e^{jw})$ centered at the harmonics $w' = 2\pi l / L$ [as depicted in figure 2.17(b) and (c)]. A bandpass filter $h_{BP}(m)$ is then used to select the appropriate image of this signal. It can be seen that to obtain the k th image, the bandpass filter must approximate the ideal characteristics

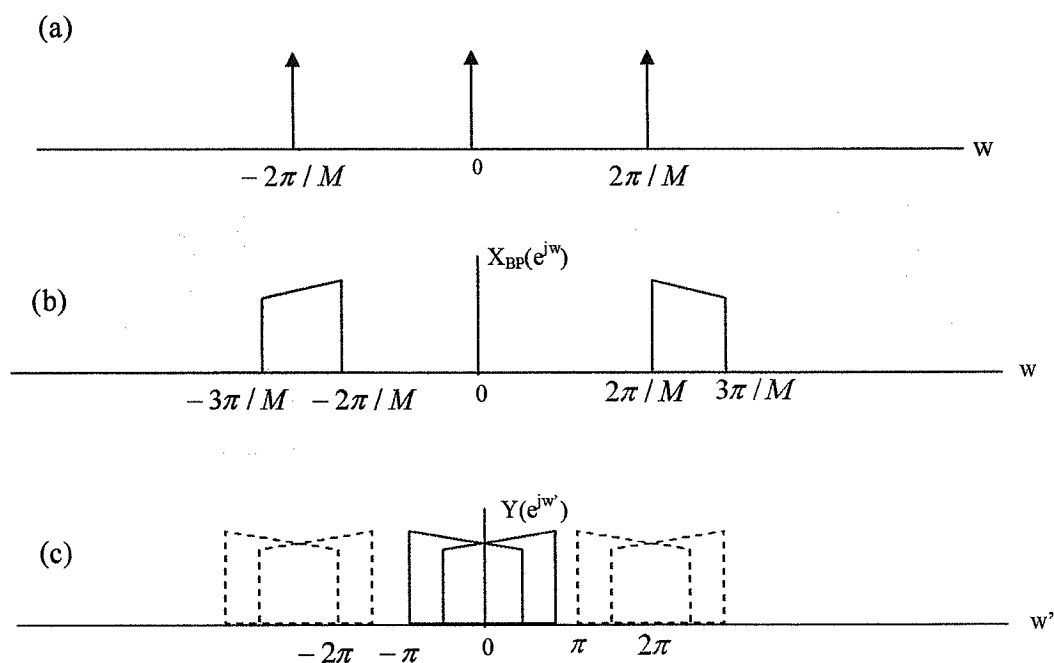


Figure 2.17 Spectral Interpretation of Integer-band Decimation when Integer-band Constraints are violated.

$$\tilde{H}_{BP}(e^{jw'}) = \begin{cases} L, & k\frac{\pi}{L} < |w'| < (k+1)\frac{\pi}{L} \\ 0, & \text{otherwise} \end{cases} \quad (2.45)$$

where $k = 0, 1, 2, \dots, L-1$. Figure 2.18(d) shows an example of the output spectrum of the bandpass signal $Y(e^{jw'})$ for the $k = 2$ and figure 2.18(e) illustrates an example for the

$k = 3$ band. As in the case of integer-band decimation, it is also seen that the spectrum of the resulting bandpass signal $x(n)$ can first be modulated by $(-1)^n$, which inverts the spectrum of the baseband and consequently the bandpass signal.

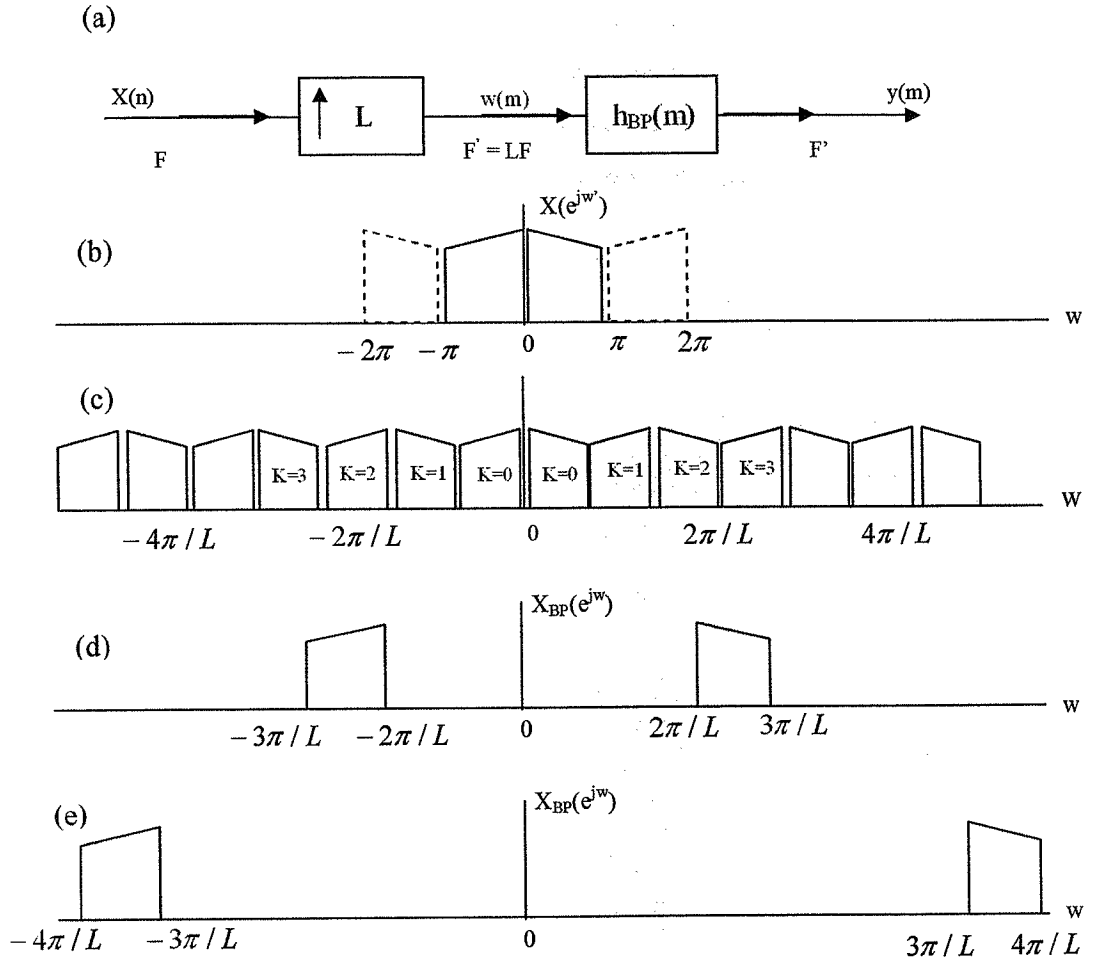


Figure 2.18 Spectral Interpretation of Integer-band Interpolation of Bandpass Signals.

2.5 Summary

This chapter has been directed at the basic concepts of digital sampling of analog lowpass and bandpass signals and at the fundamentals of converting the sampling rates of sampled signals by a direct digital-to-digital approach. Basic interpretations of the operations of sampling rate conversion have been given in terms of their analog equivalents and in terms of modulation concepts.

3. DIGITAL FILTER BANK IN MULTIRATE SIGNAL PROCESSING

3.1 Overview

There are applications, as in the case of a spectrum analyzer, where it is desirable to separate a signal into a set of subband signals occupying, usually nonoverlapping, portions of the original frequency band. In other applications, it may be necessary to combine many such subband signals into a single composite signal occupying the whole Shannon range [15].

3.2 Definitions

The digital filter bank is a set of digital bandpass filters with either a common input or summed output, as shown in figure 3.1. The structure of figure 3.1(a) is called an M-band analysis filter bank with the subfilters $H_k(z)$ known as the analysis filter. It is used to decompose the input signal $x[n]$ into a set of M subband signals $v_k[n]$ with each subband signal occupying a portion of the original frequency band. (The signal is being 'analyzed' by being separated into a set of narrow spectral bands.)

The dual of the above operation, whereby a set of subband signals $\hat{v}_k[n]$ (typically belonging to continuous frequency bands) is combined into one signal $y[n]$ is called a synthesis filter bank.

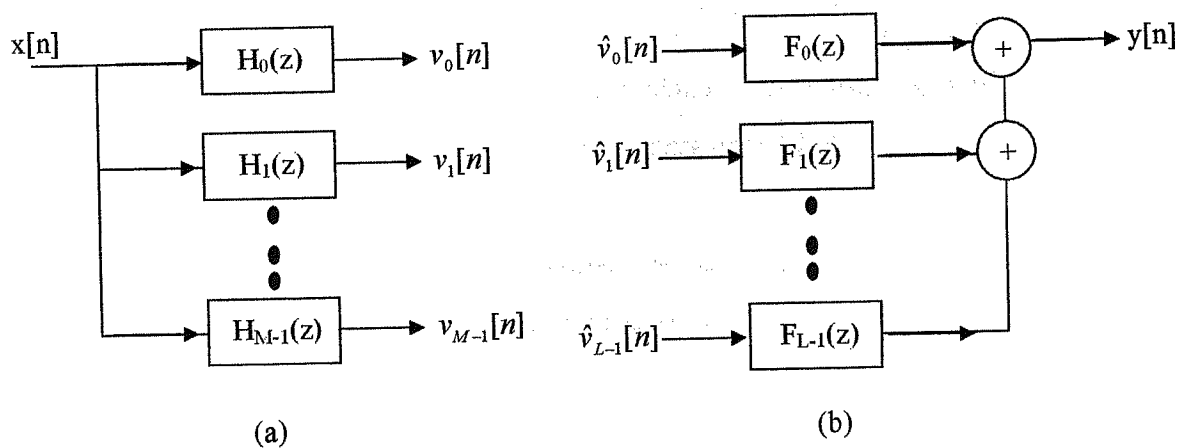


Figure 3.1 (a) Analysis Filter Bank, and (b) Synthesis Filter Bank.

3.3 Uniform DFT Filter Banks

We now outline a simple technique for the design of a class of filter banks with equal pass-band widths. Let $H_0(z)$ represent a causal low-pass digital filter with an impulse response $h_0[n]$:

$$H_0(z) = \sum_{n=1}^{\infty} h_0[n]z^{-n} \quad (3.1)$$

which we assume to be an IIR filter without any loss of generality. Let us now assume that $H_0(z)$ has its pass-band edge ω_p and stop-band edge ω_s around π/M , where M is some arbitrary integer, as indicated in figure 3.2(a). Now, consider the transfer function $H_k(z)$ whose impulse response $h_k[n]$ is defined to be

$$h_k[n] = h_0[n]W_M^{-kn}, \quad k = 0, 1, \dots, M-1 \quad (3.2)$$

where $W_M = e^{-j2\pi/M}$, thus

$$H_k(z) = \sum_{n=0}^{\infty} h_k[n]z^{-n} = \sum_{n=0}^{\infty} h_0[n](zW_M^k)^{-n}, \quad k = 0, 1, \dots, M-1 \quad (3.3)$$

i.e.,

$$H_k(z) = H_0(zW_M^k), \quad k = 0, 1, \dots, M-1 \quad (3.4)$$

with a corresponding frequency response ($Z = e^{j\omega}$):

$$H_k(e^{j\omega}) = H_0\left(e^{j\left(\omega - \frac{2\pi k}{M}\right)}\right), \quad k = 0, 1, \dots, M-1 \quad (3.5)$$

In other words, the frequency response of $H_k(z)$ is obtained by shifting the response of $H_0(z)$ to the right, by an amount $2\pi k/M$. The response of $H_1(z)$, $H_2(z)$,, $H_{M-1}(z)$

are shown in figure 3.2(b). Note that the corresponding impulse responses $h_k[n]$ are, in general, complex and hence $|H_k(e^{j\omega})|$ does not necessarily exhibit symmetry with respect to zero frequency. Figure 3.2(b) therefore represents the responses of $M-1$ filters $H_1(z)$, $H_2(z)$, ..., $H_{M-1}(z)$, which are uniformly shifted versions of the response of the basic prototype filter $H_0(z)$ of figure 3.2(a).

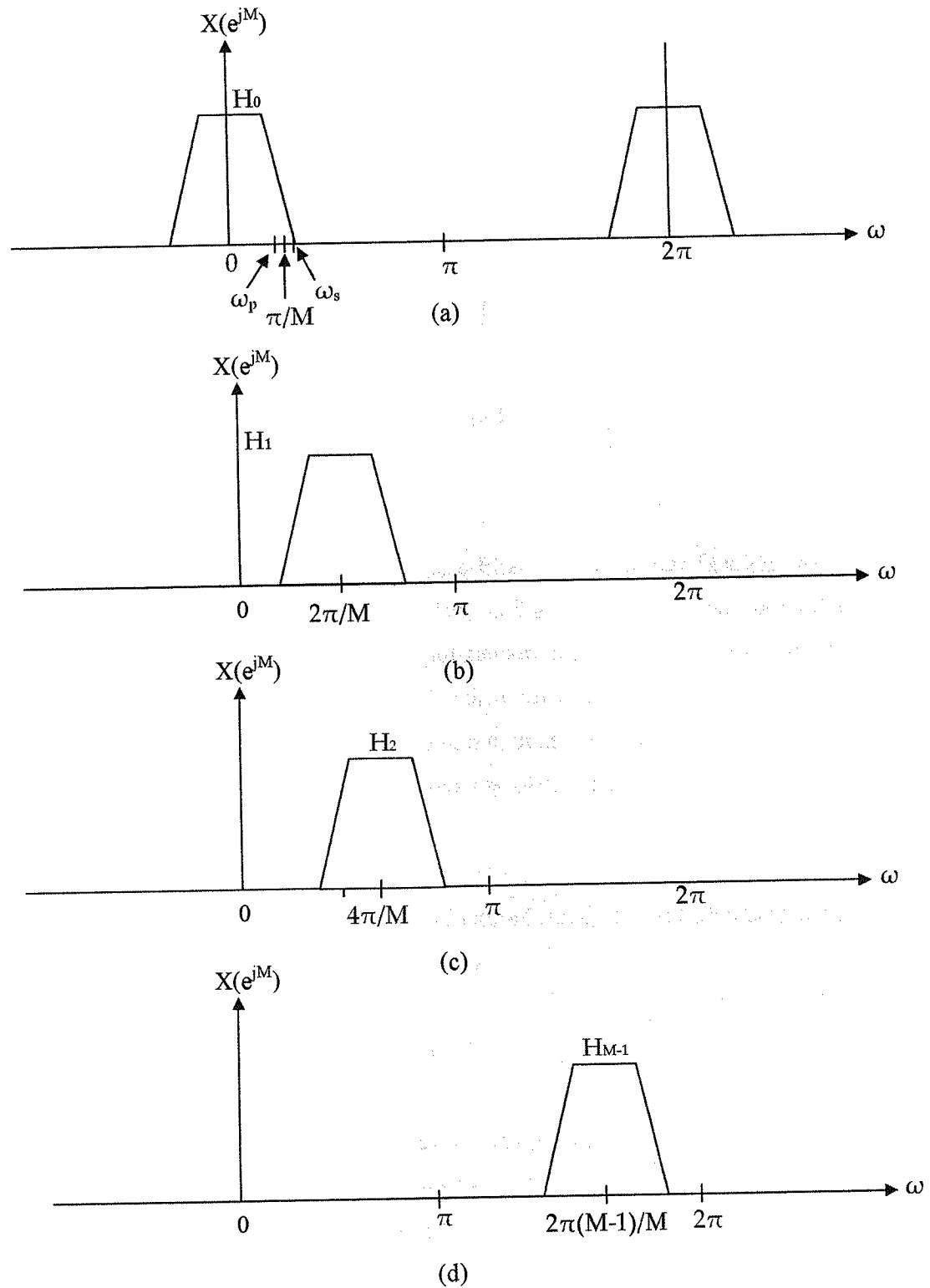


Figure 3.2 The Bank of M Filters $H_k(z)$ with Uniformly Shifted Frequency Response.

The M filters $H_k(z)$ defined by equation (3.4) could be used as the analysis filters in the analysis filter bank of figure 3.1(a) or as the synthesis filters $F_k(z)$ in the synthesis filter bank of figure 3.1(b).

Since the set of magnitude responses $|H_k(e^{jw})|$, $k = 0, 1, \dots, M-1$, are uniformly shifted versions of a basic prototype $|H_0(e^{jw})|$, i.e.,

$$|H_k(e^{jw})| = |H_0(e^{j[w - (2\pi k/M)]})| \quad (3.6)$$

the filter bank obtained is called a *uniform filter bank*.

3.3.1 Nyquist (Lth Band) Filters

We introduce a special type of low-pass filter with a transfer function that by design has certain zero valued coefficients. Due to the presence of these zero-valued coefficients, these filters are by nature computationally more efficient than other low-pass filters of the same order. In addition, when used as interpolator filters, they preserve the nonzero samples of the up-sampler output at the interpolator output. These filters, called *Lth* band filters or Nyquist filters are often used both in single rate and multirate signal processing.

Consider the factor-of- L interpolator of figure 3.15(a). The relation between the output and the input of the interpolator is given by

$$Y(z) = H(z)X(z^L) \quad (3.7)$$

If the interpolation filter $H(z)$ is realized in the L band polyphase form, then we have

$$H(z) = E_0(z^L) + z^{-1}E_1(z^L) + z^{-2}E_2(z^L) + \dots + z^{-(L-1)}E_{L-1}(z^L)$$

Assume that the k th polyphase component of $H(z)$ is a constant, i.e., $E_k(z) = \alpha$:

$$H(z) = E_0(z^L) + z^{-1}E_1(z^L) + \dots + z^{-(k-1)}E_{k-1}(z^L) + \alpha z^{-k} + z^{-(k+1)}E_{k+1}(z^L) + \dots + z^{-(L-1)}E_{L-1}(z^L) \quad (3.8)$$

Then we can express $Y(z)$ as

$$Y(z) = \alpha z^{-k} X(z^L) + \sum_{\substack{l=0 \\ l \neq k}}^{L-1} z^{-l} E_l(z^L) X(z^L) \quad (3.9)$$

As a result, $y[Ln] = \alpha x[n-k]$, i.e., the input samples appear at the output without any distortion at $n = k, k \pm L, k \pm 2L, \dots$, whereas the in-between $(L-1)$ samples determined by interpolation.

A filter with the above property is called a Nyquist filter or an L th band filter and its impulse response has many zero-valued samples, making it computationally very attractive. For example, the impulse response of the L th band filter obtained for $k = 0$ satisfies the following conditions:

$$h[Ln] = \begin{cases} \alpha, & n = 0 \\ 0, & \text{otherwise} \end{cases} \quad (3.10)$$

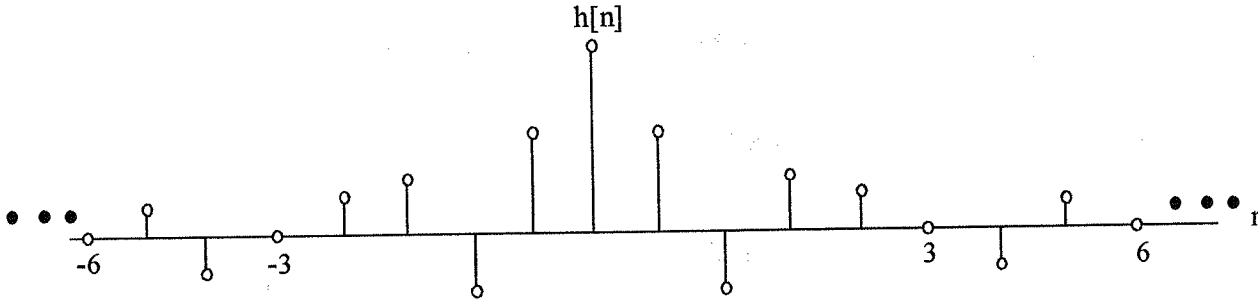


Figure 3.3 The Impulse Response of a Typical Third-band Filter.

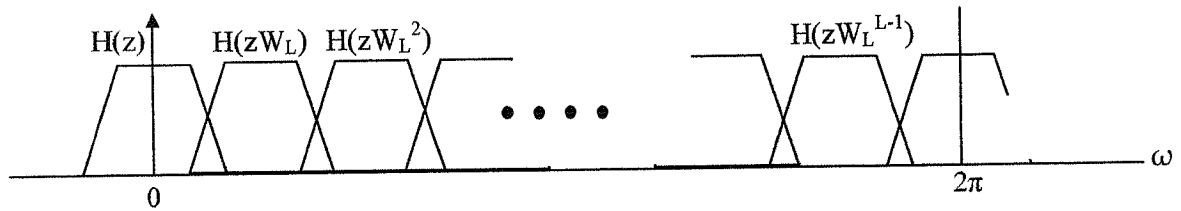


Figure 3.4 Frequency Responses of $H(zW_L^k)$ for $k = 0, 1, \dots, L-1$.

Figure 3.3 shows a typical impulse response of a third-band filter ($L=3$). If $H(z)$ satisfies equation (3.8) with $k = 0$, i.e., $H(z) = \alpha$, that it can be shown that

$$\sum_{k=0}^{L-1} H(zW_L^k) = L\alpha = 1 \quad (\text{assuming } \alpha = 1/L) \quad (3.11)$$

Since the frequency response $H(zW_L^k)$ is the shifted version $|H(e^{j(w-(2\pi k/L))})|$ of $H(e^{jw})$, the sum of all of these L uniformly shifted version of $H(e^{jw})$ add up to a constant (see figure 3.4). L th band filters can be either FIR or IIR filters [10].

3.3.2 Half-Band Filters

An L th band filter for $L = 2$ is called a half-band filter. From equation (3.8) the transfer function of a half-band filter is thus given by

$$H(z) = \alpha + z^{-1}E_1(z^2) \quad (3.12)$$

with its impulse response satisfying equation (3.10) with $L = 2$. The condition on the frequency response given by equation (3.12) reduces to

$$H(z) + H(-z) = 1 \quad (\text{assuming } \alpha = 1/2) \quad (3.13)$$

If $H(z)$ has real coefficients, then $H(-e^{jw}) = H(e^{j(\pi-w)})$, and equation (3.13) leads to

$$H(e^{jw}) + H(e^{j(\pi-w)}) = 1 \quad (3.14)$$

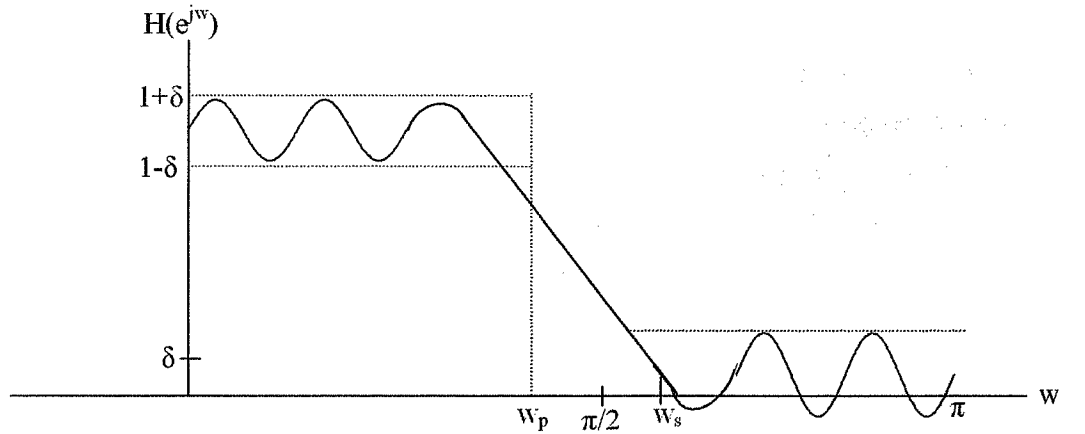


Figure 3.5 Frequency Response of a Zero-Phase Half-Band Filter.

The above equality implies that $H(e^{j((\pi/2)-\theta)})$ and $H(e^{j((\pi/2)+\theta)})$ add up to unity for all θ . In other words, $H(e^{j\omega})$ exhibits a symmetry with respect to the half-band frequency $\pi/2$, thus justifying the name 'half-band filter'. Figure (3.5) illustrates this symmetry for a half-band low-pass filter for which the pass-band and stop-band ripples are equal, i.e., $\delta_p = \delta$ and the pass-band and stop-band bandedges are symmetric with respect to $\pi/2$, i.e., $\omega_p + \omega_s = \pi$.

An important attractive property of the half-band filter is that about 50% of the coefficients of $h[n]$ are zero. This reduces the number of multiplication required in its implementation, making the filter computationally quite efficient.

For example, if $N = 101$, an arbitrary Type I FIR transfer function requires about 50 multipliers, where as a Type I half-band filter requires only about 25 multipliers.

An IIR half-band filter can be designed with linear phase. However, there is a constraint on its length. Consider a zero-phase half-band FIR filter for which $h[n] = ah^*[-n]$, with $|a| = 1$. Let the highest nonzero coefficient be $h[R]$. Then R is odd as a result of the conditions of equation (3.10). Therefore, $R = 2K + 1$ for some integer K . Thus the length of the impulse response $h[n]$ is restricted to be of the form $2R + 1 = 4K + 3$ [unless $H(z)$ is a constant].

3.4 Two-Channel Quadrature-Mirror Filter Bank

In many applications, a discrete-time signal $x[n]$ is first split into a number of subband signals $\{v_k[n]\}$ by means of analysis filter bank, the subband signals are then processed and finally combined by a synthesis filter bank resulting in an output signal $y[n]$. If the subband signals are *bandlimited* to frequency ranges much smaller than that of the original input signal, they can be down-sampled before processing. Because of the lower sampling rate, the processing of the down-sampled signal can be carried out more efficiently. After processing, these signals are up-sampled before being combined by the synthesis bank into a higher rate signal. The combined structure employed is called a quadrature-mirror filter (QMF) bank. If the down-sampling and the up-sampling factors are equal to the number of bands of the filter bank, then the output $y[n]$ can be made to retain some or all of the characteristics of the input $x[n]$ by properly choosing the filters in the structure. In this case, the filter bank is said to be a *critically*

sampled filter bank. The most common application of this scheme is in the efficient coding of a signal $x[n]$. Another possible application is in the design of an analog voice privacy system to provide secure telephone conversation.

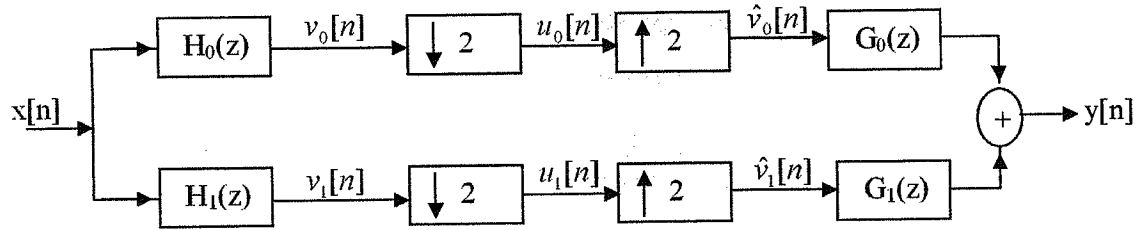


Figure 3.6 The Two-Channel Quadrature-Mirror Filter (QMF) Bank.

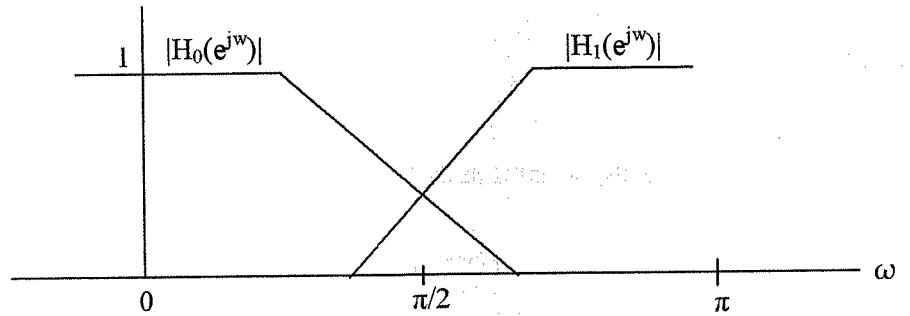


Figure 3.7 Typical Frequency Responses of the Analysis Filters.

3.4.1 The Filter Bank Structure

Figure 3.6 illustrates the basic two-channel quadrature-mirror filter (QMF) bank structure. Here, the input signal $x[n]$ is first passed through a two-band analysis filter bank containing the filters $H_0(z)$ and $H_1(z)$, which typically have low-pass and high-pass frequency responses, respectively, with a cutoff frequency at $\pi/2$, as indicated in figure (3.7). The subband signals $\{v_k[n]\}$ are then down-sampled by a factor of 2. In subband coding applications, coders are inserted after the down-sampler in each subband channel and each down-sampled subband signal is encoded by exploiting the special spectral properties of the signal, such as energy levels, perceptual importance, etc. At the receiving end, decoder are use to produce approximations of the original down-sampled signals. The decoded signal are then up-sampled by a factor of 2 and passed through a two-band synthesis filter bank composed of the filters $G_0(z)$ and $G_1(z)$ whose outputs

are then added yielding $y[n]$. The, analysis and the synthesis filters in the QMF bank are chosen so as to ensure that the reconstructed output $y[n]$ is a reasonable replica of the input $x[n]$. In practice, various *errors* are generated in this scheme. In addition to the coding error, the QMF bank itself introduces several errors due to the sampling rate alterations and imperfect filters. We ignore the coding errors and investigate only the errors generated by the down-samplers and up-samplers in the filter bank and their effects on the performance of the system.

3.4.2 An Alias-Free Realization

A very simple alias-free two-band QMF bank is obtained when

$$H_1(z) = H_0(-z) \quad (3.15)$$

The above condition, in the case of a real coefficient filter, implies

$$|H_1(e^{j\omega})| = |H_0(e^{j(\pi-\omega)})| \quad (3.16)$$

indicating that if $H_0(z)$ is a low-pass filter, then $H_1(z)$ is a high-pass filter, and vice-versa. In fact, equation (3.16) indicates that $|H_1(e^{j\omega})|$ is a mirror image of $|H_0(e^{j\omega})|$ with respect to the $\pi/2$, the quadrature frequency. This has given rise to the name quadrature-mirror filter bank.

Substituting equation (3.15) in equation (3.33), we arrive at

$$G_0(z) = H_0(z), \quad G_1(z) = -H_1(z) = -H_0(-z) \quad (3.17)$$

Equations (3.15) and (3.17) imply that the two analysis filters and the two synthesis filters in the QMF bank are essentially determined from one transfer function $H_0(z)$. Moreover, equation (3.17) indicates that if $H_0(z)$ is a low-pass filter the $G_0(z)$ is also a low-pass filter, and $G_1(z)$ is a high-pass filter. The distortion function $T(z)$ is:

$$T(z) = \frac{1}{2} \{H_0^2(z) - H_1^2(z)\} = \frac{1}{2} \{H_0^2(z) - H_0^2(-z)\} \quad (3.18)$$

A computationally efficient realization of the above alias-free two-channel QMF bank is obtained by realizing the analysis and the synthesis filters in polyphase form. Let the two-band type1 polyphase representation of $H_0(z)$ be given by

$$H_0(z) = E_0(z^2) + z^{-1}E_1(z^2) \quad (3.19a)$$

From equation (3.15) it follows then that

$$H_1(z) = E_0(z^2) - z^{-1}E_1(z^2) \quad (3.19b)$$

In matrix form equation (3.19a) and (3.19b) can be expressed as

$$\begin{bmatrix} H_0(z) \\ H_1(z) \end{bmatrix} = \begin{bmatrix} 1 & 1 \\ 1 & -1 \end{bmatrix} \begin{bmatrix} E_0(z^2) \\ z^{-1}E_1(z^2) \end{bmatrix} \quad (3.20)$$

Likewise the synthesis filters in matrix form, can be expressed as

$$\begin{bmatrix} G_0(z) & G_1(z) \end{bmatrix} = \begin{bmatrix} z^{-1}E_1(z^2) & E_0(z^2) \end{bmatrix} \begin{bmatrix} 1 & 1 \\ 1 & -1 \end{bmatrix} \quad (3.21)$$

Using equation. (3.20) and (3.21), we can redraw the two-channel QMF bank as shown in figure 3.8(a), which can be further simplified using the cascade equivalences, resulting in the computationally efficient realization of figure 3.8(b).

The expression for the distortion transfer function in this case, obtained by substituting equations (3.19a) and (3.19b) in equation (3.18), is given by

$$T(z) = 2z^{-1}E_0(z^2)E_1(z^2) \quad (3.22)$$

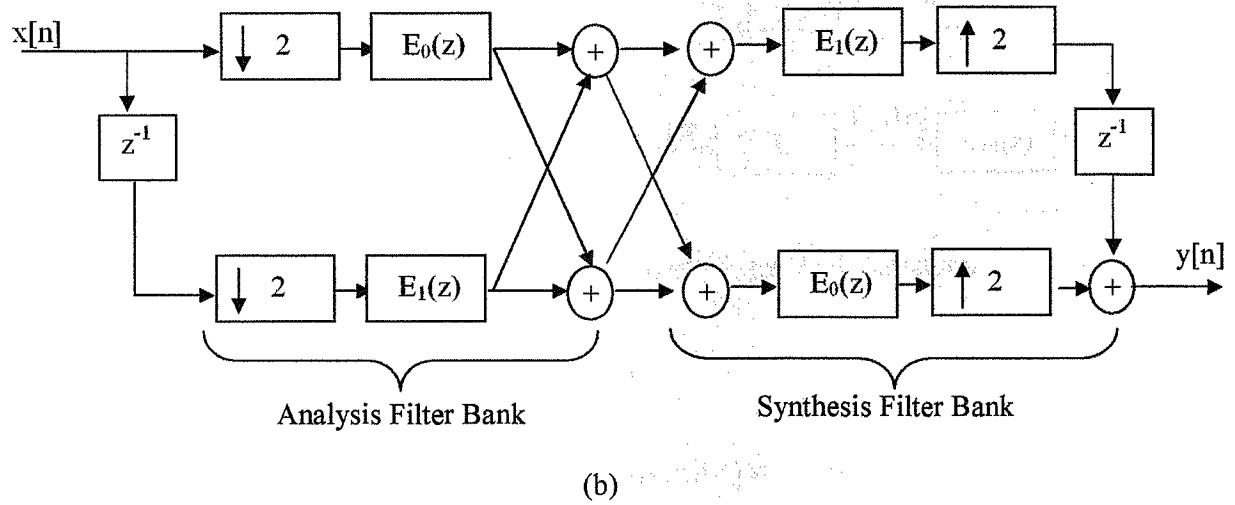
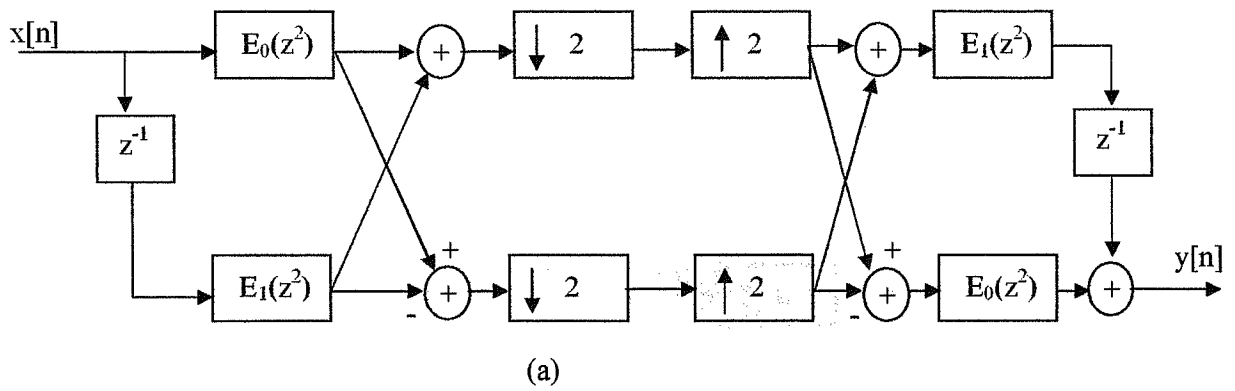


Figure 3.8 Polyphase Realization of the Two-Channel QMF Bank. (a) Direct Realization and (b) Computationally Efficient Realization.

3.5 L-Channel QMF Bank

We now generalize the discussion of the previous section to the case of a QMF bank with more than two-channels. The basic structure of the L-channel QMF bank is shown in figure 3.9

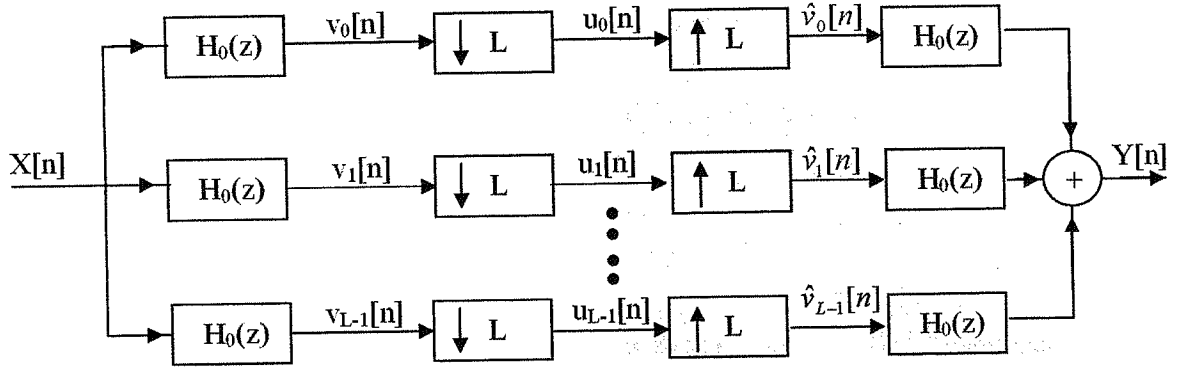


Figure 3.9 The Basic L-Channel QMF Filter Bank Structure.

3.5.1 Analysis of the L-Channel Filter Bank

We analyze the operation of the L-channel QMF bank of figure 3.9 in the z-domain. The expression for the z-transforms of various intermediate signal in figure 3.9 are given by

$$V_k(z) = H_k(z)X(z) \quad (3.23a)$$

$$U_k(z) = \frac{1}{L} \sum_{l=0}^{L-1} H_k(z^{1/L} W_L^l) X(z^{1/L} W_L^l) \quad (3.23b)$$

$$\hat{V}_k(z) = U_k(z^L) \quad (3.23c)$$

where $k = 0, 1, \dots, L-1$. The output of the QMF bank is given by

$$Y(z) = \sum_{k=0}^{L-1} G_k(z) \hat{V}_k(z) \quad (3.24)$$

From equations (3.23a), (3.23b) and (3.23c), we finally arrive at

$$Y(z) = \frac{1}{L} \sum_{l=0}^{L-1} X(zW_L^l) \sum_{k=0}^{L-1} H_k(zW_L^l) G_k(z) \quad (3.25)$$

which can be written in compact form as

$$Y(z) = \sum_{l=0}^{L-1} a_l(z) X(zW_L^l) \quad (3.26)$$

where

$$a_l(z) = \frac{1}{L} \sum_{k=0}^{L-1} H_k(zW_L^l) G_k(z), \quad 0 \leq l \leq L-1 \quad (3.27)$$

3.5.2 Matrix Representation

It is convenient to examine the operation of the L-channel QMF bank using a matrix formalism. Define

$$A(z) = [a_0(z) \quad a_1(z) \quad \dots \quad a_{L-1}(z)]^T \quad (3.28a)$$

$$g(z) = [G_0(z) \quad G_1(z) \quad \dots \quad G_{L-1}(z)]^T \quad (3.28b)$$

$$H(z) = \begin{bmatrix} H_0(z) & H_1(z) & \dots & H_{L-1}(z) \\ H_0(zW_L^1) & H_1(zW_L^1) & \dots & H_{L-1}(zW_L^1) \\ \vdots & \vdots & \ddots & \vdots \\ H_0(zW_L^{L-1}) & H_1(zW_L^{L-1}) & \dots & H_{L-1}(zW_L^{L-1}) \end{bmatrix} \quad (3.28c)$$

where the $L \times L$ matrix $H(z)$ is called the aliasing component (AC) matrix. Using the above notations, equations, (3.26) reduces to

$$LA(z) = H(z)g(z) \quad (3.29)$$

The aliasing cancellation condition can now be written as

$$H(z)g(z) = t(z) \quad (3.30)$$

where

$$t(z) = [La_0(z) \quad 0 \quad \dots \quad 0]^T = [LT(z) \quad 0 \quad \dots \quad 0]^T \quad (3.31)$$

Using equation (3.28a) and the notation

$$x(z) = \begin{bmatrix} X(z) \\ X(zW_L^1) \\ \vdots \\ X(zW_L^{L-1}) \end{bmatrix} \quad (3.32)$$

we can rewrite equation (3.26) as

$$Y(z) = A^T(z)x(z) \quad (3.33a)$$

or equivalently, as

$$Y(z) = \frac{1}{L} g^T(z) H^T(z) x(z) \quad (3.33b)$$

derived using equation (3.29)

From equation (3.28), it follows that by knowing the set of analysis filters $\{H_k(z)\}$, we can determine the desired set of synthesis filters $\{G_k(z)\}$ as

$$g(z) = H^{-1}(z)t(z) \quad (3.34)$$

provided of course $[\det H(z)] \neq 0$. Moreover, a perfect reconstruction QMF bank results if we set $T(z) = z^{-n_0}$ in the expression for $t(z)$ in equation (3.29). In practice, the above approach is difficult to carry out for a number of reasons. A more practical solution to the design of perfect reconstruction QMF bank is obtained via the polyphase representation.

3.5.3 Polyphase Representation

Consider the type I polyphase representation of the k th analysis filter $H_k(z)$:

$$H_k(z) = \sum_{t=0}^{L-1} z^{-t} E_{kt}(z^L), \quad k = 0, 1, \dots, L-1 \quad (3.35)$$

A matrix representation of the above set of equations is given by

$$h(z) = E(z^L)e(z) \quad (3.36)$$

where

$$h(z) = [H_0(z) \ H_1(z) \ \dots \ H_{L-1}(z)]^T \quad (3.37a)$$

$$e(z) = [1 \ z^{-1} \ \dots \ z^{-(L-1)}]^T \quad (3.37b)$$

and

$$E(z) = \begin{bmatrix} E_{00}(z) & E_{01}(z) & \dots & E_{0,L-1}(z) \\ E_{10}(z) & E_{11}(z) & \dots & E_{1,L-1}(z) \\ \vdots & \vdots & \ddots & \vdots \\ E_{L-1,0}(z) & E_{L-1,1}(z) & \dots & E_{L-1,L-1}(z) \end{bmatrix} \quad (3.37c)$$

The matrix $E(z)$ defined above is called the Type I polyphase component matrix. Figure (3.10a) shows the Type I polyphase representation of the analysis filter bank.

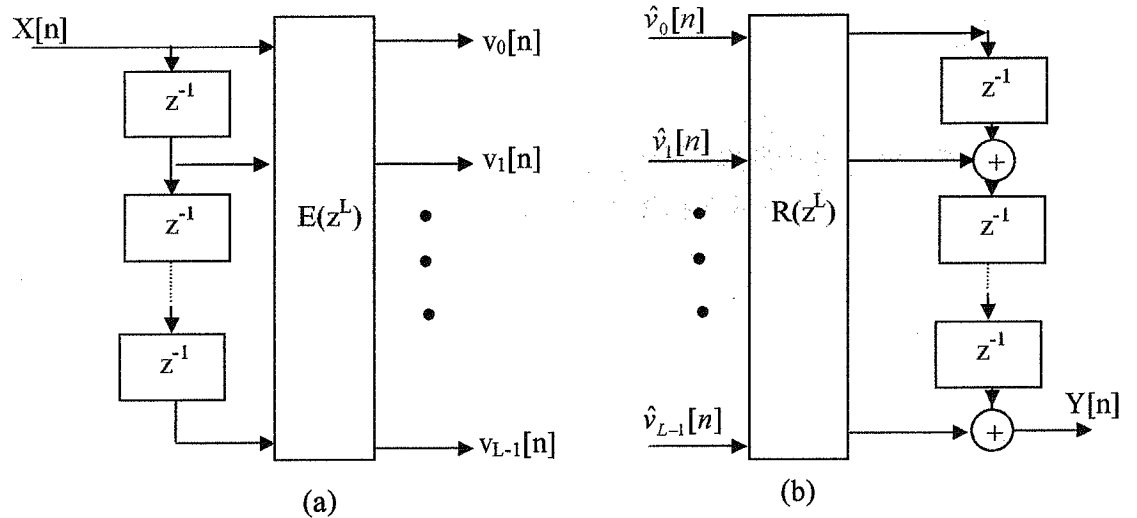


Figure 3.10 (a) Type I Polyphase Representation of the Analysis Filter Bank and
(b) Type II Polyphase Representation of the Synthesis Filter Bank.

Likewise, we can represent the L synthesis filter in a Type II polyphase form:

$$G_k(z) = \sum_{l=0}^{L-1} z^{-(L-1-l)} R_{lk}(z^L), \quad k = 0, 1, \dots, L-1 \quad (3.38)$$

In matrix form, the above set of L equation can be rewritten as

$$g^T(z) = z^{-(L-1)} \tilde{e}(z) R(z^L) \quad (3.39)$$

here

$$g(z) = [G_0(z) \ G_1(z) \ \dots \ G_{L-1}(z)]^T \quad (3.40a)$$

$$\tilde{e}(z) = [1 \ z \ \dots \ z^{L-1}] = e^T(z^{-1}) \quad (3.40b)$$

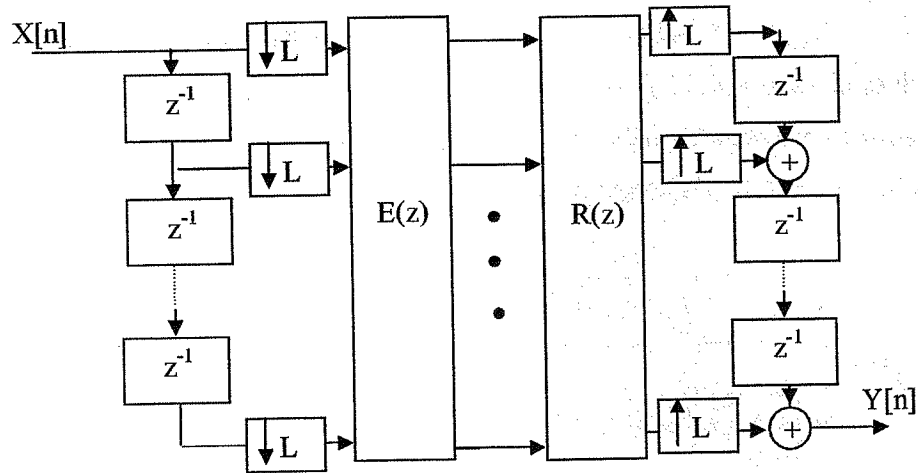


Figure 3.11 L -Channel QMF Bank Structure Based on the Polyphase Representations of the Analysis and Synthesis Filter Bank.

$$e(zW_L^k) = \Delta(z) \begin{bmatrix} 1 \\ W_L^{-k} \\ \vdots \\ W_L^{-k(L-1)} \end{bmatrix} \quad (3.41)$$

where

$$\Delta(z) = \text{diag}[1 \quad z^{-1} \quad \dots \quad z^{-(L-1)}] \quad (3.42)$$

Making use of equation (3.43) in equation (3.41), we arrive at the desired result after some algebra:

$$H(z) = D^* \Delta(z) E^T(z^L) \quad (3.43)$$

where the D is the $L \times L$ DFT matrix.

3.6 Filter Banks with Equal Pass-Band Widths

By inserting a two-channel maximally decimated QMF bank in each channel of another two-channel maximally decimated QMF bank between the down-sampler and the up-sampler, we can generate a four-channel maximally decimated QMF bank, as shown in figure 3.12.

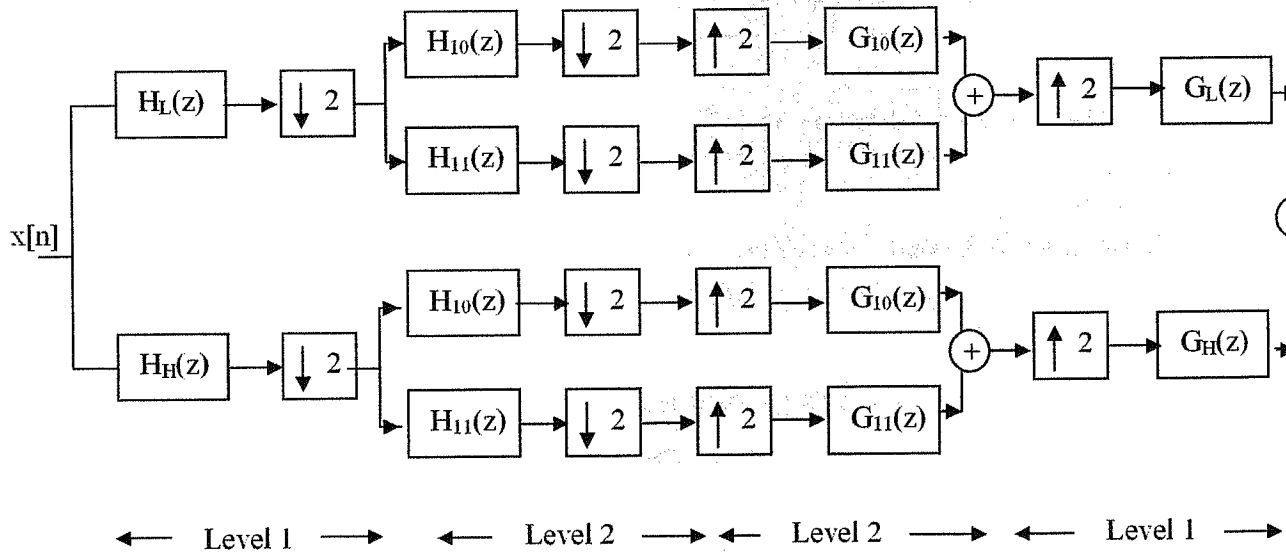


Figure 3.12 A Two-Level Four-Channel Maximally-Decimated QMF Structure.

Since the analysis and the synthesis filter banks are formed like a tree, the overall system is often called a *tree-structure filter bank*. It should be noted that in the four channel tree-structure filter bank of figure 3.12, the two 2-channel QMF bank in the second level do not have to be identical. However, if they are different QMF banks with different analysis and synthesis filters, to compensate for the unequal gains and unequal delays of the two 2-channel systems, additional delays of appropriate values need to be inserted at the middle to ensure perfect reconstruction of the overall four channel system.

An equivalent representation of the four-channel QMF system of figure 3.12 is shown in figure 3.13.

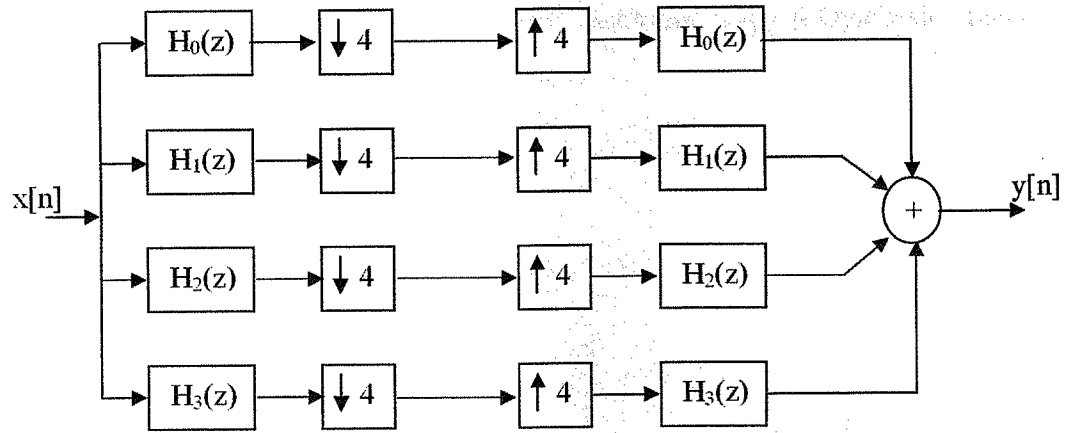


Figure 3.13 An Equivalent Representation of the Four-Channel QMF Structure of Figure 3.12.

The analysis and synthesis filters in the equivalent representation are related to those of the parent two-level tree-structured filter bank as follows:

$$H_0(z) = H_L(z)H_{10}(z^2), \quad H_1(z) = H_L(z)H_{11}(z^2) \quad (3.44a)$$

$$H_2(z) = H_H(z)H_{10}(z^2), \quad H_3(z) = H_H(z)H_{11}(z^2) \quad (3.44b)$$

$$G_0(z) = G_L(z)G_{10}(z^2), \quad G_1(z) = G_L(z)G_{11}(z^2) \quad (3.44c)$$

$$G_2(z) = G_H(z)G_{10}(z^2), \quad G_3(z) = G_H(z)G_{11}(z^2) \quad (3.44d)$$

From equations (3.44a)-(3.44d) it can be seen that each analysis filter $H_k(z)$ is a cascade of two filters, one with a single pass-band and a single stop-band and the other with two pass-bands and two stop-bands. The pass-band of the cascade is the frequency range where the pass-bands of the two filters overlap. On the other hand, the stop-band of the cascade is formed from three different frequency ranges. In two of the frequency ranges, the pass-band of one coincides with the stop-band of the other, while in the third range, the two stop-bands overlap. As a result, the gain responses of the cascade in the three regions of the stop-band are not equal, resulting in uneven stop-band attenuation characteristic.

By continuing the process, QMF banks with more than four channels can be easily constructed. It should be noted that the number of channels resulting from this approach is restricted to a power-of-2, i.e., $L = 2^v$. In addition, the filters in the analysis (synthesis) branch have pass-bands of equal width given by π/L . However, by a simple modification to the approach we can design QMF banks with analysis (synthesis) filters having pass-bands of unequal width as described next.

3.7 Filter Banks with Unequal Pass-Band Widths

Consider the two-channel maximally decimated QMF bank of figure 3.14(a). By inserting another two-channel maximally decimated QMF bank in the top subband channel between the down-sampler and the up-sampler at the position marked by a *, we arrive at a three-channel maximally decimated QMF bank, as shown in figure 3.14(b).

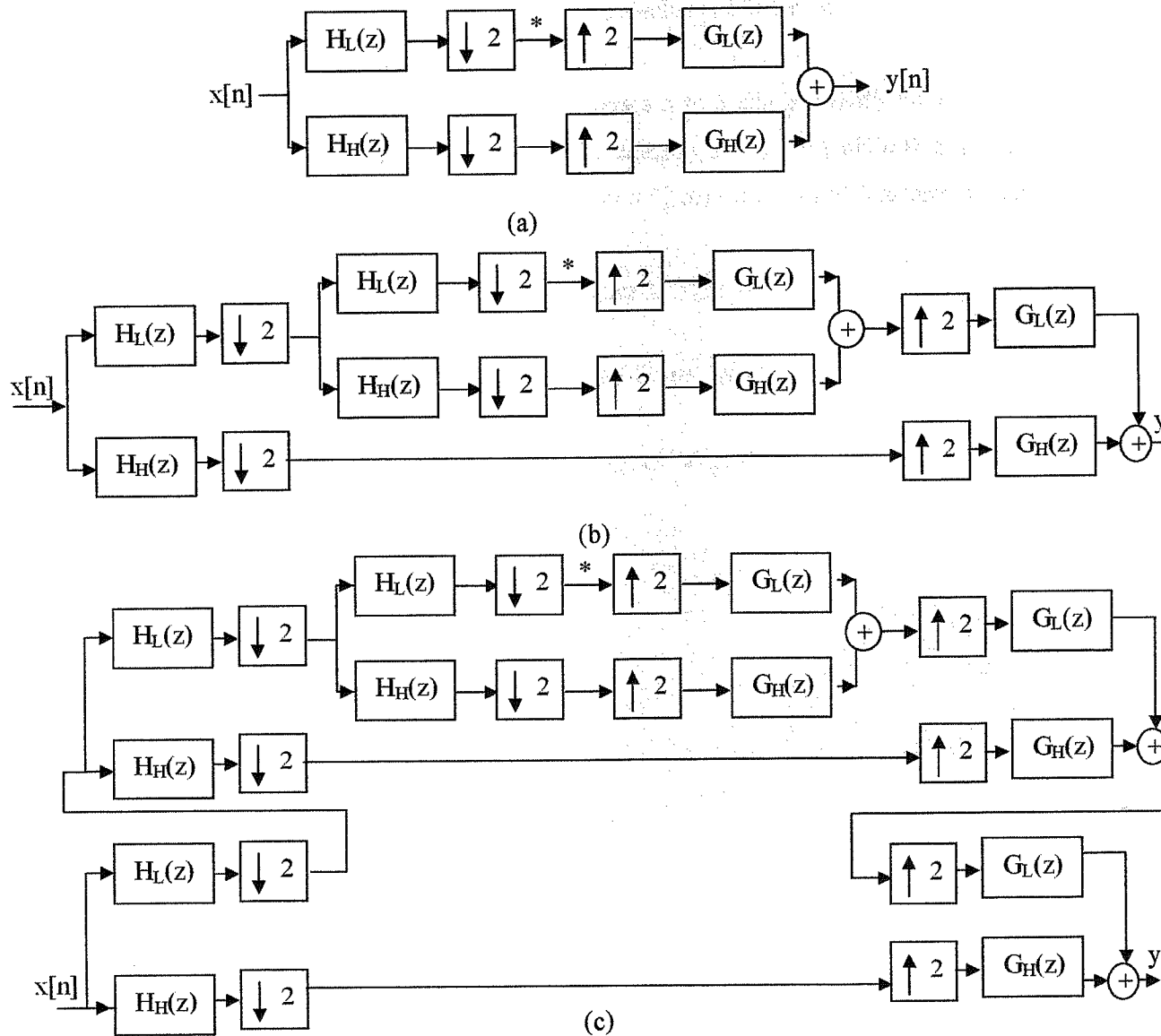


Figure 3.14 (a) a 2-Channel QMF Bank, (b) a 3-Channel QMF Bank Derived From the 2-Channel QMF Bank, (c) a 4-Channel QMF Bank Derived From the 3-Channel QMF Bank.

The equivalent representation of the generated three-channel filter bank is indicated in figure 3.15(a), where the analysis and synthesis filters are given by

$$\begin{aligned} H_0(z) &= H_L(z)H_L(z^2), & H_1(z) &= H_L(z)H_H(z^2), & H_2(z) &= H_H(z), \\ G_0(z) &= G_L(z)G_L(z^2), & G_1(z) &= G_L(z)G_H(z^2), & G_2(z) &= G_H(z) \end{aligned} \quad (3.45)$$

Typical magnitude response of the analysis filters of the two-channel QMF bank of figure 3.14(a) and that of the derived three-channel filter of figure 3.14(b) are sketched in figure 3.16(a) and (b), respectively.

We can continue this process and generate a four-channel QMF bank from the three-channel QMF bank of figure 3.14(b). By inserting a two-channel QMF bank in the top subband channel at the position marked by a *, resulting in the structure of figure 3.14(c).

Its equivalent representation is indicated in figure 3.15(b), where

$$\begin{aligned} H_0(z) &= H_L(z)H_L(z^2)H_L(z^4), & H_1(z) &= H_L(z)H_L(z^2)H_H(z^4), \\ H_2(z) &= H_L(z)H_H(z^2), & H_3(z) &= H_H(z), \\ G_0(z) &= G_L(z)G_L(z^2)G_L(z^4), & G_1(z) &= G_L(z)G_L(z^2)G_H(z^4), \\ G_2(z) &= G_L(z)G_H(z^2), & G_3(z) &= G_H(z) \end{aligned} \quad (3.46)$$

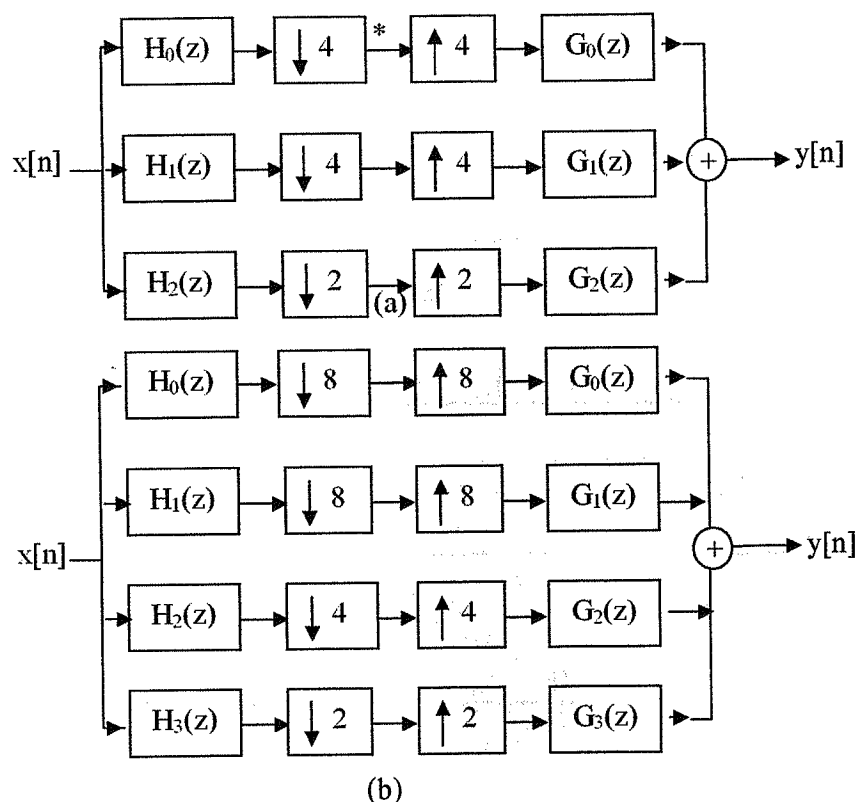


Figure 3.15 Maximally Decimated QMF Banks with Unequal Pass-Band Width Analysis (Synthesis) Filters.

Figure 3.16 (c) shows typical magnitude responses of the analysis (synthesis) filters of the four-channel QMF bank of figure 3.14(c) derived from a parent two-channel QMF bank with magnitude responses as indicated in figure 3.16(a).

Because of the unequal pass-band width of the analysis and synthesis filters, these structures belong to the class of nonuniform QMF banks. The tree-structured filter banks of figure 3.14 are also referred to as octave band QMF banks.

Various other types of nonuniform filter banks can be generated by iterating branches of a parent uniform two-channel QMF in different forms. Nonuniform filter banks are often used in speech and image coding applications [14].

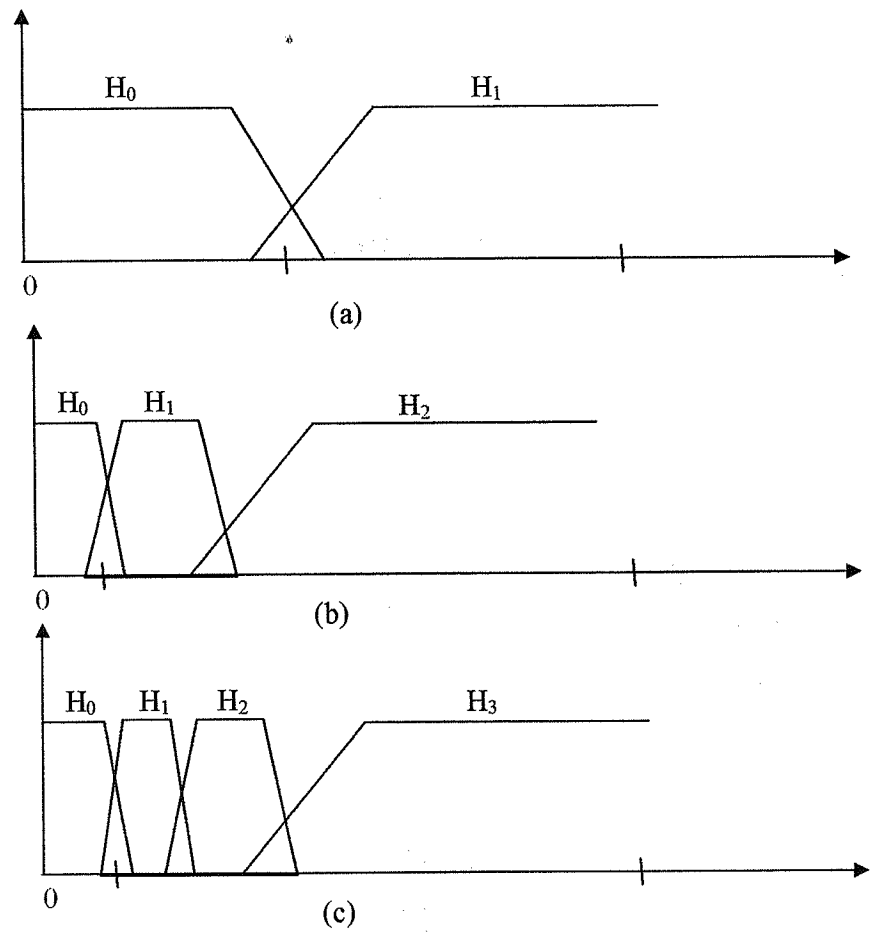


Figure 3.16 Magnitude Response of the Analysis Filters of a (a) 2-Channel QMF Bank, (b) 3-Channel QMF Bank Derived from a 2-Channel QMF Bank, and (c) 4-Channel Bank Derived from a 3-Channel QMF Bank.

3.8 Summary

The basics of the digital bank filter and its application for multirate signal processing was given. Uniform DFT filters having different central frequencies, full and half Lth band filter was presented. Design and error analysis of the 2-channel QMF bank filters was given.

4. INTERPOLATION USING ORTHOGONAL FUNCTION

4.1 Overview

The theory of orthogonal rational functions has been widely studied over the last few decades; see e.g. the comprehensive monograph [2]. A possible approach to the subject is to consider orthogonal rational functions as generalizations of orthogonal polynomials or equivalently, orthogonal polynomials form a special case of orthogonal rational functions (with all poles fixed at infinity). Many classical results from orthogonal polynomials, such as those concerning recurrence relations, quadrature formulas, Favard theorems, moment problems, Padé approximation etc. have been generalized to the case of orthogonal rational functions.

4.2 Orthogonal Functions

Let us consider a set of functions $g_1(t), g_2(t), \dots, g_n(t)$ defined over the interval $t_1 \leq t \leq t_2$ and which are related to one another in very special way that any two different ones of the set satisfy the condition

$$\int_{t_1}^{t_2} g_i(t) g_j(t) dt = 0 \quad (4.1)$$

where $i \neq j$

That is, when we multiply two different functions and then integrate over the interval from t_1 to t_2 the result is zero. A set of functions which has this property is described as being orthogonal over the interval from t_1 to t_2 .

Now we consider that we have some arbitrary function $f(t)$ and that we are interested in $f(t)$ only in the range from t_1 to t_2 , i.e., in the interval over which the set of functions $g(t)$ are orthogonal. Suppose further that we undertake to write $f(t)$ as a linear sum of the functions $g_n(t)$. That is, we write

$$f(t) = C_1 g_1(t) + C_2 g_2(t) + \dots + C_n g_n(t) = \sum_{i=1}^n C_i g_i(t) \quad (4.2)$$

in which the C 's are numerical coefficients. Assuming that such an expansion is indeed possible, the orthogonality of the g 's makes it very easy to compute the coefficients C_n . Thus to evaluate C_n we multiply both sides of equation (4.2) by $g_n(t)$ and integrate over the interval of orthogonality. We have

$$\int g_n(t) f(t) dt = C_1 \int g_n(t) g_1(t) dt + C_2 \int g_n(t) g_2(t) dt + \dots + C_n \int g_n(t) g_n(t) dt \quad (4.3)$$

Because of the orthogonality, all of the terms on the right-hand side of equation (4.3) become zero with a single exception and we are left with

$$\int_{t_1}^{t_2} f(t) g_n(t) dt = C_n \int_{t_1}^{t_2} g_n^2(t) dt \quad (4.4)$$

So that the coefficient that we are evaluating becomes

$$C_n = \frac{\int_{t_1}^{t_2} f(t) g_n(t) dt}{\int_{t_1}^{t_2} g_n^2(t) dt} \quad (4.5)$$

The mechanism by which we use the orthogonality of the function to "drain" away all the terms except the term that involves the coefficient we are evaluating is often called the "orthogonality sieve".

Next suppose that each $g_n(t)$ is selected so that the denominator of the right-hand member of equation (4.5) (which is a numerical constant) has the value

$$\int_{t_1}^{t_2} g_n^2(t) dt = 1 \quad (4.6)$$

In this case

$$C_n = \int_{t_1}^{t_2} f(t)g_n(t)dt \quad (4.7)$$

When the orthogonal functions $g_n(t)$ are selected as in equation (4.6) they are described as being normalized. The use of normalized function has the merit that the C_n 's can then be calculated from equation (4.7) and thereby avoids the need to evaluate equation (4.6)

4.3 Completeness of an Orthogonal Set, the Fourier Series

Suppose on the hand we expand a function $f(t)$ in terms of orthogonal functions as

$$f(t) = C_1s_1(t) + C_2s_2(t) + C_3s_3(t) + \dots \quad (4.8)$$

and on the other hand we expand it as

$$f(t) = C_1s_1(t) + C_3s_3(t) + \dots \quad (4.9)$$

that is, in the second case, we have deliberately omitted one term in equation (4.9). A moment's review of the procedure, described in the previous section, for evaluating coefficients makes it apparent that all the coefficients C_1, C_3 , etc., that appear in both expansions will turn out to be the same. Hence if one expansion is correct the other is in error. We might be suspicious of the expansion of equation (4.9) on the grounds that in term is missing. The point is that simply having a set of orthogonal functions and having a procedure for evaluating coefficients does not guarantee that the series so developed can represent an arbitrary function. Such can well be the case even when the orthogonal set consists of an infinite number of independent functions necessary to allow an error free expansion of an arbitrary function then the set is said to be complete.

A most important orthogonal set which is complete is the set of sinusoidal functions (both sines and cosines) which generate the Fourier series. In this case,

because of the periodicity of the functions, it is not necessary to specify the end points of the interval over which the expansion is to be valid but only to specify the length of the interval. (It may, however, be useful to specify the interval end points for the sake of computational convenience in connection with evaluating the coefficients.) Specifically, if the variable of interest is the time t and the length of time interval is T , then the Fourier expansion of a function $x(t)$ is

$$X(t) = \sum_{n=0}^{\infty} A_n \cos \frac{2\pi n t}{T} + \sum_{n=0}^{\infty} B_n \sin \frac{2\pi n t}{T} \quad (4.10)$$

We take account of the fact that $\cos 0 = 1$ and $\sin 0 = 0$, and applying the normalized procedure we can express the expression of $x(t)$ in terms of orthogonal function as

$$X(t) = \frac{A_0}{\sqrt{T}} + \sum_{n=1}^{\infty} A_n \sqrt{2/T} \cos \frac{2\pi n t}{T} + \sum_{n=1}^{\infty} B_n \sqrt{2/T} \sin \frac{2\pi n t}{T} \quad (4.11)$$

The orthogonal functions are given by

$$1/\sqrt{T}, \sqrt{2/T} \cos\left(\frac{2\pi n t}{T}\right) \text{ and } \sqrt{2/T} \sin\left(\frac{2\pi n t}{T}\right) \text{ where } n \neq 0.$$

Any two such different functions when multiplied and integrated over T yields zero and any function squared and integrated over T yields unity.

In general case an expansion is valid only over the finite interval T of orthogonality. In the case an expansion is periodic with period T . if it should happen that $v(t)$ is also periodic with period T then the expansion is valid for all t . Thus, a periodic function with period T can be expanded into a Fourier series as in equation (4.11) in which the coefficients are given by

$$A_0 = \frac{1}{\sqrt{T}} \int_T X(t) dt \quad (4.12)$$

$$A_n = \sqrt{\frac{2}{T}} \int_T X(t) \cos\left(\frac{2\pi n t}{T}\right) dt, \quad (4.13)$$

$$B_n = \sqrt{\frac{2}{T}} \int_T X(t) \sin\left(\frac{2\pi nt}{T}\right) dt \quad (4.14)$$

where $n \neq 0$

4.4 Trigonometric Polynomial Approximation

Definition: A series of the form

$$T_M = a_0 + (a_j \cos(jt) + b_j \sin(jt)) \quad (4.15)$$

is called a trigonometric polynomial of order M.

Theorem: Discrete Fourier series.

Assume that $\{(t_j, y_j)\}$, where $y_j = f(t_j)$ and that the $N+1$ points have equally spaced abscissas

$$t_j = -\pi + \frac{2j\pi}{N} \quad \text{for } j = 0, 1, \dots, N \quad (4.16)$$

If $f(x)$ is periodic with period 2π and $2M < N$, then there exist a trigonometric polynomial $T_M(t)$ of the form equation (4.15) that minimizes the quantity

$$\sum_{k=1}^N (f(t_k) - T_M(t_k))^2 \quad (4.17)$$

The coefficients a_j and b_j of this polynomial are computed with the formulas

$$a_j = \frac{2}{N} \sum_{k=1}^N f(t_k) \cos(jt_k), \quad \text{for } j = 0, 1, \dots, M \quad (4.18)$$

and

$$b_j = \frac{2}{N} \sum_{k=1}^N f(t_k) \sin(jt_k), \quad \text{for } j = 1, 2, \dots, M \quad (4.19)$$

Although formula (4.18) and (4.19) are defined with the least-square procedure, they can also be viewed as numerical approximations to the integrals in Euler's formulas. Euler's formulas give the coefficients for the Fourier series of continuous function, whereas formula (4.18) and (4.19) give the trigonometric polynomial coefficients for curve fitting to data points. The next example uses data points generated by the function $f(t) = t/2$ at discrete points. When more points are used, the trigonometric polynomial coefficients get closer to the Fourier series coefficients.

4.5 Expansion Signals in Special Orthogonal Functions

a) Legendre Polynomials

$$P_n(t) = \frac{1}{2^n n!} \frac{d^n}{dt^n} (t^2 - 1)^n \quad (4.20)$$

For the first three degree we have

$$P_0(t) = 1$$

$$P_1(t) = t$$

$$P_2(t) = (3t^2 - 1)/2$$

Legendre polynomials satisfy the following conditions:

$$P_n(-t) = \begin{cases} P_n(t) & \text{if } n \text{ is even} \\ -P_n(t) & \text{if } n \text{ is odd} \end{cases} \quad (4.21g)$$

Figure shows $P_n(t)$ for $n = 0, 1, 2, 3, 4, 5$

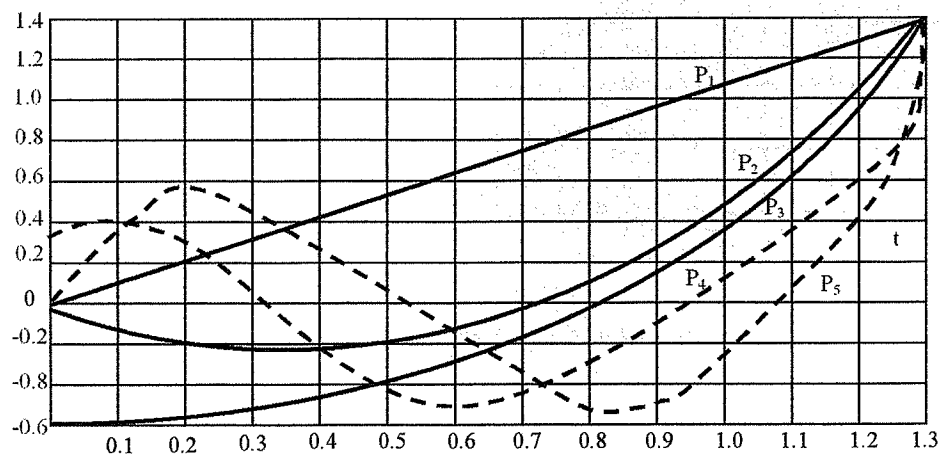


Figure 4.1 Shows $P_n(t)$ for $n = 0, 1, 2, 3, 4, 5$

The coefficients C_n are defined by

$$C_n = \sqrt{\frac{2n+1}{2}} \int_{-1}^1 f(t) P_n(t) dt \quad (4.21)$$

b) Chebyshev Polynomial

Chebyshev polynomials can be generated by the following way. Set $T_0(t) = 1$ and $T_1(t) = t$ and use the recurrence relation.

$$T_k(t) = 2tT_{k-1}(t) - T_{k-2}(t) \quad \text{for } t = 2, 3, \dots \quad (4.22)$$

Graphs of the chebyshev polynomials $T_0(t)$, $T_1(t)$, $T_2(t)$ are shown in figure 4.2.

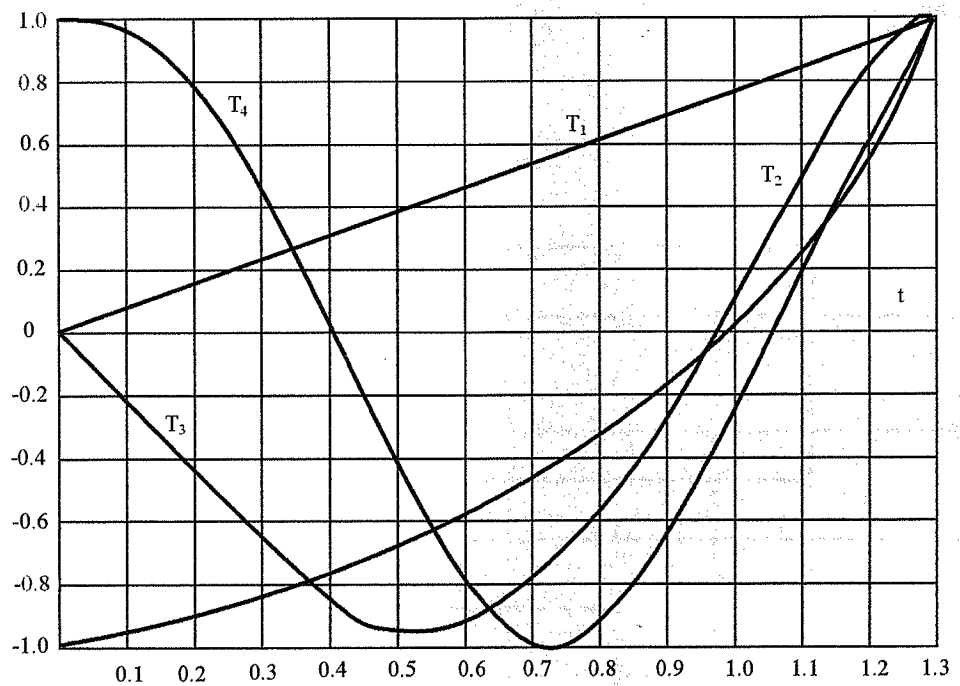


Figure 4.2 Graph of the Chebyshev Polynomials

The Chebyshev approximation can be written as

$$F(t) = \sum_{j=1}^N C_j T_j(t) \quad (4.23)$$

The coefficients C_j are computed with the formulas:

$$C_0 = \frac{1}{N+1} \sum_{k=0}^N f(t_k) T_0(t_k) = \frac{1}{N+1} \sum_{k=0}^N f(t_k) \quad (4.24)$$

and

$$C_j = \frac{2}{N+1} \sum_{k=0}^N f(t_k) \cos\left(\frac{j\pi(2k+1)}{2N+2}\right) \quad \text{for } j = 1, 2, \dots, N \quad (4.25)$$

Such an approximation is based on the nodes

$$t_k = \cos\left(\frac{j\pi(2k+1)}{2N+2}\right) \quad (4.26)$$

c) Khaar Polynomial

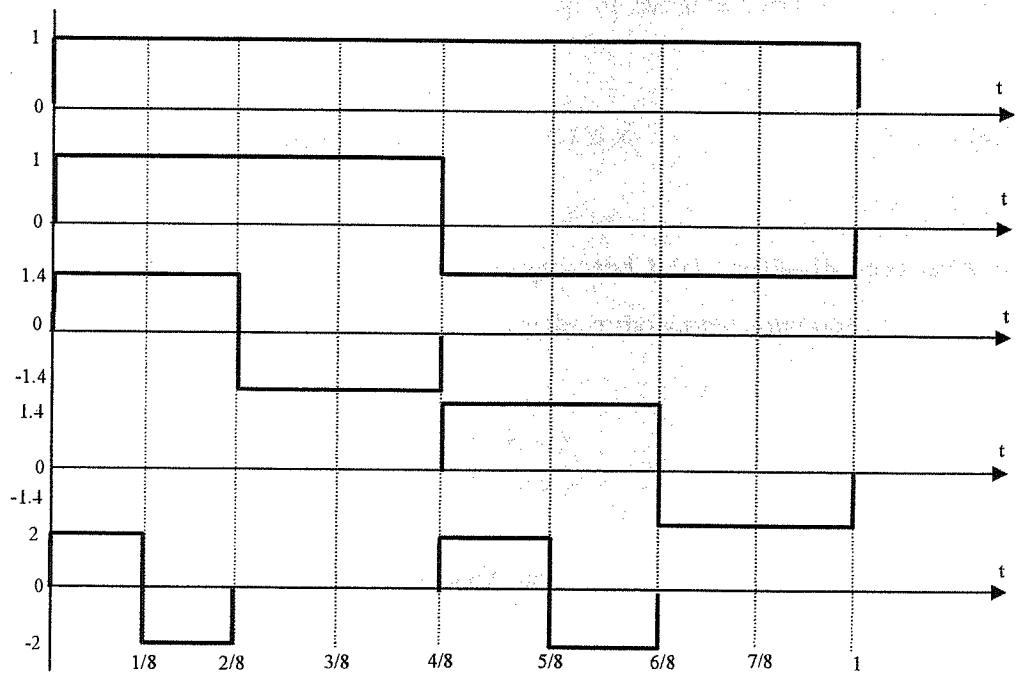


Figure 4.3 Shows some Khaar Polynomials.

Khaar polynomials are defined by

$$X_n^k(t) = \begin{cases} \sqrt{2^n} & \frac{2k-2}{2^{n+1}} \leq t \leq \frac{2k-1}{2^{n+1}} \\ -\sqrt{2^n} & \frac{2k-1}{2^{n+1}} \leq t \leq \frac{2k}{2^{n+1}} \\ 0 & t \notin [0,1] \end{cases}$$

Khaar functions are considerable practical importance because they can easily generated by digital logic circuitry and because multiplication by these functions be simply implemented by a polarity reversing switch.

4.6 Orthogonal Filters

4.6.1 Hermite Series

Consider the approximation of the noisy function by a Hermite series. The series approximates the function by a finite expansion of Hermite functions on an interval $\{-\infty, \infty\}$

$$f(t) \cong f_N(t) = \sum_{n=0}^N a_n h_n(t) \quad -\infty \leq t \leq \infty \quad (4.27)$$

where $\{a\}$ are a set of suitably chosen weights and $h_n(t)$ are the Hermite activation functions on the interval $\{-\infty, \infty\}$ which satisfy the orthonormal condition

$$\int_{-\infty}^{\infty} h_n(t) h_m(t) dt = \begin{cases} 1 & m = n \\ 0 & m \neq n \end{cases} \quad (4.28)$$

The first few Hermite functions in this series are

$$h_0(t) = \frac{\exp(-t^2/2)}{\pi^{1/4}} \quad (3.29)$$

$$h_0(t) = \frac{2t \exp(-t^2/2)}{\pi^{1/4} 2^{1/2}} \quad (3.30)$$

The remainder may be determined from the recurrence relation

$$h_{n+1}(t) = t \sqrt{\frac{2}{n+1}} h_n(t) - \sqrt{\frac{n}{n+1}} h_{n-1}(t) \quad (3.31)$$

Since the fundamental, $h_0(t)$, is the Gaussian function it can take the place of the filter function. The fundamental Hermite function

$$\hat{f}(t) \cong \hat{f}_N(t) = \int_{-\infty}^{\infty} \left\{ \sum_{n=0}^N a_n h_n(\tau) \right\} h_0(t-\tau) d\tau \quad (4.32)$$

In order to evaluate this expression the correlation between the Hermite functions of different order is required. This correlation is given by

$$\int_{-\infty}^{\infty} h_n(\tau) h_m(t-\tau) d\tau = \frac{1}{2} l_m^{n-m}(t^2/2) \quad (m \leq n) \quad (4.33)$$

where $l_m^n(t)$ is a normalized associated Laguerre function. Using this result in equation (4.32) we obtain

$$\hat{f}_N(t) = \frac{1}{2} \sum_{n=0}^N a_n l_0^n(t^2/2) \quad (4.34)$$

Note that only those associated Laguerre functions of subscript $\{m = 0\}$ contribute, which is greatly simplifying the result. The associated Laguerre functions of subscript are

$$l_0^n(t) = \frac{t^{n/2} e^{-t/2}}{\sqrt{n!}} \quad (4.35)$$

The usefulness of this expansion is that by fitting a Hermite series to the input function, one also immediately obtains the weights of the Laguerre series, $\{a_n\}$, which is the correlation of the input with a Gaussian function.

4.6.2 Hermite Rodriguez Functions

Hermite-Rodriguez functions are similar to the Hermite functions except that a Gaussian window modulates their amplitude. They are defined as

$$hr_n(t) = (\pi)^{1/4} h_n(t) e^{-t^2/2} \quad (4.36)$$

where $h_n(t)$ is an orthonormal Hermite function. The fundamental Hermite-Rodriguez function is also a Gaussian function but of different width to the fundamental Hermite function.

The fundamental is

$$hr_0(t) = \exp(-t^2) \quad (4.37)$$

The others may be determined by using the recurrence relation (equation (4.15)) for the Hermite functions and multiplying by the Gaussian function. Like the Hermite series, a simple expression also occurs for the correlation of the Hermite-Rodriguez functions. The correlation of two Hermite-Rodriguez functions is given by

$$hr_n(t) * hr_m(t) = \sqrt{\frac{(n+m)!}{2^{n+m} n! m!}} hr_{n+m}\left(t/\sqrt{2}\right) \quad (4.38)$$

Note that the scale is reduced and the order of the Hermite-Rodriguez function increased by the correlation operation. Using equation (4.38), the derivation of a Gaussian filter with the Hermite-Rodriguez functions is similar to the filter derived using the Hermite series.

4.7 Signal Duration and Bandwidth

Application requires the duration and bandwidth of the orthogonal series to be matched to the signal being modeled. The Hermite series behaves as a window in the time domain. Outside this window the Hermite functions decay exponentially, limiting the effective range over which a function may be approximated to within the window. The width of the Hermite series window is equal to the duration of the largest order Hermite function, $h_N(t)$, occurring in the series. The useful range of application of the Hermite series interpolation is then

$$|t| \leq \sqrt{2N+1} \quad (4.39)$$

where the right hand side, equal to the duration of the Hermite function of order $\{N\}$, may be determined via the Quantum mechanic solution of the Harmonic oscillator as the location where the oscillator energy becomes negative. The Fourier transform of a Hermite function is

$$F\{h_N(t)\} \rightarrow j^n h_N(w) \quad (4.40)$$

In view of this isomorphic Fourier transform, a similar windowing effect occurs in the complex frequency domain. The useful bandwidth is

$$|w| \leq \sqrt{2N+1} \quad (4.41)$$

Together, the bandwidth and window width of equation (4.27) and (4.28) define the size, N , of the neural series required to approximate a function. Unlike the Hermite series, which increases in duration with the order $\{N\}$ of the function, the Hermite-Rodriguez series is independent of N . Instead it is limited in duration by the Gaussian amplitude modulation function to the range

$$|t| \leq 3 \quad (4.42)$$

The Fourier transform of the Hermite-Rodriguez function is an associated Laguerre function

$$F\{hr_n(t)\} = (-j)^n L_n^0(w^2/2) \quad (4.43)$$

4.8 Scaling

Application to practical problems requires scaling of the orthogonal series. The procedure is illustrated for the Hermite-Rodrigues series.

The scaled Hermite-Rodriguez series is obtained by introducing the variable

$$t \rightarrow t/\alpha \quad (4.44)$$

Scaling changes the duration and bandwidth of the Hermite-Rodriguez series to,

$$|t| \leq 3\alpha \quad (4.45)$$

and

$$|w| \leq \frac{\sqrt{2N+1}}{\alpha} \quad (4.46)$$

respectively

Using scaled Hermite-Rodriguez functions, the correlation with the Gaussian function is

$$hr_n(t/\alpha) * hr_0(t/\beta) = \left(\frac{\alpha}{\gamma}\right)^n hr_n(t/\gamma) \quad (4.47)$$

where α and β are the scaling factors and

$$\gamma^2 = \alpha^2 + \beta^2 \quad (4.48)$$

4.9 Optimizing the Weights of the Orthogonal Series

The weights of the Hermite and Hermite-Rodriguez series were both obtained using the same method, which is described in this section for the Hermite series. For a continuous function defined on $\{-\infty, \infty\}$, the weights of the Hermite series are optimum with respect to the mean square error (equation (4.27)) when

$$A_n = \int_{-\infty}^{\infty} a(t) h_n(t) dt \quad (4.49)$$

We use a simple summation, similar to Euler integration, given by

$$A_n = \sum_{t=0}^{t=L} a(\Delta t i) h_n(\Delta t i) \quad (4.50)$$

where Δt is the integration step size which was fixed to the sampling rate. A feature of this type of integration is that it is also suitable for randomly sampled data. For random data, this type of numerical integration generalizes to Monte-Carlo integration. Numerical integration is only an approximation to the analytical continuous integration. In addition, the data most often encountered in practice is discrete, often corrupted with noise. To cope with these situations the gradient descent algorithm was applied after the weights had been estimated with the integration. Gradient descent reduces the mean square error between the Hermite series approximation and the discrete data by successive iterations of the following algorithm

$$A_{k, new} = A_k + \mu \left(a(t) - \sum_{n=0}^N A_n h_n(t) \right) h_k(t) \quad (4.51)$$

where μ is the feedback constant chosen in the range 0.0 to 1.0.

4.10 Summary

In this chapter different sets of orthogonal functions may be chosen to represent a given signal, and filter orthogonal, finally the expansion of the signals in special orthogonal functions was introduced.

5. PRACTICAL CONSIDERATION USING MATLAB

5.1 Overview

We investigate the process of upsampling and downsampling signal it introduces extra samples between measured original samples using lagrange interpolation and orthogonal function practical band simulation of systems are described by using MATLAB program.

5.2 MATLAB Implementation

MATLAB provides a function called bilinear to implement this mapping. Its invocation is similar to improve function, but it also takes several forms for different input-output quantities. Here is the design procedure of digital filters.

- Effect of up-sampling in the frequency domain
- use fir2 to create a bandlimited input sequence

```
>> freq=[0 0.45 0.5 1];
>> mag=[0 1 0 0];
>> x=fir2(99,freq,mag);
>> %evaluate and plot the input spectrum
>> [Xz,w]=freqz(x,1,512);
>> plot(w/pi,abs(Xz));grid
>> xlabel('Normalized frequency');ylabel('Magnitude');
>> title('Input Spectrum');
>> pause
>> %Generate the up-sampled sequence
>> L=input('Type in the up-sampling factor=');
Type in the up-sampling factor=5
>> y=zeros(1,L*length(x));
>> y([1:L:length(y)])=x;
>> %evaluate and plot the ouput spectrum
>> [Yz,w]=freqz(y,1,512);
>> plot(w/pi,abs(Yz));grid
>> xlabel('Normalized frequency');ylabel('magnitude');
>> title('output spectrum');
```

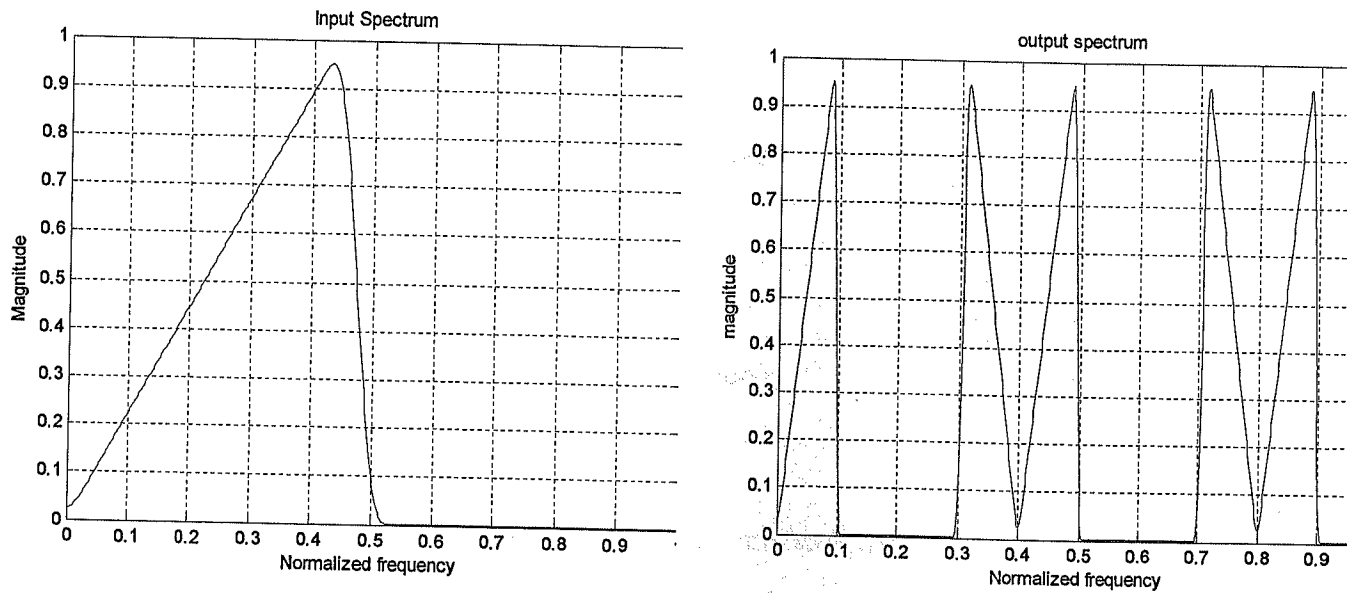



Figure 5.1 MATLAB Generated Input and Output Spectrum of a Factor of 5 Up-Sampler.

- Illustrate of up-sampling by an integer factor

```
>> N=input('Input length =');  
Input length =50  
>> L=input('Up-sampling factor =');  
Up-sampling factor =3  
>> fo=input('Input signal frequency =');  
Input signal frequency =0.12
```

- Generate the input sinusoidal sequence

```
>> n=0:N-1;
>> x=sin(2*pi*fo*n);
>> % Generate the up-sampled sequence
>> y=zeros(1,L*length(x));
>> y([1:L:length(y)])=x;
>> % Plot the input and the output sequences
>> subplot(2,1,1)
>> stem(n,x);
>> title('Input Sequence');
>> xlabel('Time index n');ylabel('Amplitude');
>> subplot(2,1,2)
>> stem(n,y(1:length(x)));
>> title(['Output sequence upsampled by',num2str(L)]);
>> xlabel('Time index n');ylabel('Amplitude');
```

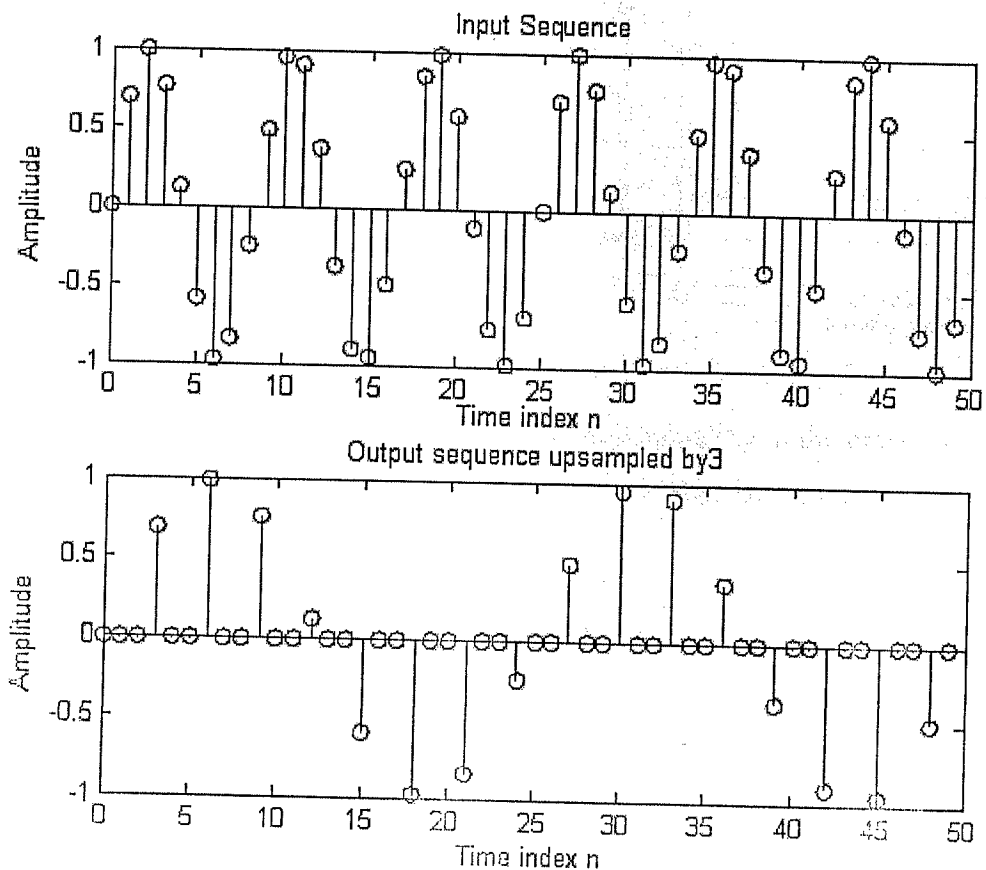


Figure 5.2 MATLAB Generated Illustrate of Up-Sampling by an Integer Factor.

- Effect of down-sampling in the frequency domain
- use fir2 to create a bandlimited input sequence

```
>> freq=[0 0.42 0.48 1];  
>> mag=[0 1 0 0];  
>> x=fir2(101, freq, mag);  
>> % Evaluate and plot the input spectrum  
>> [Xz, w]=freqz(x,1,512);  
>> plot(w/pi,abs(Xz));grid  
>> xlabel('Normalized frequency');ylabel('Magnitude');  
>> title('Input Spectrum')
```

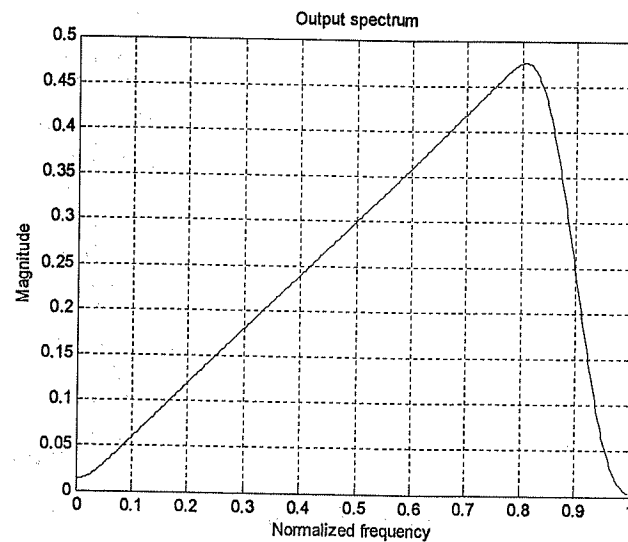
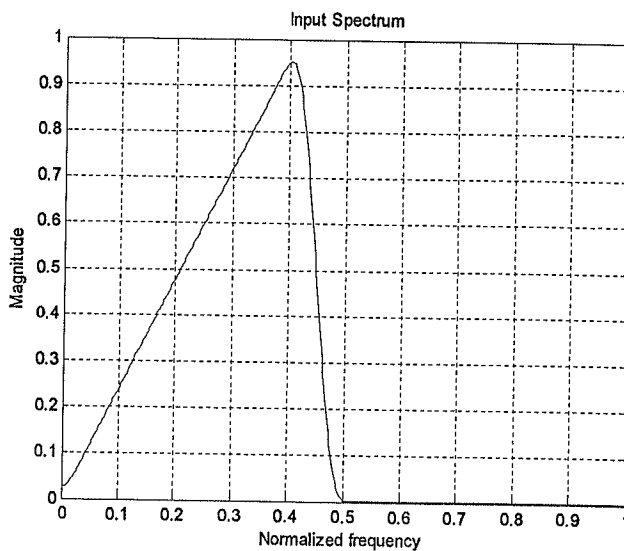


Figure 5.3 MATLAB Generated Effect of Down-Sampling in the Frequency Domain using FIR to create a band-limited Input Sequence.

- Illustration of decimator process

```
>> clf
>> N=input('length of input signal =');
length of input signal =100
>> M=input('down-sampling factor =');
down-sampling factor =2
>> f1=input('Frequency of first sinusoidal =');
Frequency of first sinusoidal =0.043
>> f2=input('Frequency of second sinusoidal =');
Frequency of second sinusoidal =0.031
>> n=0:N-1;
>> % Generate the input sequence
>> x=sin(2*pi*f1*n)+sin(2*pi*f2*n);
>> %generate the decimated output sequence
>> y=decimate(x,M,'fir');
>> %Plot the input and output sequences
>> subplot(2,1,1)
>> stem(n,x(1:N));
>> title('Input sequence');
>> xlabel('Time index n');ylabel('Amplitude');
>> subplot(2,1,2)
>> m=0:N/M-1;
>> stem(m,y(1:N/M));
>> title('Output sequence');
>> xlabel('Time index n');ylabel('Amplitude');
```

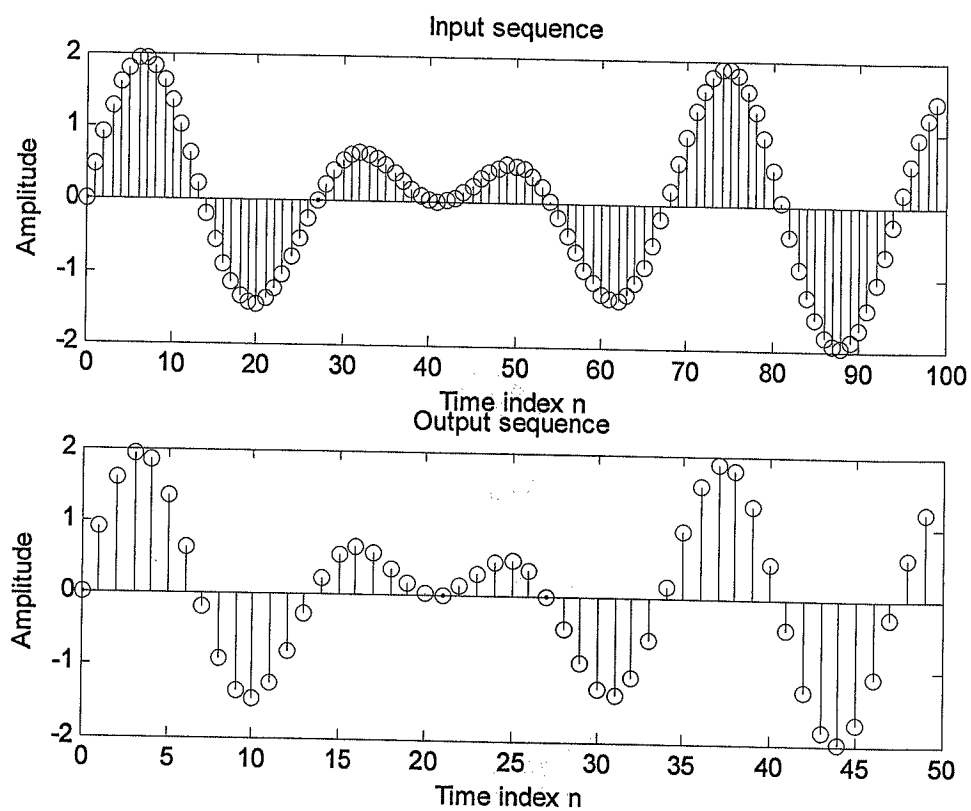


Figure 5.4 MATLAB Generated Effect of Decimator Process.

- Illustration of Interpolation process

```
>> clf
>> N=input('Length of input signal =');
Length of input signal =50
>> L=input('Up-sampling factor =');
Up-sampling factor =2
>> f1=input('Frequency of first sinusoidal =');
Frequency of first sinusoidal =0.043
>> f2=input('frequency of second sinusoidal =');
frequency of second sinusoidal =0.031
>> % Generate the input sequence
>> n=0:N-1;
>> x=sin(2*pi*f1*n)+sin(2*pi*f2*n);
>> % Generate the interpolated output sequence
>> y=interp(x,L);
>> %plot the input and output sequence
>> subplot(2,1,1)
>> stem(n,x(1:N));
>> title('Input sequence');
>> xlabel('Time index n');ylabel('Amplitude');
>> subplot(2,1,2)
>> m=0:N*L-1;
>> stem(m,y(1:N*L));
>> title('Output sequence');
>> xlabel('Time index n');ylabel('Amplitude');
```

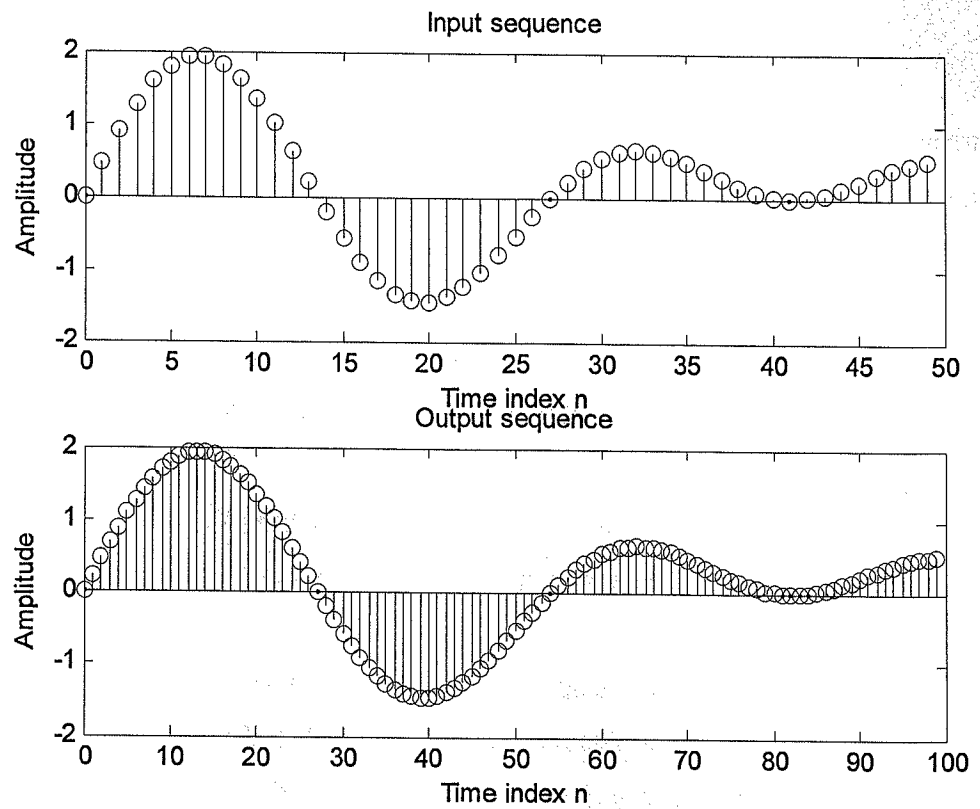


Figure 5.5 MATLAB Generated Illustration of Interpolation Process.

5.3 Design of Algorithms and Devices for Upsampling

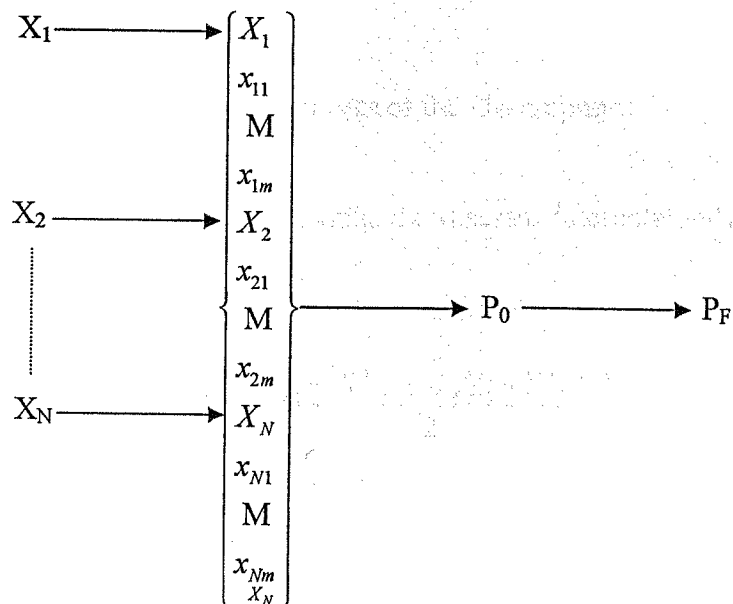
For the digital control and signal processing system the main problem is the reconstruction of a continuous-time signal from its samples when the rate of sampling is not sufficient. This problem becomes more complicated if the process has difficulty of access. For this purpose interpolator filter is used.

The application of complicated reconstruction functions is accomplished by performing mathematical operations such as multiplication, division and generation different orthogonal functions.

Application of the filtering in these cases yields to the exponential and sharply form reconstruction missing values between interpolating nodes. Therefore this problem is actual.

The proposed algorithm of reconstruction of a signal is described below.

1. Let the samples X_1, X_2, \dots, X_N be the principal (measure) samples.
2. Using X_1, X_2, \dots, X_N generating intermediate samples $x_{11}, \dots, x_{1m}; x_{21}, \dots, x_{2m}; \dots, x_{N1}, \dots, x_{Nm}$.



3. The intermediate samples are filtered by the filtering operator P_F through staircase approximation (operator P_0). To obtain intermediate samples any orthogonal or power series polynomials can be used.

Application of this hybrid algorithm upsampling allow controlling the interpolation process between the nodes of the interpolation and perform desired smooth interpolation. Figure 5.6 shows the process of the upsampling.

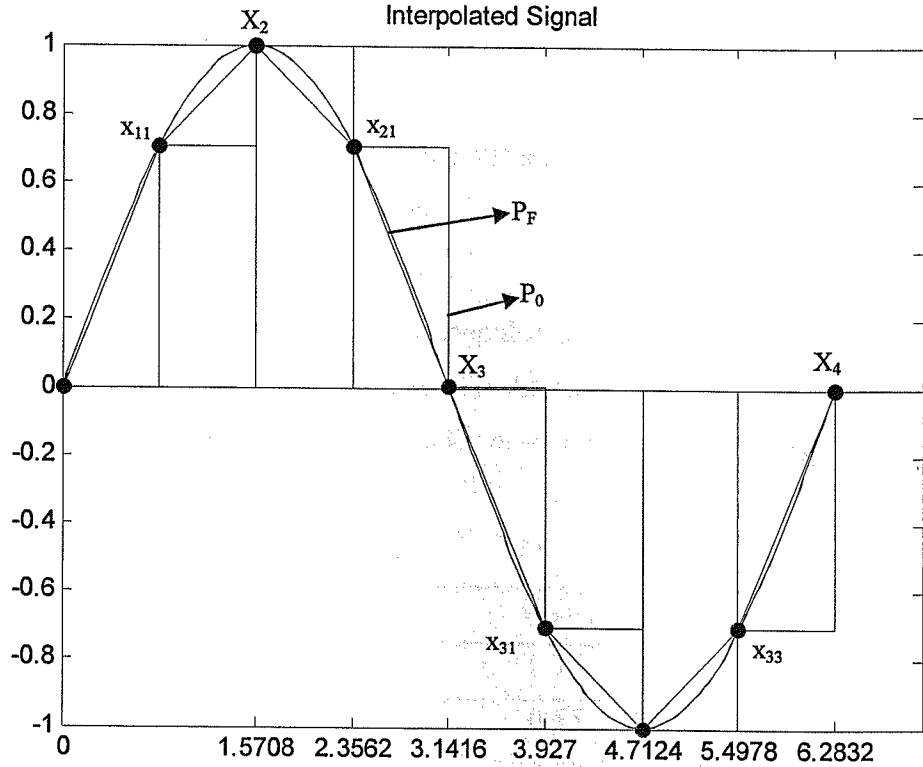


Figure 5.6 The Process of the Upsampling.

Now consider the principle of designing the discrete interpolators that realize Newton polynomial of second order.

From

$$U(t) = U_n + (U_{n+1} - U_n)(t-1) + \frac{(U_{n+2} - 2U_{n+1} + U_n)(t+1)(t+2)}{2}$$

By substituting

$$t = 1 + \frac{k}{i+1} = z \text{ we have}$$

$$U_m = G_{ni}U_n + G_{(n+1)i}U_{n+1} + G_{(n+2)i}U_{n+2}; \quad i = 1, 2, 3, \dots, m; \quad n = 0, 1, 2, 3, \dots, N$$

where N is the total number of samples and m is the total number of intermediate samples.

$$G_{ni} = 3 + 0.5Z^2 - 0.5Z;$$

$$G_{(n+1)i} = 4Z - Z^3 - 3;$$

$$G_{(n+2)i} = 0.5Z^2 - 1.5Z + 2;$$

$$U_{ni} = \sum_{i=1}^3 G_{ni} U_i; \quad i = 1, 2, 3, \dots, m$$

We limit with $m = 1$, in this case the values of the intermediate samples are determined by the following equation

$$U_i = 0.375U_n + 0.75U_{n+1} - 0.125U_{n+2}$$

This signal is the output of a finite impulse response filter with the impulse responses 0.375, 0.75, -0.124. Table 5.1 shows the coefficients of the digital filter to generate intermediate samples for $m=2$ and $n = 3$

Table 5.1 Coefficients of Digital Filter

m	G_{ni}	$G_{(n+1)i}$	$G_{(n+2)i}$
1	0.375	0.75	-0.125
2	0.55	0.55	-0.11
	0.22	0.88	-0.11
3	0.65	0.44	-0.09
	0.37	0.75	-0.125
	0.16	0.94	-0.094

Ratio of resistances on each point is defined in accordance to the table 5.1

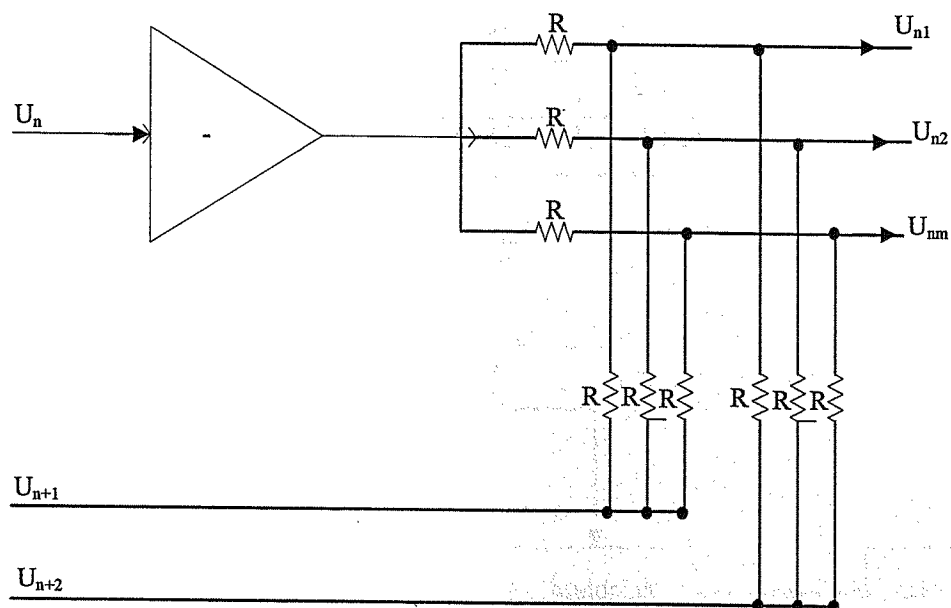


Figure 5.7 Shows the Realization of Digital Filter using the Voltage Dividers..[12].

The mathematical basic to design of the discrete interpolator realizing sinc(t) function is obtained by the following expressions

$$X(t) = \sum_{n=-\infty}^{\infty} X[nT] \frac{\sin w(t - nT)}{w(t - nT)}$$

The value coefficients in table 5.1 can be determined as

$$G_{ni} = \sum_{k=-n_0}^{n_0} \frac{\sin \pi [(m+1)^{-1}i - (i + N_k)]}{\pi [(m+1)^{-1}i - (i + N_k)]}$$

Table 5.2 Coefficients of FIR Filters for $n_0 = 100$; $N = 4$

m	G_{1i}	G_{2i}	G_{3i}	G_{4i}
1	0.604	0.604	-0.105	-0.102
2	0.843	0.330	-0.052	-0.122
3	0.467	0.732	-0.122	-0.075

Realization of filter is shown in figure 5.8

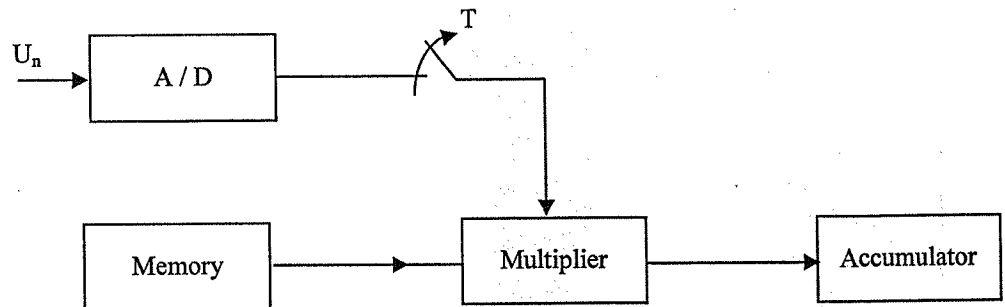


Figure 5.8 Filter Realization

Taking into account the advantages of the digital FIR filters (easily both software and hardware implementation) it is possible to generate intermediate samples in any form, in real time systems.

Efficiency of reconstruction is increased if there is some priory information about the behavior of the process. In this case the criterion of the selection of the interpolating function is based on the desired precision and pattern of reconstruction.

- Reconstructed Signal from its Samples with 5 Samples

```
>> x=0:pi/100:2*pi;
>> y=sin(x);
>> plot(x,y);
>> title('Original Signal')
figure
>> hold on
>> x=0:pi/2:2*pi;
>> y=sin(x);
>> stem(x,y,'fill');
>> title('Sampled Signal')
figure
>> hold on
>> stem(x,y,'fill');
>> stairs(x,y);
>> title('Stair Signal')
figure
>> set(gca,'xtick',[0*pi/4 pi/2 3*pi/4 pi 5*pi/4 6*pi/4 7*pi/4 2*pi]);
>> x=0:2*pi/100:2*pi;
>> y=sin(x);
>> xi=0:pi/2:2*pi;
>> yi=interp1(x,y,xi);
>> plot(x,y,xi,yi)
>> title('Interpolated Signal')
```

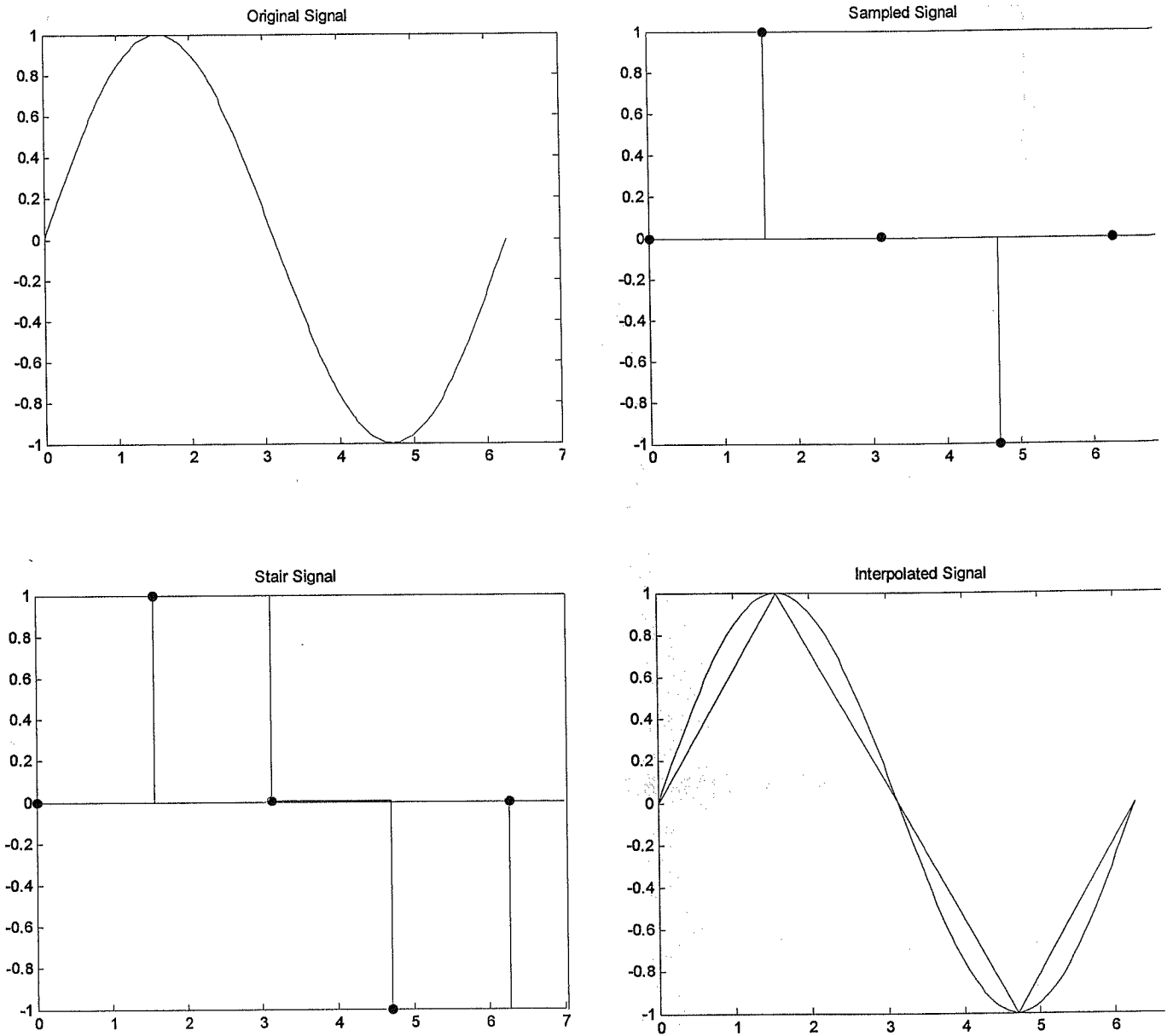


Figure 5.9 MATLAB Implementation for Reconstructed Signal from its Samples with 5 Samples.

By 5 samples we cannot reconstruct the signal as shown in the figure.

- Reconstructed Signal from its Samples with 9 Samples.

```
>> x=0:pi/100:2*pi;
>> y=sin(x);
>> plot(x,y);
>> title('Original Signal')
figure
>> hold on
>> x=0:pi/4:2*pi;
>> y=sin(x);
>> stem(x,y,'fill');
>> title('Sampled Signal')
figure
>> hold on
>> stem(x,y,'fill');
>> stairs(x,y);
>> title('Stair Signal')
figure
>> set(gca,'xtick',[0*pi/4 pi/2 3*pi/4 pi 5*pi/4 6*pi/4 7*pi/4 2*pi]);
>> x=0:2*pi/100:2*pi;
>> y=sin(x);
>> xi=0:pi/4:2*pi;
>> yi=interp1(x,y,xi);
>> plot(x,y,xi,yi)
>> title('Interpolated Signal')
```

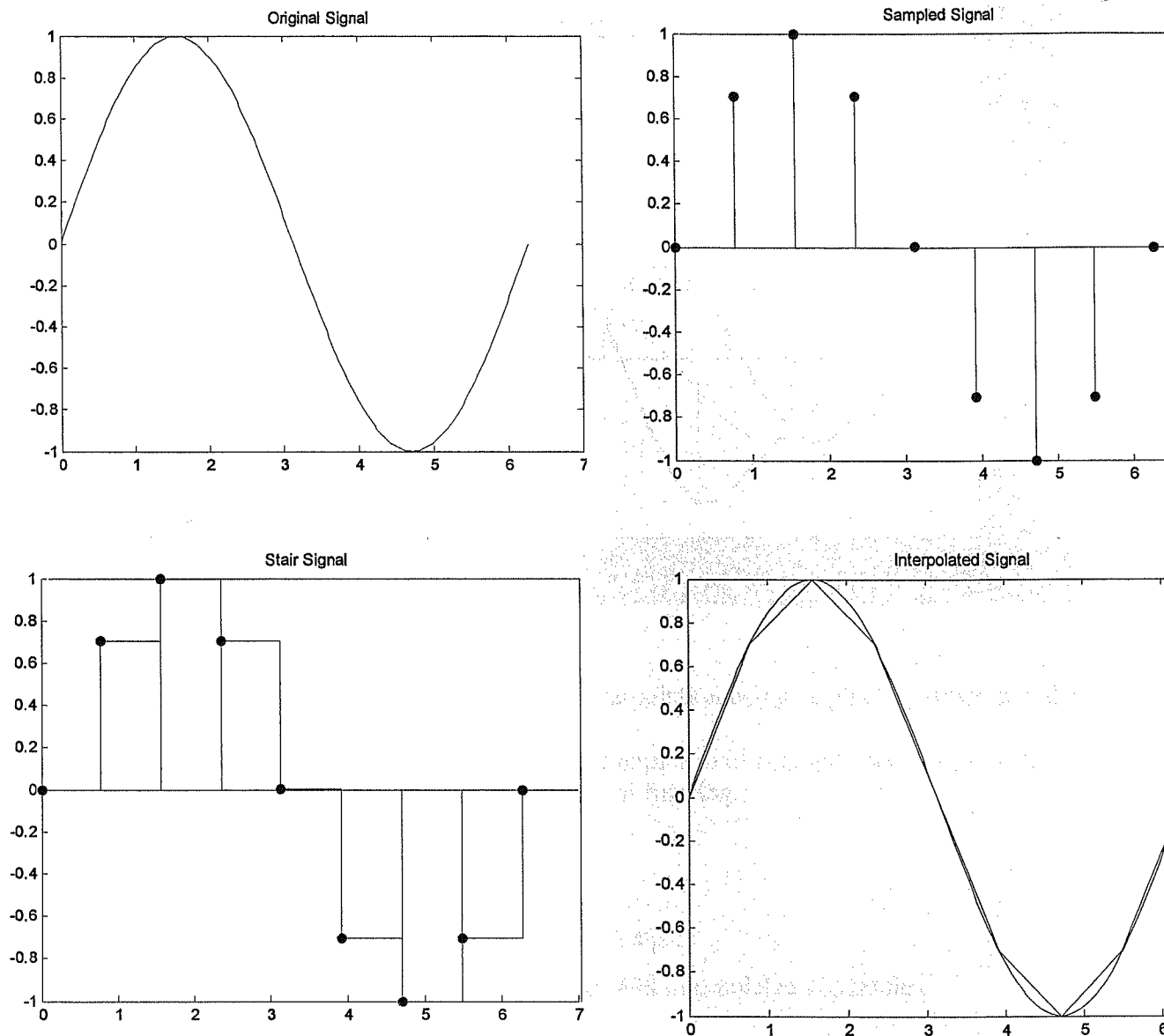


Figure 5.10 MATLAB Implementation for Reconstructed Signal from its Samples with 9 Samples.

By 9 samples we could reconstruct the original signal (very closed to original signal) this means if we increase the number of samples we can reconstruct and if decrease we cannot.

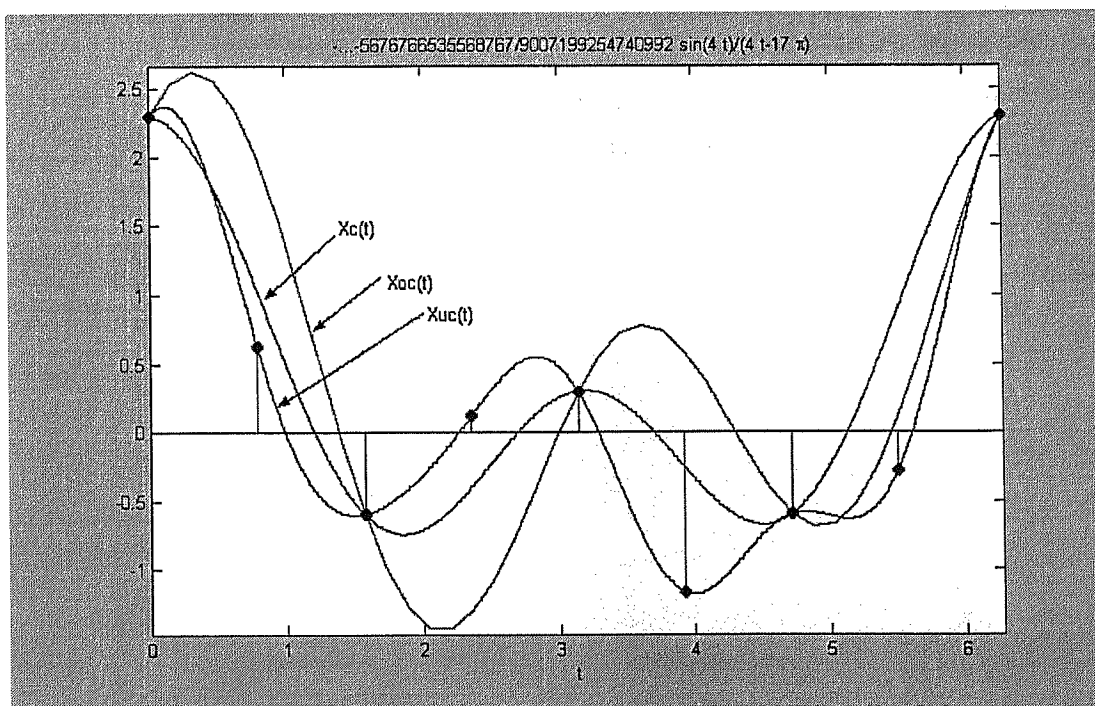


Figure 5.11 Original signal and result of interpolation using original upsampled nodes

In figure 5.11 after inserting a new value of samples to old samples we can reconstruct the signal from its samples by using orthogonal filtering.
The program is shown in appendix 2.

$X_o(t)$ - Original signal

$X_{oc}(t)$ - Reconstructed signal from original samples

$X_{uc}(t)$ - Signal reconstruction using original and interpolated upsampled

5.4 Summary

Extra samples between measured original samples using lagrange interpolation and orthogonal function practical and simulation of systems was described by using MATLAB program.

5.4 Summary

Extra samples between measured original samples using lagrange interpolation and orthogonal function practical and simulation of systems was described by using MATLAB program.

CONCLUSION

The problem of sampling and reconstruction of bandlimited signals were considered.

Interpolation properties of different orthogonal and power series functions were analyzed, Established that using any of orthogonal and Lagrange polynomials can not give desired result, when the number of samples less than the number of samples defined by Shannon.

To increase precision of reconstruction was proposed inserting extra intermediate samples between the original samples and then orthogonal filtering the combination of original and extra samples.

Inserting extra samples (upsampling) between original samples was realized by different ways by changing the number of extra samples and by modifying and by selecting method of computing.

Laboratory implantation using digital signal processing toolbox of Matlab based on different data were established that proposed method allow to increase precision of reconstruction of signal, by compare of parabolic interpolation that is equivalent $MAEc_0 = 0.5380$ and $MAEc = 0.715$

REFERENCES

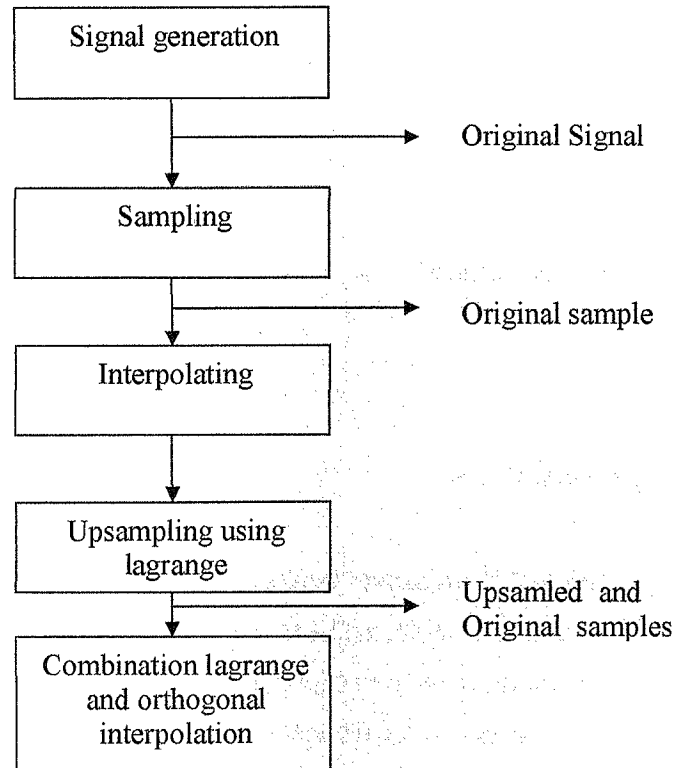
- [1] Alan. V. Oppenheim & Ronald. W. Schafer. (1998). *Discrete-Time Signal Processing. International Edition*. Prentice Hall
- [2] Coutautiue H. Houpis, Gary B. Lamout. (1992). *Digital Control Systems*. International Edition. McGraw-Hill
- [3] Garne E. Brayn. (1999). *Telecommunications Primer, Data, Voice and Video Communications*. International Edition. Prentice Hall
- [4] Gibson J. D. (1993). *Principles of Digital and Analog Communication*. 2'nd Edition. Macmillan
- [5] Haykin S.S. (1986). *Adaptive Filter Theory*. Prentice Hall
- [6] L A. Glover & P. M Gran. (1998). *Digital Communications*. Prentice Hall
- [7] LE.E.E. Communication Magazine Vol20 No:3 .(1982). *The Discrete Fourier Transform Applied to a Time Domain Signal Processing*.
- [8] John.G.Pproakis and Masoud Salehi. (1994). *Communication Systems Engineering*. Prentice Hall
- [9] I. S. Um & A. V. Oppenheim. (1988). *Efficient Fourier Transform and Convolution Algorithms Advanced Topics in Signal Processing*. Prentice Hall
- [10] L. W Couch. (1990). *Digital and Analog Communication Systems*. 3'rd Edition. Macmillan
- [11] F. Mamedov F. S. (1981). *Adaptive Sampling*. Patent No:79258.2. 1981
- [12] F. Mamedov F. S. (1982). *Reconstruction of Analog Signals from its Samples*. Patent No: 877572. 1982
- [13] R. J. Marks. (1991). *Introduction to Shannon Sampling and Interpolation Theory*. Springer-Valey
- [14] R. I. Damper. (1995). *Introduction to Discrete-Time Signals and Systems*. Charpman & Hall
- [15] Simon Haykin. (1994). *Communication Systems*. 3'rd Edition.

- [16] WILEY Steven C. Chatra and Reymond P. Canale. (1988). *Numerical Methods for Engineers*. International Edition. McGraw-Hill
- [17] Widrow B. (1986). *Adaptive Filters Fundamentals*. Tech.Report No:6764-6 (From E.M. University Bookstore)
- [18] Ziemer R E & Tranter W. H. (1990). *Principles of Communication Systems Modulation and Noise*. Macmillan

APPENDIX 1

DIAGRAM OF MATLAB PROGRAM

Diagram of program reading combination of lagrange and orthogonal polynomials is drawn below.



Result of reconstruction

APPENDIX 2

MATLAB PROGRAM AND RESULT

```
t=0:2*pi/40:2*pi;
s=0.35+sin(t+pi/2)+1.34*sin(2*t+pi/4);
plot(t,s,'r')
```

Signal Generation

```
hold on
axis([0 7 -2 3])
t=0:2*pi/4:2*pi;
s=0.35+sin(t+pi/2)+1.34*sin(2*t+pi/4);
stem(t,s,'fill','k')
```

Original Sample

Interpolating Signal

```
syms t k
x1=sin(2*(t-(4*k*pi/2)))/(2*(t-(4*k*pi/2)));z1=symsum(x1,k,-2,2);
x2=sin(2*(t-(4*k+1)*pi/2))/(2*(t-(4*k+1)*pi/2)); z2=symsum(x2,k,-2,2);
x3=sin(2*(t-(4*k+2)*pi/2))/(2*(t-(4*k+2)*pi/2)); z3=symsum(x3,k,-2,2);
x4=sin(2*(t-(4*k+3)*pi/2))/(2*(t-(4*k+3)*pi/2)); z4=symsum(x4,k,-2,2);
x5=sin(2*(t-(4*k+4)*pi/2))/(2*(t-(4*k+4)*pi/2)); z5=symsum(x5,k,-2,2);
hold on
xc=2.2975*z1-0.5975*z2+0.2975*z3-0.5975*z4; ezplot(xc,[0 2*pi])
```

Upsampled and Original Sampled

```
hold on
k1=0.3; k2=-0.2; k3=-0.6;
s11=s(1)*k1+s(2)*k2+s(3)*k3;
s21=s(2)*k1+s(3)*k2+s(4)*k3;
s31=s(3)*k1+s(4)*k2+s(1)*k3;
s41=s(4)*k1+s(1)*k2+s(2)*k3;
x1c=sin(4*(t-(8*k*pi/4)))/(4*(t-(8*k*pi/4)));z11=symsum(x1c,k,-2,2);
x2c=sin(4*(t-(8*k+1)*pi/4))/(4*(t-(8*k+1)*pi/4)); z22=symsum(x2c,k,-2,2);
```

Upsampled and Original Sampled

```
x3c=sin(4*(t-(8*k+2)*pi/4))/(4*(t-(8*k+2)*pi/4)); z33=symsum(x3c,k,-2,2);
x4c=sin(4*(t-(8*k+3)*pi/4))/(4*(t-(8*k+3)*pi/4)); z44=symsum(x4c,k,-2,2);
x5c=sin(4*(t-(8*k+4)*pi/4))/(4*(t-(8*k+4)*pi/4)); z55=symsum(x5c,k,-2,2);
x6c=sin(4*(t-(8*k+5)*pi/4))/(4*(t-(8*k+5)*pi/4)); z66=symsum(x6c,k,-2,2);
x7c=sin(4*(t-(8*k+6)*pi/4))/(4*(t-(8*k+6)*pi/4)); z77=symsum(x7c,k,-2,2);
x8c=sin(4*(t-(8*k+7)*pi/4))/(4*(t-(8*k+7)*pi/4)); z88=symsum(x8c,k,-2,2);
ss=[s(1) s11 s(2) s21 s(3) s31 s(4) s41]
```

Combination Lagrange and Orthogonal Interpolation

```
xc1=s(1)*z11+ s11*z22+ s(2)*z33+ s21*z44+ s(3)*z55+ s31*z66+ s(4)*z77+ s41*z88;
ezplot(xc1,[0 2*pi])
```

hold on

```
ss=[s11 s21 s31 s41];
tt=[pi/4 pi*3/4 pi*5/4 pi*7/4];
stem(tt,ss,'fill','m')
```

Result of Reconstruction

ss =

```
2.2975 0.6302 -0.5975 0.1198 0.2975 -1.1698 -0.5975 -0.2802
```

n=1;

new_xc1= [];

new_Xc = [];

for t=0:2*pi/40:2*pi

new_Xc(n)=Xc;

new_xc1(n)= xc1;

tt(n)=t;

n=n+1;

end

plot(tt,new_Xc,'r:')

plot(tt,new_xc1,'r:')

```
c=new_Xc-s1;  
c0=new_xc1-s1;
```

```
er_c=load('c.m');  
er_c0=load('c0.m');
```

```
MAEc=mean(abs(er_c))
```

```
RMSEc=sqrt(mean(er_c.^2))
```

```
MAEc0=mean(abs(er_c0))
```

```
RMSEc0=sqrt(mean(er_c0.^2))
```

```
total=[s1' new_Xc' new_xc1' er_c er_c0]
```

```
MAEc0 =
```

```
0.5380
```

```
MAEc =
```

```
0.7156
```

```
RMSEc0 =
```

```
0.6120
```

```
RMSEc =
```

```
0.9061
```

The comparison of original signal with parabolic and proposed interpolation signal.

Original signal S1	Parabolic interpolation new_Xc	proposed interpolation new_xc1	rorEr c	Error c0
2.2975	2.2970	2.2970	0	0
2.5316	2.2259	2.3657	-0.3057	-0.1659
2.6246	2.0466	2.1644	-0.5780	-0.4602
2.5645	1.7739	1.7452	-0.7906	-0.8193
2.3530	1.4293	1.1993	-0.9237	-1.1537
2.0046	1.0395	0.3762	-0.9652	1.6284
1.5461	0.6339	0.1280	-0.9122	-1.4182
1.0136	0.2425	-0.2504	-0.7711	-1.2640
0.4494	-0.1073	-0.4860	-0.5567	-0.9354
-0.1019	-0.3927	-0.5919	-0.2908	-0.4900
-0.5975	-0.5975	-0.5975	0	0
-1.0004	-0.7133	-0.5335	0.2871	0.4669
-1.2825	-0.7400	-0.4209	0.5425	0.8616
-1.4275	-0.6857	-0.2698	0.7418	1.1577
-1.4317	-0.5655	-0.0858	0.8663	1.3460
-1.3046	-0.3998	0.0738	0.9048	-1.1848
-1.0674	-0.2126	0.3217	0.8548	1.3890
-0.7506	-0.0284	0.4803	0.7222	1.2310
-0.3914	0.1297	0.5499	0.5211	0.9414
-0.0293	0.2427	0.4933	0.2721	0.5226
0.2975	0.2975	0.2975	0	0
0.5563	0.2880	-0.0158	-0.2683	-0.5720
0.7224	0.2157	-0.3917	-0.5067	-1.1142
0.7825	0.0900	-0.7550	-0.6925	-1.5375
0.7349	-0.0733	-1.0312	-0.8082	-1.7661
0.5904	-0.2532	-0.6238	-0.8436	0.4206
0.3706	-0.4258	-1.1600	-0.7964	-1.5306
0.1056	-0.5668	-1.0340	-0.6724	-1.1396
-0.1686	-0.6535	-0.8544	-0.4849	-0.6858
-0.4148	-0.6677	-0.6918	-0.2530	-0.2770
-0.5975	-0.5975	-0.5975	0	0
-0.6875	-0.4385	-0.5839	0.2491	0.1036
-0.6645	-0.1945	-0.6173	0.4700	0.0472
-0.5195	0.1222	-0.6284	0.6417	-0.1089
-0.2562	0.4921	-0.5366	0.7482	-0.2804
0.1096	0.8898	-1.5738	0.7802	-1.4642
0.5507	1.2865	0.1576	0.7359	-0.3931
1.0314	1.6520	0.7366	0.6207	-0.2948
1.5107	1.9577	1.3654	0.4471	-0.1452
1.9460	2.1790	1.9242	0.2330	-0.0218
2.2975	2.2975	2.2975	0	0